ABSTRACT

Title of Dissertation:	ESTIMATING RISK OF AIRBORNE INFLUENZA TRANSMISSION IN A CONTROLLED ENVIRONMENT
	Paul Jacob Bueno de Mesquita, Doctor of Philosophy, 2019
Dissertation directed by:	Professor Donald K. Milton, Department of Epidemiology and Biostatistics, Maryland Institute for Applied Environmental Health

Pandemic preparedness is weakened by uncertainty about the relative importance of influenza transmission modes, particularly airborne droplet nuclei (aerosols). A human-challenge transmission trial in a controlled environment was conducted to address this uncertainty. Healthy, seronegative volunteer 'Donors' (N=52) were randomly selected for intranasal challenge with influenza A/Wisconsin/67/2005 (H3N2) and exposed to seronegative 'Recipients' randomized to intervention (N=40) or control (N=35) groups. Intervention recipients wore face shields and hand sanitized frequently to limit large droplet and contact transmission. A transmitted infection, confirmed by serology in a control recipient, yielded a 1.3% SAR overall. This was significantly less than the expected 16% SAR ($p < 0.001$) based on a proof-of-concept study that used half as many Donors and exposure days. The main difference between these studies was mechanical building ventilation in the follow-on study, suggesting a

possible role for aerosols. The extent to which Donor viral shedding was similar to that of mild, natural infections and may be useful for studying transmission was investigated. The only available aerosol shedding comparison data comes from a population of adults with influenza A H3 infection enrolled on the basis of febrile illness plus cough or sore throat, or positive Quidel QuickVue rapid test (N=83). Systematic differences in case selection compared with Donors yielded more severe cases and introduced bias. To account for differences in illness severity, propensity score matching, stratification, and inverse weighting ultimately demonstrated that the experimental and naturally infected groups were too different to compare without bias. While acknowledging the uncertainty in the generalizability of the current challenge model, observed aerosol shedding and CO_2 were used in the rebreathed-air version of the Wells-Riley equation to compute average quantum generation rates (95% CI) 0.029 (0.027, 0.03) and 0.11 (0.088, 0.12) per hour for infected Donors and fine aerosol shedding Donors, respectively. Donors shed 1.4E+5 (1.0E+5, 1.8E+5) airborne viral RNA copies per quantum (ID_{63}). This dissertation provides evidence for airborne transmission, presents a methodology for estimating an airborne dose, and suggests a role for building ventilation in reducing risk and the need for future observational studies to evaluate transmission modes in non-experimental settings with greater generalizability.

ESTIMATING RISK OF AIRBORNE INFLUENZA TRANSMISSION IN A CONTROLLED ENVIRONMENT

by

Paul Jacob Bueno de Mesquita

Dissertation submitted to the Faculty of the Graduate School of the
University of Maryland, College Park, in partial fulfillment
of the requirements for the degree of
Doctor of Philosophy
2019

Advisory Committee:
Professor Donald K. Milton, Chair
Associate Professor Shuo Chen
Associate Professor Robin Puett
Professor Jelena Srebric
Associate Professor Paul Turner

Dedication

To our interconnected global community.

Acknowledgements

I thank my advisor and mentor Dr. Donald Milton for his teaching, encouragement, grit, graciousness, and joyful spirit to do meaningful and meticulous research. I am very grateful to be your student. Thanks to the other members of the dissertation committee (Dr. Shuo Chen, Dr. Robin Puett, Dr. Jelena Srebric, and Dr. Paul Turner) for shepherding me into this transdisciplinary, environmental health field. I thank the EMIT Consortium for their many efforts to advance influenza transmission work and promote public health. Thanks to Michael Grantham for laboratory training, Jing Yan for a trail of notes, Muhiuddin Haider for philosophical debate, and Chang Chen for statistical consultation. Thanks to the entire *C.A.T.C.H. The Virus Study* team. Thanks to Rosie Sokas and Phil Hagan for introducing me to this field of study and the social justice that drives it. Thanks to Linda Kirk, Rick Roush, and the Union County Health Department for introducing me to practical, community-based public health service delivery. Lots of love and gratitude for friends and family.

This doctoral program was supported by the University of Maryland Graduate School, University of Maryland School of Public Health, The Maryland Institute for Applied Environmental Health, The US Centers for Disease Control Prevention Cooperative Agreement 1U01IP000497, and The Defense Advanced Research Projects Agency (DARPA) BTO under the auspices of Col. Matthew Hepburn through agreement N66001-17-2-4023 and N66001-18-2-4015, and. The findings and conclusions in this report are those of the authors and do not necessarily represent the

official position or policy of funding agencies and no official endorsement should be inferred.

Table of Contents

CHAPTER I

RESEARCH AIMS AND INTRODUCTION

Specific Research Aims

Seasonal and pandemic influenza remain global threats. Seasonal flu kills up to 650,000 people each year and pandemics have the potential to cause millions of deaths and disrupt societies. Despite this being the 100th year anniversary of the 1918-19 global influenza pandemic with a death toll estimated over 50 million, present day non-pharmaceutical prevention strategies as well as vaccines remain inadequate. It is widely appreciated that the quest for improved non-pharmaceutical controls and vaccines is dependent upon knowledge of influenza virus transmission via direct contact, large droplet spray, and fine-particle aerosol inhalation. However, the infection risk posed by each mode is not well known. Influenza intervention trials showed that use of hand hygiene and surgical masks to reduce contact and large droplet exposure resulted in only mild risk reduction among susceptible household contacts of influenza cases, and may have facilitated more airborne transmission (Cowling et al., 2013a). Human challenge studies have shown that infection initiated through aerosols, compared with nasal instillation (Alford et al., 1966; Henle et al., 1946), required a lower dose and resulted in more severe disease. Inhalation of bioaerosols is likely important for other acute, viral, respiratory infections and was convincingly implicated by airborne viral transport computational fluid dynamic

models for a deadly SARS-coronavirus outbreak (Yu et al., 2004). The capacity to directly measure the extent and intensity of transmission risk posed by bioaerosols represents a major uncertainty for which research is urgently needed. Failure to quantify the contribution of exhaled bioaerosols impedes the implementation of effective control measures and facilitates population vulnerability during seasonal epidemics and pandemics.

The long-term goal is to achieve valid estimates of airborne transmission risk for respiratory viruses to support optimization of prevention strategies. We build upon the quantum theory of airborne infection (Wells, 1955) by quantifying influenza in exhaled breath aerosols, and by describing an approach to directly measure airborne risk from confirmed transmission events. The central hypothesis is that risk of influenza A virus transmission by the airborne mode can be estimated from a human challenge transmission trial as a function of exposure to contaminated exhaled breath indoors. This research supports the theoretical underpinnings for innovative epidemiologic research that moves the field closer to reliably measuring and predicting airborne risk, which informs disease control efforts. This research takes advantage of data collected from the CDC-funded human influenza challenge transmission trial (Evaluating Modes of Influenza Transmission, ClinicalTrials.gov number NCT01710111) that tested the effect of transmission mode using face shields and hand hygiene randomized exposure groups in a controlled environment. Specific aims tested the following hypotheses:

1. The fraction of secondary cases attributable to airborne transmission will be greater than those attributable to contact and large droplet spray.
2. The shedding strength of natural, community-acquired influenza cases are well approximated by artificial infection initiated by nasal instillation of virus.
3. The infectious quantum generation rate for influenza is estimated as a function of the quantity of infectious aerosols exhaled by infectious cases, and the rate of airborne virus removal mainly driven by ventilation, given the susceptible immune status of the trial volunteers.

These hypotheses focus on achieving knowledge to support the scientific underpinnings of new frameworks to drive investigation of influenza transmission risk assessment. Findings lead support future epidemiologic study designs under which longitudinal surveillance of contact networks can revolutionize understanding of airborne infection transmission by pinpointing transmission routes and refining estimates of infection risk by airborne and other modes in indoor spaces. Results from this and future work provide key information for guiding the strategic use of prevention methods to protect against seasonal epidemics and pandemics, especially in shared air spaces and among immunologically vulnerable communities.

Disease burden and public health significance

The Forum of International Respiratory Societies emphasizes that acute respiratory infections are the greatest contributors to the global disease burden, responsible for 4

million deaths annually. CDC reports that influenza resulted in 9-36 million illnesses and up to 56,000 deaths each year since 2010 in the US, with annual estimated direct and indirect costs of $87 billion (Molinari et al., 2007). Respiratory infections cost over $15 billion annually in the UK (Burki, 2017). Globally, seasonal influenza kills up to 675,000 people each year and influenza pandemics have the potential to cause millions of deaths and severe societal disruption. The health and economic burdens are amplified in developing nations with less access to health services (Fischer et al., 2014). Trends in spillover of pathogenic avian influenza to humans, and an increasingly interconnected world create an urgent case for improved prevention methods.

Prevention of these substantial population health threats cannot rely solely on vaccines, which are often poorly matched to rapidly evolving strains. During pandemics, lag time in the production and dissemination of vaccines leads to widespread vulnerability and underscores the need for interventions based on viral exposure reduction to interrupt transmission. It is widely appreciated that the quest for improved non-pharmaceutical prevention methods (e.g., reducing exposures through building ventilation or social distancing), and vaccines is dependent on understanding transmission risk via contact, large droplet spray, and fine-particle aerosol respiration (i.e., airborne) (Erbelding et al., 2018). Although the risk contribution by each of these modes is not well characterized, there is strong evidence supporting the critical role of airborne transmission, and it is well-recognized that infection initiated by the airborne route is likely to cause more severe symptoms

compared to infections initiated by contact or large droplet spray (Alford et al., 1966; Henle et al., 1946).

CDC recommends protective behaviors such as washing hands, covering coughs, and donning masks to reduce contact and droplet exposure, but does not provide specific guidance to mitigate fine-particle aerosols that are capable of penetrating and circumventing surgical masks. Intervention trials showed that use of hand hygiene and surgical masks to hinder contact and droplet exposure resulted in only mild risk reduction among susceptible household contacts of nearly 800 influenza cases, and may have promoted a greater proportion of airborne transmission (Cowling et al., 2013a). Furthermore, those most likely to be exposed to airborne influenza, due to use of hand hygiene plus surgical mask, tended to present with more severe symptoms characterized by fever and cough. Despite some delays in intervention initiation and imperfect adherence, such trial conditions reflect realistic population usage, while randomization and robust sensitivity analyses support internal validity to the extent possible. Thus, the state of the science urgently demands investigation to quantify airborne transmission risk. In the absence of accurate risk estimation, the strategic design and implementation of control programs remains elusive.

Prevailing uncertainty about intervention effectiveness permits seasonal epidemics and pandemic vulnerability. A clear, dose-response relationship between dormitory rebreathed air fraction and likelihood of retrospective, self-reported ARI was observed in a study of 3,712 students in Tianjin, China (Sun et al., 2011). A separate

airborne infection risk model suggested that increased clean air supply can effectively control population spread for ARIs including influenza, but may not have much effect on highly contagious infections like measles (Rudnick and Milton, 2003a). However this study used estimated values of influenza contagiousness based on an airplane outbreak (Moser et al., 1979a), where there was uncertainty about outdoor air exchange and all secondary influenza cases were assumed to be connected to the index.

While modulating airflow and ventilation can influence airborne contamination quantities and human exposure, unequivocal evidence from benchtop exposure chambers demonstrates the inactivation of aerosolized influenza (McDevitt et al., 2012) and TB (Riley and Nardell, 1989) under exposure to UV-C light, representing another promising strategy for airborne transmission control. But whereas current control techniques are unlikely to be strategically deployed, improved characterization of risk by transmission mode enable the most effective use of already existing control strategies. In the absence of accurate risk estimation, the strategic design and implementation of control programs remains elusive. Likewise, the motivation to invest by public health officials and community members dwindles. Elucidating airborne transmission risk is the next step toward optimizing the control of influenza and other respiratory infections and maximizing population health impact.

Premise for human-transmission trial

A meeting of globally recognized influenza transmission experts was convened by CDC in 2010 to address knowledge gaps about the relative importance of influenza transmission modes that are reflected in uncertainty about hospital care and general population prevention guidelines (Snider et al., 2010). The meeting discussed possible animal and human transmission experiments and explored the possibilities of conducting epidemiological studies with engineering and/or personal protective interventions. Although there was great enthusiasm for studies of population infection surveillance with upper room germicidal irradiation (UVGI) or other airborne control interventions, preliminary work in this area was lacking. Ultimately it was determined that a human challenge-transmission study with interventions to control for transmission mode, and surveillance of aerosol shedding, environmental conditions, and comparison of aerosol infectivity of experimental and naturally infected influenza cases would represent a the most scientifically sound approach.

Aerobiologic pathway

An abundance of laboratory evidence substantiates the aerobiologic pathway for influenza and other acute respiratory infections (ARIs) and supports new epidemiologic studies of transmission. The aerobiologic pathway (Roy and Milton, 2004), consists of: a) generation of particles containing infectious microbes from the respiratory tract or environmental sources, b) maintenance of infectivity and

persistence in the air before reaching a susceptible host, and c) deposition in at least one vulnerable locus in the respiratory tract of the new host.

With respect to infectious particle generation, exhaled breath particles contain respiratory fluid lining of the small airways and are generated by small airway closure and reopening (Almstrand et al., 2010; Fabian et al., 2008; Johnson and Morawska, 2009). Our group observed 218 half-hour exhaled breath samples from 142 symptomatic influenza cases. We detected culturable influenza virus in 39% of fine-particle aerosols with geometric means of 37 infectious particles by fluorescent focus assay and $3.8x10^4$ RNA copies by qRT-PCR (geometric standard deviations 4.4 and 13, respectively) (Yan et al., 2018). Using a G-II bioaerosol collection device to sample natural breathing (including incidental coughs), this research clearly shows that influenza cases can generate many virus-laden particles.

Once generated, infectious aerosols maintain infectivity and persist in the air before reaching a susceptible host. The airborne movement of infectious particles has been implicated in human and animal transmission for influenza and other respiratory pathogens. Computational fluid dynamics and multi-zone models simulating a three-dimensional aerosol plume rising upwards and around an apartment building with a SARS-coronavirus index case predicted the location of secondary cases (Yu et al., 2004). Noti et al., 2012 measured infectious influenza in aerosols that had traveled across a room. Upward dispersion of aerosols with slow settling velocity has been confirmed by influenza A transmission between infected guinea pigs housed >100cm

below exposed animals (Mubareka et al., 2009). Numerous ferret studies report similar results. The ability for airborne particles to travel and initiate disease was implied by two postal workers who became infected with Anthrax following a known release of spores and no other known exposures (Fennelly et al., 2004). Biologically active airborne particles carry public health significance given the potential for prolonged suspension and scenarios of exposure before removal occurs or through recirculated air that has not been filtered or sterilized. Studies of biological decay in aerosolized virus maintained in a rotating drum demonstrated infectious potential for influenza (Harper, 1961) and coronavirus (Ijaz et al., 1985) after 23 hours and 6 days, respectively. Although the exact sizes of the laboratory generated aerosols used were not reported, these studies demonstrate prolonged infectiousness in particles <10μm. The rate of biological decay as a function of temperature and relative humidity has been characterized through laboratory manipulation of viral laden droplets in Yang et al., 2012; and through airborne simulations with bacteriophage Phi6, a surrogate for influenza and coronaviruses, in Prussin et al., 2018. Reduced decay corresponded with lower droplet salt concentrations associated with high and low vapor pressures, consistent with epidemiologic observation of peak transmission during the hot and rainy season in the tropics, and the cold and dry season in temperate climates. However other research using aerosolized virus from human airway epithelial fluid suggests that influenza virus remains infectious independent of relative humility (Kormuth et al., 2018). This latter work may be more convincing given the use of a more realistic human model.

Inhalation of airborne virus and deposition at a vulnerable locus in the respiratory tract can initiate infection. A human challenge study demonstrated an infectious dose for inhaled influenza A aerosols as low as 0.6-3 $TCID_{50}$ (Alford et al., 1966). A study of exhaled breath from confirmed influenza cases showed that 99 and 87% of particles were less than 5 and 1µm, respectively (Fabian et al., 2008). This shows that exhaled breath aerosols are well within the size range to penetrate the lower lung. Fine particle aerosols exhaled from naturally infected influenza cases have been shown to carry infectious virus (Lindsley et al., 2015, 2010; Milton et al., 2013; Noti et al., 2012; Yan et al., 2018). Given that epidemiologic, laboratory, and challenge studies fail to definitively confirm human airborne transmission and produce valid risk models, there is an urgent need for methods that maximize external validity to community settings and enable confirmation of transmission modes for a range of ARIs. Observation of community transmission provides an ideal platform to validate risk models that parameterize the aforementioned aerobiologic path – viral aerosol generation, persistence, and deposition – leading to valid estimation of infectious dose. Observation of exposed, asymptomatic individuals satisfies the concerns of Fraser et al., 2004, which identified asymptomatic cases as key to pushing R_0 above 1.

Studies of influenza transmission mode and the anisotropic hypothesis

Hand hygiene and face masks have been assessed for their potential to reduce influenza transmission and gain information about transmission mode-related risk.

Cluster-randomized trial with hand hygiene and facemask interventions found mild reductions in risk among intervention users (effect for hand hygiene and facemask groups, separately) that did not reach statistical significance (Aiello et al., 2012). This finding was consistent with those from studies performed in Hong Kong and Bangkok that showed the effect of hand hygiene plus facemask to be small at best (Cowling et al., 2013a, 2009; Simmerman et al., 2011). A similar result was observed for crowded, urban households in upper Manhattan after 19 months of follow-up in 509 households (Larson et al., 2010). However a meta-analysis showed that hand hygiene plus facemask interventions were associated with a statistically significant 27% reduction in transmission risk, while hand hygiene alone had no significant effect, showed a trend toward reducing risk under higher humidity and suggesting a predominance of aerosol transmission in temperate climates that is weakened in tropical climates (Wong et al., 2014). Given that facemasks have been assessed to reduce viral RNA copies contained in coarse aerosols by 25-fold and fine aerosols by 2.8-fold, if such reductions are associated with reduced transmission risk, then the meta-analysis findings make sense (Milton et al., 2013). Several other studies and review papers provide make a case for the role of airborne particles in influenza transmission (Nikitin et al., 2014; Tellier, 2009; Tellier et al., 2019).

The hypothesis that influenza is anisotropic (Milton, 2012)– that the route of transmission influences disease presentation (Tellier et al., 2019) – is supported by early studies of human exposure to influenza contained in aerosols and nasal droplets (Alford et al., 1966; Knight et al., 1965). Aerosol exposure was more likely to result

in typical, influenza-like disease characterized by fever and cough, compared with nasal mucosa exposure representative of contact and droplet routes. Henle et al., 1946 observed similar findings for those with nasal inoculation. Furthermore, community infected cases documented by Knight and colleagues exhibited similar symptomatology as Alford's infected volunteers, suggesting a natural tendency toward aerosol transmission. These findings were recently borne out in ferrets where aerosol-infected animals not only presented with more severe symptoms but also shed more virus than their nasally-inoculated counterparts (Gustin et al., 2011).

Overview of thesis

The human challenge-transmission trial, Evaluating Modes of Influenza Transmission (EMIT), used in this research was designed to achieve an expected 40% SAR, however achieved an actual SAR of 1.3%. This finding on its own fails to provide definitive results regarding transmission modes. Comparison of this result with the proof-of-concept study that achieved an SAR of 8.3% under much lower exposure and ventilation motivates discussion about the role of ventilation and exposure to airborne pathogens (Killingley et al., 2012). The next question is whether the EMIT human volunteers experimentally infected by intranasal droplets simulate naturally-acquired infections to a comparable degree. Fortunately, to address this question EMIT funded a study of community influenza cases presenting with influenza-like illness. Finally, using the CO_2 data from the transmission trial, and knowledge of aerosol viral shedding by experimentally infected primary cases (known as 'viral

Donors'), we can apply the rebreathed-air equation, a modification of the Wells-Riley equation, to estimate an infectious quanta generation rate and RNA copy number per infectious quanta (Rudnick and Milton, 2003a). Findings from these analyses generate new knowledge about influenza infection, disease, and transmission and inform future studies aimed at improving our understanding influenza transmission.

CHAPTER II

MINIMAL TRANSMISSION IN AN INFLUENZA A (H3N2) HUMAN CHALLENGE-TRANSMISSION MODEL WITH EXPOSURE EVENTS IN A CONTROLLED ENVIRONMENT

By Jonathan S. Nguyen-Van-Tam, Ben Killingley, Joanne Enstone, Michael Hewitt, Jovan Pantelic, Michael Grantham, P. Jacob Bueno de Mesquita, Robert Lambkin-Williams, Anthony Gilbert, Alexander Mann, John Forni, Catherine J. Noakes, Min Z. Levine, LaShondra Berman, Stephen Lindstrom, Simon Cauchemez, Werner Bischoff, Raymond Tellier, and Donald K. Milton, for the EMIT Consortium.
A complete list of the EMIT Consortium can be found in the Supporting Information.

Abstract

Background

Uncertainty about the relative importance of modes of influenza transmission, particularly airborne droplet nuclei (aerosols), fuels controversy concerning recommendations for healthcare worker protection during pandemics. In-depth review by an expert panel, a proof-of-concept study, and an international workshop concluded that human challenge-transmission studies in well-controlled environments would be the most promising approach to fill this critical knowledge gap.

Methods

Healthy, seronegative volunteer 'Donors' (N=52) were randomly selected for intranasal challenge with influenza A/Wisconsin/67/2005 (H3N2). Seronegative 'Recipients' randomised to Intervention (IR, N=40) or Control (CR, N=35) groups

were exposed to Donors for four days. IRs wore face shields and hand sanitised frequently to limit large droplet and contact transmission. Numbers of Donors and days of Recipient exposure were increased compared to proof-of-concept to increase secondary attack rate (SAR). Symptoms were monitored and viral shedding in nasopharyngeal swabs and exhaled breath viral aerosols were quantified by reverse-transcriptase PCR (qRT-PCR). Serological specimens were analysed for evidence of seroconversion. (ClinicalTrials.gov number NCT01710111).

Findings

Intranasal inoculation produced an infection rate of 81% (42/52); 60% (25/42) of infected Donors had influenza-like illness, 14% (6/42) had fever, and 26% (11/42) had mild or no symptoms. Viral aerosol shedding was observed from 26% (11/42) of the infected Donors. One transmitted infection was confirmed by serology in a CR, yielding a SAR of 2·9% among CR, 0% in IR ($p = 0{\cdot}47$ for group difference), and 1·3% overall.

Interpretation

The SAR observed was significantly less than 16% ($p < 0{\cdot}001$) expected based on the proof-of-concept study SAR considering that there were twice as many Donors and days of exposure to Recipients. The main difference between these studies was mechanical building ventilation in the follow-on study, suggesting a possible role for aerosols. The low SAR limits this study's ability to provide definitive evidence regarding modes of transmission.

Research in context

Evidence before this study

The evidence base for influenza transmission is derived from studies that have assessed: virus deposition and survival in the environment; the epidemiology of disease in hospitals, nursing homes and other closed or semi-closed settings, pharmaceutical and non-pharmaceutical interventions in the setting of natural, and experimental infection, animal models, and mathematical models of transmission. These approaches have so far failed to produce conclusive answers quantifying the relative importance of human-to-human transmission modes. Influenza challenge studies in humans have been conducted over several decades to investigate disease pathogenesis and the efficacy of antivirals and vaccines. Until recently, experimental challenge-transmission studies assessing human-to-human transmission had not been performed. In 2009, we demonstrated proof-of-concept that healthy seronegative volunteers inoculated intranasally with influenza A/Wisconsin/67/2005 (H3N2) would develop symptoms of influenza-like illness (ILI) and, during two days of household-like conditions without environmental controls, transmit infection to other seronegative volunteers. However, the routes of transmission in the proof-of-concept study were not determined and in retrospect, the outcome criteria for secondary infection in the proof-of-concept study were judged to be insufficiently rigorous.

Added value of this study

To our knowledge, this is the largest human influenza challenge-transmission study undertaken to date. The control of indoor air quality during exposure, of exposure modes via randomized intervention groups, and the analysis of viral shedding from the mucosa and exhaled breath were designed to allow for a comprehensive understanding of viral shedding and the potential for transmission by the various modes. The low overall secondary attack rate shows that, as currently implemented, the challenge-transmission model results in negligible transmission. The significantly lower than expected secondary attack rate, based on the results of the prior proof-of-concept study, was possibly attributable to greater ventilation in the current study, and adds to evidence that limiting exposure to infectious droplet-nuclei (aerosols) may make an important contribution to controlling influenza transmission.

Implications of all the available evidence

Understanding the relative importance of influenza modes of transmission informs strategic use of preventive measures to reduce influenza risk in high-risk settings such as hospitals and is important for pandemic preparedness. Given the increasing evidence from epidemiological modelling, exhaled viral aerosol, and aerobiological survival studies supporting a role for aerosol transmission and the potential benefit of respirators (and other precautions designed to prevent inhalation of aerosols) versus surgical masks (mainly effective for reducing exposure to large droplets) to protect healthcare workers, more studies are needed to evaluate the extent of risk posed by different modes of transmission. Future human challenge-transmission studies should be carefully designed to overcome limitations encountered in the current study.

However, the low secondary attack rate also suggests that the current challenge-transmission model may no longer be a more promising approach to resolving questions about transmission modes than community-based studies employing environmental monitoring and newer, state-of-the-art deep sequencing-based molecular epidemiological methods.

Introduction

Influenza virus is a pathogen of global public health significance, but human-to-human transmission remains poorly understood. In particular, the relative importance of the different modes of transmission (direct and indirect contact, large droplet, and aerosols (airborne droplet nuclei)) remains uncertain during symptomatic and asymptomatic infection (Brankston et al., 2007; Killingley and Nguyen-Van-Tam, 2013; Tellier, 2009, 2006).

The evidence base for influenza transmission is derived from studies that have assessed: virus deposition and survival in the environment; the epidemiology of disease; pharmaceutical and non-pharmaceutical interventions; animal models; and mathematical models of transmission. Those approaches have so far failed to produce conclusive data quantifying the relative importance of human-human transmission modes (Brankston et al., 2007; Killingley and Nguyen-Van-Tam, 2013).

Infection control guidance for pandemic and seasonal influenza assumes that most transmission occurs during symptomatic infection, predominantly via large droplet spread at short range (1-2m).(Brankston et al., 2007) Thus, social distancing measures are often proposed to mitigate the spread and impact of a pandemic; and hand washing and respiratory etiquette are promoted as ways to reduce transmission of seasonal and pandemic influenza. Evidence to support the possibility of aerosol transmission has grown over recent years (Cowling et al., 2013b; Kormuth et al., 2018; Yan et al., 2018) and leads to controversies about when and if filtering facepiece respirators (and other precautions designed to prevent inhalation of aerosols) versus surgical masks (mainly capable of reducing large droplets and some fine particles) should be used to protect healthcare workers, particularly during a severe pandemic (Bischoff et al., 2013; Brankston et al., 2007; Makison Booth et al., 2013; Milton et al., 2013; Tellier, 2009, 2006).

An expert panel, after in-depth review of the challenges facing community- and workplace-based intervention studies and their failure thus far to provide definitive evidence regarding the relative contribution of the various modes, concluded that a human challenge-transmission study would be a more promising direction for future research.(Killingley et al., 2011) Influenza challenge studies in humans have been conducted to investigate disease pathogenesis and the efficacy of antivirals and vaccines. Challenge studies assessing human-to-human transmission had not been performed (Killingley et al., 2011). In 2009, we demonstrated proof-of-concept that healthy seronegative volunteers inoculated intranasally with influenza

A/Wisconsin/67/2005 (A/WI), an H3N2 virus, would develop symptoms of influenza-like illness (ILI) and, under two days of household-like conditions without environmental controls, transmit infection to other seronegative volunteers. This suggested that larger scale human challenge-transmission models might be useful to evaluate modes of transmission. A subsequent international workshop discussed these findings and the potential that human challenge-transmission studies, with appropriate interventions, monitoring of aerosol shedding, and environmental controls, could provide definitive results (Snider et al., 2010). Here, we report a large follow-on study, including design factors aimed at assessing the importance of aerosol transmission in human-to-human transmission of influenza virus.

Materials and Methods

The randomized challenge-transmission trial took place from March to June 2013 in a closed quarantine facility, was conducted with written informed consent from healthy volunteers in accordance with the principles of the Declaration of Helsinki, in full compliance with UK regulatory and ethical (IRB) requirements, and registered with ClinicalTrials.gov (number NCT01710111). Volunteers, screened for serologic susceptibility, were randomly selected for intranasal challenge with A/WI (Killingley et al., 2012) – becoming 'Donors' (D). After allowing for a short incubation period, Donors were then introduced to other sero-susceptible volunteers – 'Recipients' (R) – under controlled household-like conditions for four days. Recipients were randomised to be Intervention Recipients (IR) or Control Recipients (CR). IRs wore face shields

evaluated to interrupt large droplet transmission but to be permissive to aerosols (**SI Appendix 2.1**); in addition, IRs hand sanitised (using alcohol-based Deb® InstantFOAM, 72% ethyl alcohol) once every 15 minutes to minimise the possibility of contact transmission. IRs were only allowed to touch face via single use wooden spatulas. Thus, IRs would be exposed to influenza only via aerosols. CRs did not wear face shields or use hand sanitiser and were allowed to touch face freely; therefore, CRs would have been exposed via all routes of transmission consistent with close proximity human-human contact. An overview of the study design is shown in ***Figure 2.1***.

Influenza Virus

Influenza A/WI manufactured and processed under current good manufacturing practices (cGMP) was obtained from Baxter BioScience, (Vienna, Austria). Stocks of this virus preparation have been sequenced and its evolution in the upper respiratory track of inoculated volunteers extensively analysed (Sobel Leonard et al., 2016).

Screening

Volunteers were screened from 3-56 days in advance of the experiment to determine humoral immunity to A/WI before undergoing further screening against inclusion and exclusion criteria (**SI, Appendix 2.2**). Volunteers needed to be healthy, between the ages of 18 and 45 years, not living with anyone deemed at high risk of influenza complications on discharge, and not to have had a seasonal influenza vaccine in the last 3 years. Blood samples from volunteers were collected immediately before

quarantine entry for repeat serology, although results were not available until after the study. An initial screening haemagglutination inhibition assay (HAI) titre of ≤10 was considered evidence of susceptibility to infection.

Power calculation

We calculated, based on the reported SAR of the proof-of-concept study,(Killingley et al., 2012) (**SI, Appendix 2.2**) that over a range of scenarios the statistical power of the whole study would be between 63% and 84%, typically 80% in the most realistic scenario, if a sample size of 125 Recipients was achieved (70 IR, 55 CR). To increase the SAR from that observed in the proof-of-concept study, we opted to inoculate 4 (rather than 2) Donors per 5 Recipients and to conduct exposure events on days 1-4 (rather than 2-3) post inoculation.

Study Design and Conduct

Pre-exposure

Screened, eligible, volunteers entered a closed, quarantine unit on Day -2 and were randomised to Donor or Recipient (IR and CR) groups; thereafter Donors and Recipients were segregated. Donors and Recipients were immediately screened for a panel of 7 imported 'contaminant' respiratory viruses (influenza A, B; adenovirus; respiratory syncytial virus; parainfluenza 1, 2, 3) by a direct fluorescence antibody assay (DFA) (LIGHT DIAGNOSTICS™ SimulFluor1 Respiratory Screen, Merck Millipore) and any with a positive test were immediately discharged. On day 0 (zero) Donors were inoculated intranasally, via pipette while in a supine position, with

0.5ml per nostril of a suspension containing 5·5 $\log_{10}TCID_{50}$/ml of influenza A/WI (Zaas et al., 2013, 2009).

Exposure Events

The study was conducted in three separate identically-designed quarantine events (Q1, Q2, and Q3). From Day 1 to Day 4 of each quarantine event, all volunteers took part in an Exposure Event (EE). Individual Donors and Recipients were each allocated to a single exposure room per day where they interacted at close distances for approximately 15 hours/day, for four consecutive days. In-room staff supervised activities such as playing board games, watching films, playing pool and table football, whilst ensuring that volunteers mixed freely, and that IR volunteers complied with face shield use, hand sanitisation and no-touch-face rules. Donor, IR and CR groups were moved into different corners of the rooms for meal breaks, and Donor and Recipient groups were housed separately at night, including further separation and withdrawal of any Recipients with symptoms to prevent any contamination of the results by Recipient-Recipient secondary transmission. Five exposure rooms were used ranging from 17-30m^2 floor area and 50-87m^3 volume. Four Donors were non-randomly allocated to each exposure group to ensure even distribution of subjects actively shedding virus. This was achieved by assessing symptom scores and the results of influenza rapid tests (Quidel Sofia®) performed on Days 1 and 2. From Day 2 onwards, Donors remained in their allocated group and were not redistributed further. Once assigned to an exposure group, Recipients remained in the same group until the end of the EE or until they developed influenza-

like illness (ILI) and were withdrawn to a separate isolation area. On each day of EE, each exposure group rotated to a different exposure room.

Environmental controls

Each exposure room was assessed pre-quarantine by building and ventilation engineers and thereafter modified to achieve a ventilation rate of approximately 4L/second/person (based on planned occupancy during the study), temperature range 18-22^{o}C, and relative humidity 45-65%, to produce conditions favourable to influenza transmission,(Lowen et al., 2007) balanced against tolerability for occupants, and the capability of the building systems to provide a controlled environment comparable across all three quarantine studies. During each EE, rooms were monitored at 5-minute intervals for CO_2 concentration (as a proxy for ventilation rate), temperature and humidity; heating, cooling and humidity were then remotely adjusted to maintain optimal conditions.

Clinical assessment

All subjects underwent thrice daily monitoring of respiratory and systemic symptoms; each symptom was reported as grade 0 (not present) to 3 (severe). Paired venous blood specimens for serology were taken on Day -2 and Day 28. Nasopharyngeal swabs (NPS) were taken daily from all subjects. Respiratory specimens were analysed by quantitative reverse-transcriptase PCR (qRT-PCR) and serological specimens by HAI and microneutralisation (MN) assays. The qRT-PCR and HAI were performed in duplicate at the MRC University of Glasgow Centre for Virus Research (with Fast

Track Diagnostics qRT-PCR kit) and the U.S. Centers for Disease Control and Prevention (CDC), Atlanta; MN assays were performed by CDC as described previously.(World Health Organization, 2011)

Exhaled breath sampling

Donors were assigned to provide exhaled breath samples on two, randomly selected days within the exposure event, collected using a Gesundheit-II cone collection apparatus allowing for fractionation of particle sizes into 'fine' <5μm and 'coarse' ≥5μm aerosol samples (McDevitt et al., 2013; Milton et al., 2013). Each sample collection session lasted for 30 minutes. Breath samples were concentrated, extracted, stored at -80˚C, and evaluated by qRT-PCR using protocols and materials specified by the CDC with RNA copy number estimated as previously described (Yan et al., 2018).

Discharge

After completion of the EE, Donors were discharged on active treatment with oseltamivir (75mg b.i.d. 5 days), whereas Recipients were observed for 7 days, then discharged with oseltamivir on day 8. All volunteers attended for 28-day (+/-3 days) post virus exposure outpatient follow-up and study dismissal.

Outcome Definitions

Respiratory symptoms, defined as self-reported grade ≥1 of runny nose, stuffy nose, sneeze, sore throat, cough, or shortness of breath 'lasting ≥24 hours' (**SI, Appendix 2.2**). Fever was defined as temperature >37·9 °C.

Symptomatic was defined as evidence of any respiratory symptom lasting ≥24 hours during study days 1-6.

Influenza-like Illness (ILI) was defined as an illness >24 hours duration with: either fever and at least one respiratory symptom; or two or more symptoms of grade ≥1, one of which must have been respiratory; eligible non-respiratory symptoms were headache, muscle/joint ache, and malaise.

Laboratory confirmed infection was defined as: a 4-fold or greater rise in HAI or MN titres between Day -2 (baseline) and Day 28; or two or more positive NPS test results by qRT-PCR. These differed from the proof-of-concept study, which used seroconversion or a single positive nasal wash (**SI, Appendix 2.5**).

Comparisons were made between groups using Fisher's exact test for binomial proportions and between observed and expected outcomes using binomial tests.

Results

Participation and safety

Between January and June 2013, 496 seronegative (HAI ≤ 10) volunteers underwent study-specific screening and 166 entered the quarantine unit, of whom 127 proved suitable for final study entry. Thirty-nine subjects were discharged before inoculation or exposure per protocol as described in methods. Three separate quarantine EEs took place in March, April, and June 2013 involving Q1: 41 (20 D; 11 CR; 10 IR), Q2: 31 (12 D; 9 CR; 10 IR) and Q3: 55 (20 D; 15 CR; 20 IR) subjects respectively, with 4 Donors and 4 to 7 Recipients per exposure group. No serious adverse events were recorded in volunteers who commenced the study. Information about volunteer baseline characteristics and group randomisation is given in SI Appendices 3 and 4.

Environmental control

In Q1 relative humidity averaged 40% (Standard Deviation 9%), room temperature averaged 20·2 ºC (0·4 ºC) and CO_2 concentration averaged 1430ppm (110ppm). For Q2 and Q3, respectively, the corresponding values were 44% (4%), 21·4ºC (0·3 ºC), 1810ppm (160ppm), and 57% (4%), 21·4ºC (0·3 ºC), 1810ppm (160ppm). Outdoor CO_2 concentration proxies, taken from the average of CO_2 measurements during 2:00am-3:00am were 418, 435, and 422 ppm, for Q1, Q2, and Q3, respectively.

Donor status

Donor status is summarised by quarantine study in ***Table 2.1***. Over all quarantines combined, intranasal inoculation produced an infection rate of 81% (42/52) among inoculated volunteers. Of the 42 lab-confirmed infected Donors 25 (60%) had ILI and 10 (24%) were classified as asymptomatic (4 in Q1, 4 in Q2, and 2 in Q3).

Ten Donors had greater than anticipated immunity on admission, as identified by retrospective serology (HAI > 10 or MN ≥ 80). Four of the 10 seroconverted (i.e. had a 4-fold rise in HAI or MN titres) between admission to quarantine and follow-up. Five of the 10 met laboratory case definition by qRT-PCR including all four who seroconverted. The one additional qRT-PCR positive case had positive swabs on study days 2 and 3 in Q2.

Virus shedding by donors

Overall, 36 Donors had NPS that tested positive by PCR for A/WI. Of these 36: 53% (n=19) were positive on day 1 post-challenge; 94% (34) on day 2; 97% (35) on day 3; 86% (31) on day 4; 92% (33) on day 5; and 67% (24) on day 6 (***Figure 2.2***).

Aerosol shedding was determined for 25 Donors on day 1, 31 on day 2, 30 on day 3, and 24 on day 4, and for a total of 36 person-days in Q1, 34 person-days in Q2, and 40 person-days in Q3. Aerosol shedding from infected Donors, detected in Gesundheit-II samples, is summarised in ***Table 2.2***. Six (7%) of the coarse and 14 (16%) of the fine aerosol samples had detectable viral RNA. We observed aerosol shedding from 11 (26%) of the 42 successfully infected Donors. The geometric mean (GM) and geometric standard deviation (GSD) for coarse and fine aerosol viral RNA copy numbers per 30-min sample were 3·1E+3 (3·3) and 5·3E+3 (4·6), respectively. The maximum levels of shedding into coarse and fine aerosols were 2·79E+4 and 8·02E+4 RNA copies respectively (***Figure 2.2***).

Recipient status

Recipient status is shown in ***Table 2.3***. There were similar rates of symptomatic non-ILI and ILI in both IR and CR groups; no Recipient developed fever. One infection was confirmed by serology (HAI increased from ≤10 to 40 and MN increased from 10 to 320) in a CR subject who was symptomatic and whose symptoms met the definition of ILI, but whose qRT-PCR evaluations were persistently negative. Two other CR were transiently qRT-PCR positive but neither met laboratory criteria for PCR positivity. Both were asymptomatic and had no change from baseline serology. Thus, there was only one confirmed transmission event. The CR and IR group SARs (2·9% and 0%) were not significantly different (p = 0·47).

To compare these results with the SAR from the proof-of-concept study, we recomputed the latter results using the current more stringent outcome criteria. The adjusted proof-of-concept SAR was 8·3% giving an expected SAR of 16%. The observed SAR for the current study was not significantly different than that of the adjusted SAR from the proof-of-concept study, but was significantly lower than the expected doubling of the SAR (1·3% overall, p < 0·0001; and 2·9% for CR, p = 0·035). Comparisons of observed and expected SAR using the proof-of-concept study outcome definitions were also statistically significant (p < 0.0001, **SI Appendix 2.5**).

Discussion

To our knowledge, this is the largest human influenza challenge-transmission study undertaken to date. We applied measures to control and standardise environmental conditions and ventilation rates within and between exposure events, to emulate as far as possible indoor winter conditions when respiratory virus spread is maximal. We particularly sought to maintain low humidity conditions which have been associated with enhanced transmission (Lowen et al., 2007) and increased virus viability (Yang et al., 2012), together with a low ventilation rate to maximise recipient exposure to airborne virus. The near absence of transmission to control Recipients suggests that contact and large droplet spray did not contribute substantially to transmission under the conditions used in these EEs. The significantly lower than expected SAR in this study compared with the proof-of-concept study suggests aerosols as an important mode of influenza virus transmission in this model. The overall low SAR suggests that Donors in this model were minimally contagious and prevents definitive assessment of the modes of transmission.

Having reported an SAR of 25% (3/12) in our earlier proof-of-concept study, we expected to observe an SAR of >25%, having doubled both the duration of the exposure and the number of Donors in each quarantine (Killingley et al., 2012). Indeed, the study was designed to examine an SAR of 40% in CR versus 20% in IR which would have required 125 Recipient volunteers; this was not met (R=75) and the study was underpowered.

However, the outcome criteria used in the proof-of-concept study, which included as positive a single NPS positive by qRT-PCR without seroconversion, were made more stringent in the present study by requiring two or more NPS positive by qRT-PCR in the absence of seroconversion (**SI Appendix 2.5**). Applying the proof-of-concept criteria to the current study gives an SAR of 4% (3/75) overall, while applying the stricter criteria used in this study to the proof-of-concept study gives an SAR of 8·3% (1/12) rather than 25%. Given the lower than planned enrolment and the stricter outcome criteria, this study was doubly underpowered.

The SAR reported here were well below expectations and were significantly lower than the expected SAR based on design changes developed to at least double the SAR. These observations raise two questions: 1) Why were SARs, using stringent criteria, low in both studies and what are the implications for future human challenge-transmission studies? 2) Why was the SAR significantly lower in the present study compared with the expected doubling of the rate observed for the proof-of-concept?

The low SAR in these studies suggests that, unless a much greater SAR can be achieved, type II error associated with underpowering will be a major obstacle to successful use of human challenge-transmission studies. Potential areas to consider addressing in order to raise the SARs in future studies include the virus used, the route of inoculation, susceptibility of the human volunteers, the rate of viral shedding into NPS and aerosols, and reducing ventilation of exposure rooms.

In the proof-of-concept (2009) and follow-on (2013) studies we used a GMP A/WI challenge virus manufactured by Baxter BioScience (Vienna, Austria). Both studies produced similar clinical and serological infection rates (typically 60-70% and 70-75%, respectively) after inoculation via nasal instillation, and similar spectrums of clinical illness severity in Donors. The illnesses we observed were similar to the range seen in healthy adults in the community, from asymptomatic to febrile symptomatic infection (Hayward et al., 2014). Thus, skewed illness severity does not seem to explain the low SAR.

The virus preparation used in this study has been used in other human challenge studies with similar rates of infection via nasal instillation (Sobel Leonard et al., 2016). Using deep sequencing, Sobel Leonard and colleagues showed that a sample of the Baxter stock "was at least partially adapted" to the egg and/or tissue environments in which it was produced (Sobel Leonard et al., 2016). They also found that nasal instillation of the stock into human volunteers resulted in rapid purification selection, although a fixed variant in the HA gene remained. We have performed a BLAST search and identified the fixed variant (G70A/D8N) in deposited sequences of wild-type H3N2 viruses. This suggests that, on its own, the fixed HA variant is unlikely to have been a key alteration. These results suggest that it is unlikely that the virus stock was the primary cause of the low SARs. But, the impact of positive selection of the challenge virus for growth in the production environment, rather than for human transmissibility, remains a potential contributing factor to consider in choosing challenge viruses for future transmission studies.

The route of infection with influenza virus is known to matter in the setting of experimental infection, with aerosolized virus infectious at lower doses and more likely to result in 'typical influenza-like disease' (fever plus cough) than intranasal inoculation (Alford et al., 1966; Henle et al., 1946). This anisotropic property (Milton, 2012) of influenza virus is not unique among respiratory viruses; e.g. it is exploited by the live, unattenuated adenovirus vaccine (Couch et al., 1963). The implication for human challenge-transmission studies, however, may be that increased rates of lower respiratory tract infection via aerosol inoculation might be required to achieve sufficiently high rates of donors with fever, cough, and contagiousness to achieve a useful SAR.

In the current quarantine-based human challenge-transmission model, consistent with historical precedent, screening for susceptibility was undertaken primarily by HAI antibody screening, although it is recognised that screening by MN titre or other assays (Park et al., 2018; Tang, 2012) could be an alternative or adjunctive approach. However, the exact correlates of immunity and severity using novel immunological assays have not been validated and selecting subjects based on these assays would have added substantial complexity and costs. Six Donors and five Recipients in the present study were discovered, in retrospect, to have seroconverted during the 3 to 56-day interval prior to entering the quarantine facility, despite having as short a delay as possible between final screening for HAI and quarantine entry. However, the majority of Donors and Recipients were susceptible according to the results of

microneutralization tests. Prior immunity, as measured by the HAI and MN assays, does not therefore, appear to have been a major limitation nor account for failure to transmit from readily infected Donors to identically screened Recipients. Regarding future studies, however, as novel immune correlates of influenza protection and severity become established, additional approaches beyond HAI and MN assays could be employed for volunteer selection. This might enable selection of those likely to become infected, febrile, and have greater symptomatology including more frequent and greater levels of cough and runny nose. Unfortunately, such screening might also dramatically reduce the yield of suitable volunteers and substantially increase overall study costs.

Results from serial nasopharyngeal swabs in Donors indicate that over 80% were positive by qRT-PCR testing on one or more post-challenge days. Thus, failure to shed virus into nasal secretions cannot explain the low SARs. The results from breath sampling with the Gesundheit-II device indicate that 26% (11/42) of infected Donors had virus detectable in exhaled air during the same period. By comparison, virus shedding into exhaled breath was detected in 84% (119 of 142) of symptomatically presenting influenza cases sampled on one to three days post onset of symptoms, mostly recruited from young adults on a college campus (Yan et al., 2018). When compared on a per-sample basis, infected Donors shed detectable virus less frequently than naturally infected college campus cases (Yan et al., 2018) in both coarse (7% and 40%, respectively) and fine aerosols (15% and 76%); all assays for both groups were performed in the same laboratory using the same methods. However, when the

comparison was limited to positive aerosol samples from each study population, the average quantities of virus detected were similar (within 1 log), for the Donors as for the college community cases (GM coarse 3·1E+3 and 1·2E+4, GM fine 5·3E+3 and 3·8E+4, respectively). The maximum exhaled breath viral aerosol from the 11 Donors was two to four logs lower than from the college campus cases (maximum coarse 2·8E+4 and 4·3E+8, and maximum fine 8·0E+4 and 4·4E+7, respectively) (Yan et al., 2018). While this difference may merely represent the low probability of sampling from the tail of a log-normal distribution with only 11, as compared with 119 cases, it may be relevant to the low SAR in the challenge-transmission model if aerosols disseminated by rare supershedders account for most transmission. If aerosols are largely derived from the lower respiratory tract, as has been suggested by analysis of the college community cases, this would also suggest that future challenge-transmission studies should employ methods designed to increase the frequency of lower respiratory tract infection.

The proof-of-concept study was conducted in a hotel room with closed windows and thermal control provided only by a recirculating air conditioning unit. While the ventilation rate was not measured, it was likely to have been extremely low for the number of occupants, with only a small, intermittent, bathroom extract and natural building infiltration providing fresh air. The ventilation rate of 4 l/s/person during the main study was low compared to 10 l/s/person recommended in UK design standards (Chartered Institution of Building Services Engineers, 2015) but was likely substantially greater than in the proof-of-concept study. This would have produced

significantly higher viral aerosol concentrations during the proof-of-concept EEs, assuming similar generation rates from Donors in both experiments. Given that the Donors in the two studies were similar in other respects, differences in shedding rates seem unlikely. Therefore, the difference in SAR between this study and the expected SAR based on design changes and prior results are possibly due to differing ventilation conditions. The implication for future challenge-transmission studies, given that the ventilation rate in the current study was as low as possible with a single pass ventilation system, is that recirculating air conditioning systems similar to that in the proof-of-concept study should be employed to limit dilution ventilation and maximize exposure to aerosols. This will be especially important if Donors in future studies continue to represent the lower end of the aerosol shedding spectrum seen in naturally infected cases.

Achieving temperature and humidity to simulate winter conditions was challenging, particularly in Q3, conducted in June 2013 when the average external conditions were 16^{o}C and 64% relative humidity. It was necessary to strike a balance between volunteer comfort and conditions favourable to transmission, both of which were constrained by the capability of the mechanical systems in the building. However, the relative humidity in the current study overlapped with that during the proof-of-concept study, which ranged between 38 and 53%, and thus, eliminated humidity as a potential explanation for the difference in transmission rates.

Despite this study not having produced the planned SAR, it yields important findings. First, although fewer viral challenged subjects had virus-laden aerosols than seen in people with natural infections presenting with influenza-like symptoms, those volunteers who did produce viral aerosols did so at a rate similar to the average symptomatic naturally infected case. Second, given that a subset of the infected volunteers had moderate viral aerosol shedding in this model, observation of transmission via aerosols in quarantine studies may be strongly dependent on the dilution ventilation rate. Third, low risk of transmission to Control Recipients suggests that contact and large droplet spray transmission were not important modes of transmission in this model. The overall low SAR compared to that observed in the proof-of-concept study suggests that, given the main difference between the studies was the indoor air ventilation rate, aerosol transmission may be an important mode of influenza virus transmission between adults. Finally, sensitivity of transmission to details of the Donors selected, environment, and activity during exposure events, suggest that if a successful transmission model can be developed, carefully designed studies may be useful for investigating specific, targeted intervention strategies for prevention of specific transmission modalities. However, sensitivity to experimental conditions also demonstrates that it will be challenging to generalise the results of the quarantine-based transmission model to broad conclusions about the relative importance of aerosol, droplet spray, and contact modes of transmission. These complexities of the challenge-transmission model suggest that community-based transmission studies employing deep-sequencing based molecular epidemiologic methods in natural experiments, e.g. comparing high and low ventilation dormitories

or barracks, may be more attractive alternatives than previously thought. Unfortunately, although an important role for aerosols in transmission of influenza, at least between adults, is hinted at when comparing the proof-of-concept and current studies, this challenge model cannot provide a definitive answer to the importance of this mode for influenza virus transmission between humans.

Tables

Table 2.1. Infected Donor Status

		Clinical Illness N (% of Infected)			Laboratory Confirmed Infection Criteria[4] N (% of Infected)		
Quarantine #	**Infected/Inoculated N/N (%)**	**Symptomatic[5]**	**Febrile[6]**	**ILI[7]**	**PCR Confirmed Infection**	**PCR Confirmed Infection and Seroconversion**	**Seroconversion by HAI : MN : Either**
1[1]	15/20 (75)	11 (73)	4 (27)	8 (53)	12 (80)	11 (73)	12 : 14 : 14
2[2]	11/12 (92)	7 (64)	0 (0)	5 (45)	10 (91)	8 (73)	9 : 7 : 9
3[3]	16/20 (80)	14 (88)	2 (12)	12 (75)	14 (88)	12 (75)	14 : 11 : 14
Total	42/52 (81)	32 (76)	6 (14)	25 (60)	36 (86)	31 (74)	35 : 32 : 37

1 Via retrospective serology, on admission to quarantine four donors were found to have greater than anticipated immunity: three by HAI (>10), one of which seroconverted, and one by MN (≥80, and this donor also seroconverted).

2 Via retrospective serology, on admission to quarantine two donors were found to have greater than anticipated immunity: one by MN and one by both HAI and MN. Neither of these donors seroconverted.

3 Via retrospective serology, on admission to quarantine four donors were found to have greater than anticipated immunity prior to inoculation: two by HAI, one of which seroconverted; one by MN, and one by both HAI and MN, and this donor seroconverted.

4 Laboratory confirmed infection was defined by evidence of acute infection based on: Seroconversion (four-fold or greater rise in either HAI or MN titres between the day -2 and day 28 serum specimens), and/or PCR confirmed infection (two or more positive NPS test results by qRT-PCR).

5 Symptomatic was defined as evidence of any respiratory symptom lasting ≥24 hours during study days 1-6, where "respiratory symptom" means self-reported grade ≥1 of runny nose, stuffy nose, sneeze, sore throat, cough, or shortness of breath, and where "lasting ≥24 hours" means evidence of a respiratory symptom during 3/3 symptom observations within a single day, or evidence of a respiratory symptom over two consecutive days at any frequency (i.e., occurring ≥1 out of three symptom observations on two consecutive days).

6 All febrile cases met criteria for symptomatic.

7 Influenza-like illness (ILI) was defined as an illness lasting ≥24 hours, during study days 1-6, with either: fever >37·9°C plus at least 1 respiratory symptom of grade ≥1, or ≥2 symptoms of grade ≥1, at least one of which must be a respiratory symptom, where "respiratory symptom" and "lasting ≥24 hours" are as defined above and where the possible non-respiratory symptoms include headache, muscle/joint ache, and malaise.

Table 2.2. Exhaled Breath Viral RNA Detection and Copy Number Among Infected Donors by Quarantine Event and Aerosol Fraction

			Coarse Aerosol (>5µm)			Fine Aerosol (≤5µm)		
Quarantine #	**N Subjects**	**N Samples**	**Positive Subjects (%)**	**Positive Samples (%)**	**Mean of Positive Samples***	**Positive Subjects (%)**	**Positive Samples (%)**	**Mean of Positive Samples***
1	15	27	1 (7)	1 (4)	2.79e+04	3 (20)	5 (19)	3.32e+04
2	11	30	3 (27)	3 (10)	2.16e+03	3 (27)	4 (13)	1.80e+04
3	16	32	2 (12)	2 (6)	1.73e+03	5 (31)	5 (16)	1.70e+03
Total	42	89	6 (14)	6 (7)	6.31e+03	11 (26)	14 (16)	1.76e+04

* The arithmetic mean RNA copy number used data from positive samples only. The geometric means (GM) and geometric standard deviations (GSD) over all positive samples were 3·14E+3 (3·33) and 5·31E+3 (4·59) for coarse and fine aerosol samples, respectively

Table 2.3. Recipient Status

			Clinical Illness (% of Exposed)			Laboratory Confirmed Infection Criteria[4] (% of Exposed)		
Quarantine #	**Recipient Classification**	**Infected/ Exposed (%)**	**Symptomatic[5]**	**Febrile**	**ILI[6]**	**PCR Confirmed Infection**	**PCR Confirmed Infection and Seroconversion**	**Seroconversion by HAI : MN : Either**
1[1]	Control (CR)	0/11 (0)	4 (36)	0 (0)	3 (27)	0 (0)	0 (0)	0 : 0 : 0
	Intervention (IR)	0/10 (0)	2 (20)	0 (0)	1 (10)	0 0	0 (0)	0 : 0 : 0
2[2]	Control (CR)	1/9 (11)	2 (22)	0 (0)	2 (22)	0 (0)	0 (0)	1 : 1 : 1
	Intervention (IR)	0/10 (0)	3 (30)	0 (0)	2 (20)	0 0	0 (0)	0 : 0 : 0
3[3]	Control (CR)	0/15 (0)	6 (40)	0 (0)	4 (27)	0 (0)	0 (0)	0 : 0 : 0
	Intervention (IR)	0/20 (0)	6 (30)	0 (0)	2 (10)	0 0	0 (0)	0 : 0 : 0
Total	**Control (CR)**	**1/35 (3)**	**12 (34)**	**0 (0)**	**9 (26)**	**0 (0)**	**0 (0)**	**1 : 1 : 1**
	Intervention (IR)	**0/40 (0)**	**11 (28)**	**0 (0)**	**5 (12)**	**0 0**	**0 (0)**	**0 : 0 : 0**

1 Via retrospective serology one of 11 CR were found to have greater than anticipated immunity prior to inoculation by HAI, and two of 11 CR were found to have greater than anticipated immunity prior to inoculation by MN. None of these CR seroconverted. One of 10 IR were found to have greater than anticipated immunity prior to inoculation by HAI, and two of 10 IR were found to have greater than anticipated immunity prior to inoculation by MN. None of these IR seroconverted.

2 Via retrospective serology none of the nine CR were found to have greater than anticipated immunity prior to inoculation. None of the 10 IR were found to have greater than anticipated immunity prior to inoculation.

3 Via retrospective serology one of 15 CR were found to have greater than anticipated immunity prior to inoculation by HAI, and two of 11 CR were found to have greater than anticipated immunity prior to inoculation by MN. None of these CR seroconverted. Two of 20 IR were found to have greater than anticipated immunity prior to inoculation by MN. Neither of these IR seroconverted.

4 Laboratory confirmed infection was defined as described in ***Table 2.1*** and methods.

5 Symptomatic was defined as defined in ***Table 2.1*** and methods.

6 Influenza-like illness (ILI) was defined as described in ***Table 2.1*** and methods.

Figures

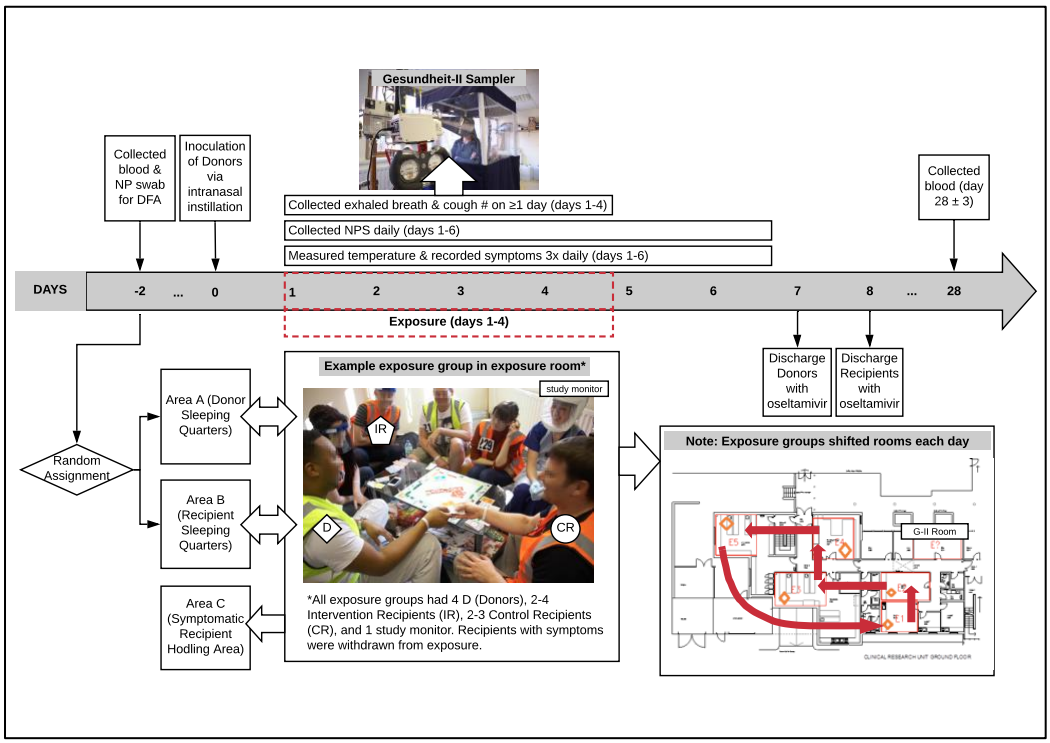

Figure 2.1. Schematic showing study timelines, physical segregation arrangements and volunteer movements during quarantine study.

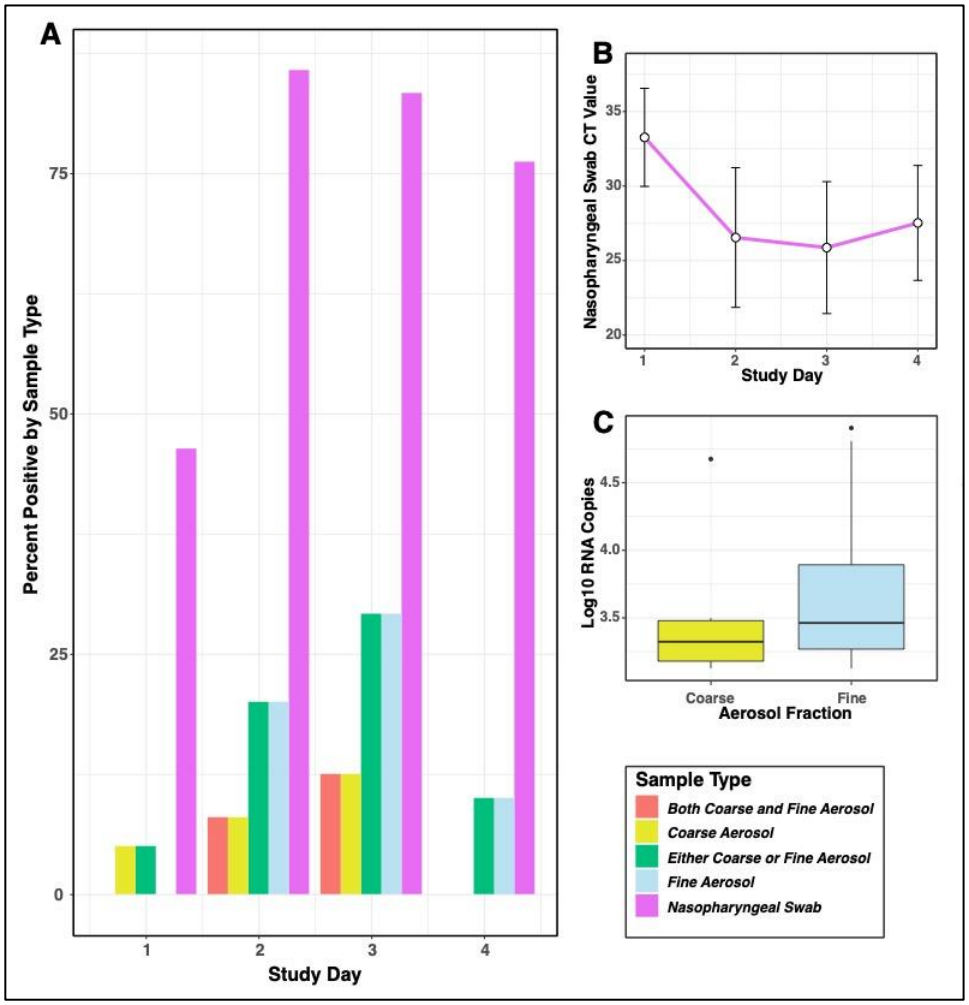

Figure 2.2. Viral detection in donors by day of exposure event. A) Columns show the proportion of all 42 infected donors who were positive for viral shedding as determined by qRT-PCR for coarse (>5μm) and fine (≤ 5μm) aerosols, and nasopharyngeal swabs. B) Mean and standard deviation error bars for qRT-PCR cycle threshold values from the positive nasopharyngeal swabs. C) Virus quantified from exhaled coarse and fine breath aerosols by qRT-PCR; the boxes show the inner-quartile range (IQR) with a band to indicate the median, and whiskers extending to highest and lowest data points within 1.5 IQR.

CHAPTER III

COMPARISON OF INFLUENZA A VIRAL SHEDDING IN EXHALED BREATH AEROSOLS FROM EXPERIMENTALLY INFECTED VOLUNTEERS AND NATURALLY INFECTED COMMUNITY CASES

Abstract

It has long been known that nasal inoculation with influenza A virus tends to produce mild infections. Whether these infections are similar to mild natural infection and may be useful for studying human-to-human transmission remains an open question. We compared the influenza A viral aerosol shedding from volunteers nasally inoculated with A/Wisconsin/2005 (H3N2) and adults naturally infected with influenza A H3 recruited from a college community during 2012-13, selected for influenza-like illness with objectively measured fever or a positive Quidel QuickVue A&B test. Propensity scores were used to control for differences in symptom presentation observed between experimentally and naturally infected groups. Among 39 experimentally infected influenza H3 cases with qRT-PCR positive nasopharyngeal swabs, symptom scores peaked on day 3 post nasal inoculation; Among 83 naturally infected influenza H3 cases, symptom scores were maximal on the first day post-onset of symptoms. On the day of peak aerosol shedding, median symptom scores for experimental infection were upper respiratory 4 (IQR 2, 5), lower respiratory 0 (0, 1), systemic 1 (0, 2), cough 0 (0, 1), and cough count 0 (0, 6) and for natural infections 7 (5, 9), 3 (2, 4), 6 (4, 8), 2 (2, 3), and 22 (8, 40) respectively.

Twenty-eight percent of experimental and 86% of natural cases shed into fine particle aerosols ($p<0.001$). The geometric means (geometric standard deviation) of positive fine aerosol samples for experimental and natural cases were 5.1E+3 (4.72) and 3.9E+4 (15.12), respectively. To compare the fine aerosol shedders (11 experimental, 71 naturally infected) on their peak day of shedding, accounting for differences in illness severity, we computed 14 sets of propensity scores based on various combinations of symptom scores (upper, lower, systemic, total, cough), cough count during aerosol sampling, fever (> 37.9ºC), temperature, nasopharyngeal swab Ct value. Using each set of propensity scores for matching, stratification, and inverse weighting, demonstrated the almost complete lack of overlap between groups (standardized group difference 86% in best model) such that a propensity score adjusted shedding comparison could not be performed.

Introduction

There is uncertainty about the extent to which mucosal contact versus expiratory droplets contribute to influenza virus infection risk between humans. Studies that challenged humans by nasal instillation of virus, and others that challenged with aerosolized virus suggest that upper respiratory mucosal exposure, as opposed to airborne exposure results in more mild, afebrile illnesses (Alford et al., 1966; Little et al., 1979; Henle et al., 1946). Anisotropic infection is defined by Milton as infection whereby transmission mode influences illness presentation (Milton, 2012), has been used to characterize human influenza (Tellier et al., 2019). To minimize health risk associated with experimental human influenza infection, recent human challenge

models have adopted viral inoculation by nasal instillation (Killingley et al., 2011). Temporal associations between symptomatology and nasal and throat mucosal viral load following symptom onset have been reported among volunteers receiving intranasal influenza virus challenge and secondary household cases in Hong Kong (Carrat et al., 2008; Ip et al., 2016; Lau et al., 2010). Other analyses of the Hong Kong household transmission data did not observe temporal associations between symptom severity and upper respiratory viral load (Lau et al., 2013), and observed upper respiratory mucosal viral loads (Tsang et al., 2016, 2015) or respiratory symptoms (Wardell et al., 2017) to be poorly predictive of transmission to household secondary cases, suggesting that other biomarkers of contagion such as exhaled breath aerosols should be explored. The current study compares fine aerosol shedding between influenza A/H3 nasally inoculated and naturally infected cases to test whether experimentally nasally infected have similar risk and rate of fine aerosol shedding compared with mild, natural cases infected by any mode. Selection bias was introduced by sampling from symptomatic naturally infected cases with a positive QuickVue rapid test or febrile illness >37.8C plus cough or sore throat, whereas the true symptomatology profile for all naturally-acquired infections is likely to include a range of illness including many asymptomatic infections (Hayward et al., 2014). Propensity scores were used in an attempt to reduce the impact of this selection bias and isolate the mode of infection as the main difference between the experimental and naturally infected populations.

Methods

Study design and data collection

Study design and data collection procedures for the EMIT human-transmission trial and the observational study of naturally infected influenza cases University of Maryland campus community of are described in Nguyen-Van-Tam et al., 2019 and Yan et al., 2018, respectively. Relevant to current analyses, viral shedding was measured from nasopharyngeal (NP) swabs taken daily during the four days of quarantine exposure (days 1-4 post inoculation of experimental, nasally inoculated cases, or viral 'Donors') and on up to three days post-symptom onset for the naturally infected. Each experimental case provided half-hour exhaled breath specimens into a Gesundheit-II bioaerosol sampler (G-II) (McDevitt et al., 2013) on two to four days within four days of nasal inoculation. The G-II collects exhaled breath aerosols in fine (≤5μm) and coarse (>5μm) fractions. Among the naturally infected, participants who met case definition for influenza (either positive QuickVue rapid test, or oral temperature >37.8 C plus cough or sore throat) and presented within the first three days of symptom onset, were invited to provide G-II exhaled breath specimens for up to three consecutive days. Exhaled breath from both studies were evaluated using the standard CDC qRT-PCR primers and probes at the University of Maryland laboratory. Nasopharyngeal swabs from experimental and natural case were evaluated by qRT-PCR in separate labs using the same reagents. Assays were not tested against

a plasmid standard for experimental cases, thus limiting comparison of swabs to the cycle threshold (Ct) values.

Symptom scores were measured three times per day for experimental cases and once per day for natural cases during a research clinic visit where exhaled breath was collected. In the analysis, as opposed to averaging multiple symptom score measurements per day for experimentally infected cases, scores taken closest in time to exhaled breath collection were selected for analysis. Upper respiratory score was sum of runny nose, stuffy nose, sneezing, sore throat, earache symptom scores (range 0-15). Lower respiratory score was the sum of shortness of breath, and cough scores (range 0-6). Systemic symptom score was the sum of malaise, headache, muscle/join ache scores (range 0-9). Observed cough counts were recorded during breath collection. Experimental cases were defined as those with a qRT-PCR-positive a nasopharyngeal swab test on at least two of six follow-up days, or on one day plus serological evidence of infection. Natural cases were defined as those who met case criteria and had a single, qRT-PCR-positive nasopharyngeal swab on the day of enrollment.

Statistical Analysis

Tobit regression was used impute fine aerosol RNA copy number for qRT-PCR replicates below detection limit where one or more replicates for a sample had detectable RNA. Imputation of RNA copies was not done for samples without any replicates above detection limit, as done in Yan et al., 2018. It was more reasonable to

impute, as done by Yan and colleagues, all aerosol replicates below detection limit because there were a minority of fine aerosol samples below detection limit (14%). It is less reasonable to do the same for the experimentally infected population where 72% of the observations would be imputed. In the current analysis exhaled breath samples were run in duplicate except for a few instances where assays were repeated in which case there were more than two replicates per sample. Here, Tobit regression to impute non-detectable replicates was performed only for positive samples (i.e., samples with qRT-PCR detectable RNA in at ≥1 replicate) for both experimentally and naturally infected cases, to maximize comparability. When performed, the Tobit regression predicted RNA copy numbers for all replicates in positive samples with ≥1 nondetectable replicates was used. For both experimentally and naturally infected populations, Tobit models consisted of fixed effects of cough and study day with random effect of person. Fixed effects for these models were selected based on a priori evidence of an association with fine aerosol shedding (Yan et al., 2018).

Cough count was imputed for 5/84 missing observations for experimental and 3/146 for the natural cases. For the experimental case group, a linear mixed effect model with fixed effects of cough symptom score, study day, and sex, with a random effect of subject was used to predict cough count. Given that the unstandardized residuals were all within plus or minus 5 coughs (with 3 instances between 5 and 10 coughs), the model was accepted and used to impute the 5 missing cough counts in the experimental case group. To impute missing cough counts in the naturally infected group, we first used Tobit regression with fixed effect of study day and random effect

of person to estimate fine aerosol shedding values for each of the 146 observations. Next, to estimate a cough count for each of the three missing cough observations we used a linear mixed effect model with fixed effects of cough, estimated fine aerosols shedding, sex, age, BMI, and day post-symptom onset.

The naturally infected cases used in this analysis were sampled from a symptomatic population and selected on the basis of positive QuickVue rapid test or febrile illness >37.8C plus cough or sore throat. On the other hand, experimentally infected cases were not selected on the basis of their symptoms, but rather on RT-PCR evaluation of their nasopharyngeal swab viral loads. This approach may result in a symptom distribution more representative of that of the overall population of influenza infections, which include a range in illness severity including many asymptomatic infections (Hayward et al., 2014). Thus, we expected differences in study design to introduce imbalance in symptom severity between groups. If symptoms are associated with aerosol shedding in an unselected population, then this would be an important variable to control for with the goal of assessing the mode of infection on shedding. To minimise the effect of this bias, we attempted to balance covariate distributions between populations with propensity score models. We evaluated model specifications by the standardized differences and variance ratios between comparison groups for each covariate, after adjustment by propensity score matching, stratification, and inverse probability weighting.

Data were cleaned and analyzed in R (v3.5.1 R Development Core Team, Vienna, Austria) and SAS Studio (Release 3.7 (Enterprise Edition), v9.4M6, Cary, NC). Unadjusted effects on risk and rate of fine aerosol shedding were estimated for symptom scores, observed cough count, age, and sex. Analysis of shedding risk used all exhaled breath observations. Analysis of shedding quantity was refined to the maximum shedding day for each aerosol shedder. All analysis scripts and readme files required to reproduce analyses are maintained on GitLab and are available upon request.

Results

For 39 experimental and 83 naturally infected influenza A H3 cases, there were 84 and 146 exhaled breath collection instances respectively. Of the 39 confirmed experimental cases, 36 were qRT-PCR positive two or more days, 31 of whom also had serological evidence of infection; three were qRT-PCR positive on one day only and also had serological evidence of infection. There were three, other, inoculated challenge study volunteers with serological evidence of infection but never a qRT-PCR positive result. None of these shed virus at detectable levels into aerosols. A total of 52 challenge study volunteers were inoculated, giving an infection rate under the current criteria of 75%. The naturally infected influenza A H3 case population was drawn from a broader group of cases with various influenza subtypes including influenza B, Pandemic H1, and dual infections, is described in Yan et al., 2018 and ***Appendix 3.1***.

Cough count data was missing in five (6.0%) of the 84 exhaled breath collection instances for experimental cases and three (2.1%) of the 146 instances for the natural cases and missing values were imputed. Both study populations of young adults were generally healthy. The experimental group were on average 10 years of age older than the naturally infected group however the naturally infected group had a wider range of ages. The experimental cases were more likely to be male while naturally infected cases were balanced by sex (***Table 3.1***). Experimental cases were asymptomatic (12.8%) or had illness mostly characterized by mild, upper respiratory symptoms. There were small peaks in upper respiratory, lower respiratory, systemic, and cough scores, and cough counts on day 3 post inoculation. Naturally infected cases had much more severe symptoms scores and greater cough counts, with symptom scores peaking on day 1 post symptom onset and observed cough count during exhaled breath collection peaking on day 2 post symptom onset. Given the respective peaks in symptom severity, the day 3 post inoculation best aligned with day 1 post symptom onset (***Figure 3.1***). For all days combined, mean symptom scores and cough counts are substantially higher in natural compared with experimental infections (***Table 3.1***). Using the repeated symptom measures taken at all exhaled breath visits in both groups (84 experimental, 146 natural), scaled, density plots of upper respiratory symptoms and observed cough count showed the greatest similarity between the two populations with a substantial offset (***Figure S3.1***).

The risk of shedding virus into coarse and fine aerosols for experimentally infected was 6/39 (15%) and 11/39 (28%), and for naturally infected 45/83 (54%) and 71/83 (86%) respectively (***Table 3.2***). These differences in proportions for coarse and fine shedding between experimental and natural groups were significant with $p<0.001$. Shedding quantity by geometric mean and percentile is displayed in ***Table 3.2***. Median coarse and fine aerosol shedding quantity between the groups was significantly higher for natural cases (coarse $p<0.001$; fine $p<0.001$). This finding remained significant after restricting Wilcoxon rank sum comparisons to positive samples (coarse $p=0.032$; fine $p<0.003$). Geometric mean (GM) (geometric standard deviation, GSD) for coarse and fine aerosols was 2.7E+3 (3.26) and 5.1E+3 (4.72) for experimental cases, and 1.8E+4 (13.9) and 3.9E+4 (15.12) for natural cases. Peak aerosol shedding was observed on day 3 post inoculation and day 1 post symptom onset for experimental and natural cases, respectively. ***Figure 3.2*** aligns the two populations on these peak shedding days. Peak aerosol shedding days matched those of peak symptom scores (***Figure 3.1***). Elevated shedding risk and rate for naturally compared to experimentally infected cases is shown in ***Figure S3.2***. On the day of peak aerosol shedding, median symptom scores for experimental infection were upper respiratory 4 (IQR 2, 5), lower respiratory 0 (0, 1), systemic 1 (0, 2), cough 0 (0, 1), and cough count 0 (0, 6) and for natural infections 7 (5, 9), 3 (2, 4), 6 (4, 8), 2 (2, 3), and 22 (8, 40) respectively.

When using all of the detectable qRT-PCR nasopharyngeal swab samples from days 1-6 post inoculation (N=179) and 1-3 post symptom onset (N=143), nasopharyngeal

swab Ct values were notably lower for naturally compared with experimentally infected cases (***Figure S3.3***). We aligned peak (lowest) Ct values temporally: day-1 post symptom onset in naturally infected cases with day-3 post inoculation; differences in Ct values increased after this alignment day.

To improve comparability between groups, we selected maximum aerosol shedding day observations for each volunteer and naturally infected case. Comparisons between shedding restricted to day 3 post inoculation against day 1 post symptom onset would have resulted in substantial loss of data since there was not always an exhaled breath sample collected on day 3 post inoculation. Restricted to maximum shedding observations for fine and coarse shedding, the GM (GSD) for coarse and fine aerosols was 2.7E+3 (3.26) and 5.0E+3 (5.83) for experimentally, and 2.1E+4 (16.47) and 5.1E+4 (17.04) for naturally infected cases. ***Figure S3.4*** shows shedding frequency and strength from maximum shedding instances for each group.

Predictors of shedding risk and rate were restricted to maximum observed fine aerosol samples per study subject since the number of positive coarse samples was small. ***Table 3.3*** provides the mean and standard deviation for continuous covariates, with frequencies and proportions for categorical variables, for all covariates for the maximum fine shedding observations in experimental and natural cases. Symptom scores and cough counts were all much higher for naturally compared with experimentally infected cases. Upper respiratory symptoms score distributions overlapped the most between groups, while differences in the distributions of lower

respiratory, systemic, and cough symptoms scores, and cough count were more pronounced (***Figure 3.3***).

Crude analysis of maximum observed fine aerosol shedding quantity with each covariate as the sole effect variable in the absence of covariate adjustment showed that only febrile status (>37.9ºC) and body temperature were statistically significant predictors when experimentally and naturally infected cases were combined (***Table 3.4*)**. Compared with afebrile cases, febrile cases shed 3.66E+6 (95% CI 3.8E+5 – 6.9E+6) more viral RNA copies into fine aerosols. For a single degree Celsius increase in body temperature, cases shed 2.1E+6 (95%CI 1.6E+5, 4.0E+6) more viral RNA copies per half hour sample. There were no significant predictors of shedding rate among experimental cases alone and among natural cases, only febrile status (>37.9ºC) was significantly associated with viral shedding with febrile cases shedding 4.5E+6 (95% CI 7.1E+5 - 8.3E+6) RNA copies. Confidence bounds were wide for all effects. Of the experimentally infected, only males shed virus into aerosols.

We also performed univariate analysis of fine aerosol shedding risk using data from all 84 and 146 exhaled breath collection visits from experimentally and naturally infected cases and controlling for random effect (***Table S3.1***). For the experimental cases, with the exception of systemic symptom score and body temperature all symptom-related covariates were significantly associated with fine aerosol shedding risk. For naturally infected cases, lower respiratory symptom, cough symptom, and cough count were significantly associated with fine aerosol shedding risk. For

experimental and naturally infected cases, respectively, the odds (95% CI) of shedding into fine aerosols were 6.49 (1.14 – 37.09) and 1.35 (1.04 – 1.76) higher for a single unit increase in lower respiratory score, 7.49 (1.28 – 43.91) and 1.9 (1.2 – 2.99) for a unit increase in cough score, and 1.29 (1.02 – 1.62) and 1.02 (1.00 – 1.04) for a single unit increase in observed cough count. Nasopharyngeal swab qRT-PCR cycle threshold (ct) value had a negative effect on shedding risk, as expected, and this effect was significant in experimental and combined cases. Although ct values in the experimental group were not standardized to an influenza A plasmid, as was done in analysis of naturally infected cases, lower ct values for a specific amplicon within qRT-PCR assays indicate higher RNA copy number.

Propensity score models were used in an attempt to balance symptom and demographic covariates in order to reduce bias introduced by the selection of influenza cases in the experimental and naturally infected studies. We tested 14 propensity model specifications based on various combinations of symptom scores (upper, lower, systemic, total, cough), cough count during aerosol sampling, fever (>37.9ºC), temperature, nasopharyngeal swab Ct value. Model specifications were guided by the strength and statistical significance of univariate analyses (***Table 3.4, Table S3.1***). All covariates that were significantly associated with risk or strength of shedding for experimental, naturally infected, or combined groups were included. Additional covariates that had strong effects, on shedding risk or strength, yet were not significant at p = 0.05 level, were added to models. Each propensity score model provided a set of propensity scores (i.e., probability of membership in the naturally

versus the experimentally infected group) as well as a set of corresponding, linearized propensity scores. These propensity scores were then used to adjust the experimental and natural cases to improve overlap of all symptom and demographic covariates in an attempt to achieve population balance closer to randomization. We tried matching on the propensity score, stratifying the propensity score by sextiles, quintiles, quartiles, and tertiles, and inverse probability weighting by average treatment effect for the treated (ATT), and average treatment effect (ATE) where the naturally infected group was considered the "treatment" group (***Table S3.2***).

Propensity score model 13 (covariates: fever, body temperature, and upper respiratory symptom score) and adjustment by inverse probability weighting for ATE minimized the standardized differences between the populations with a mean absolute value standardized difference of 86. After inverse probability weighting adjustment with model 13, balance improved for some covariates, however not to the point where they could be considered similar (***Table 3.5***). Although it is recommended (citation) that absolute standardized differences for covariates be close to zero and no greater that 10% between comparison groups, and that variance ratios be close to one (perhaps between 0.5 and 2), this optimized model with weighted adjustment had a wide range (provide range) of absolute value standardized difference beyond 10% and variance ratios of up to 29.06 (***Figure 3.4***). The substantial differences between covariate distributions did not support the use of propensity score adjusted approaches for making comparisons between these populations. ***Appendix 3.3*** includes further discussion of the propensity score approach used here.

Discussion

We compared aerosol shedding in influenza A cases infected naturally and by nasal instillation under experimental conditions. A minority of experimental cases shed virus into aerosols (28%) and all who shed into fine aerosols also shed into coarse aerosols. Although a far greater proportion of the naturally infected study population shed into fine aerosols (86%, unadjusted p-value <0.001), it is uncertain to what extent this is reflective of all naturally-acquired infections. Among the experimentally infected who did shed, the fine aerosol RNA copy GM was within a $\log_{10}$ of that for naturally infected cases (***Table 3.2***), which may not be meaningfully different (despite parametric test type-I error rate below 0.001). A more substantial difference in fine aerosol shedding rate was observed at the level of the overall distribution, with naturally infected cases more likely to shed at the highest observed levels and Wilcoxon Rank Sum test indicating very low chance of median overlap (p <10E-13). Compared with naturally infected cases at the 95^{th} percentile of fine aerosol shedding, experimentally infected cases shed about 3 $\log_{10}$ fewer RNA copies. RNA copies shed into aerosols peaked on day 3 post nasal inoculation aligns with peak shedding on day 1 post symptom onset in naturally infected cases (***Figure 3.2***). This represents a peak in aerosol shedding of one day later than that observed in upper respiratory mucosal shedding reported in previous challenge studies (Carrat et al., 2008). Aerosol shedding peak is consistent with the 1-2 day post symptom onset nose and throat swab viral load peak observed in Hong Kong household contact surveillance studies

(Ip et al., 2016). Fine aerosol shedding was detected on days 2, 3, and 4 post inoculation in 45% (5/11), 64% (7/11), and 18% (2/11) volunteers with positive aerosol shedding respectively, supporting day 3 post inoculation as the peak day for shedding frequency among experimentally infected cases. There is no available data with which to compare temporal dynamics of experimental or natural infection aerosol shedding.

If we take previous estimates of ~1-2 days (25^{th}-75^{th} percentile) as the influenza A incubation period (Lessler et al., 2009), plus about 1 day post symptom onset to reach peak aerosol shedding in the naturally infected population, then we would observe ~2-3 days following exposure to virus, to reach peak aerosol shedding. This is consistent with the observed peak in aerosol shedding in the experimentally infected cases at 3 days post exposure by intranasal instillation, suggesting that the progression of infection from exposure to replication is similar. Observations of less significant decline in viral load from nasopharyngeal swabs compared with fine aerosols following peak shedding at day 1 post symptom onset (Yan et al., 2018), and a tendency for nasal viral load to overestimate transmission risk after day 3 post symptom onset (Tsang et al., 2015), suggests that aerosol shedding may better fit epidemiologically observed transmission dynamics over time in the household setting.

The presentation of natural influenza A infection has been reported as asymptomatic in a majority of infections (Hayward et al., 2014; Leung et al., 2015) and selection of

naturally infected cases from the community based on positive QuickVue rapid test or febrile illness plus cough or sore throat, was expected to inflate proportions of moderate and severe illness. Experimental cases were asymptomatic (12.8%) or mildly symptomatic with little variation over four days post inoculation (***Figure 3.1***). Temporal trends in symptom severity are mildly supportive that day 3 post nasal inoculation aligns with day 1 post symptom onset in naturally infected cases (***Figure 3.1***). Our findings are consistent with peak symptom score on day 3 post H3N2 inoculation reported in a meta-analysis of human challenge studies (Carrat et al., 2008). A multi-year household surveillance study in Hong Kong showed mean systemic and respiratory scores peaked on day of symptom onset (Ip et al., 2016). Although our naturally infected population did not have symptom observations on day of illness onset, peak symptom scores on day 1 post symptom onset (i.e., the first day of symptom follow-up in our study) could approximate this previous finding. When comparing symptom observations on the peak day of detectable fine aerosol shedding, naturally infected cases had higher symptom scores and observed cough counts (***Table 3.3***).

Peak symptom severity and aerosol shedding coincided for both experimental and naturally infected cases, consistent with the temporal dynamics of other studies (Carrat et al., 2008; Ip et al., 2016; Lau et al., 2010). However, in regression analyses that restricted observations to the peak day of fine aerosol shedding, the effects of symptoms on fine aerosol shedding rate were generally weak and contained within wide confidence intervals. Only fever >37.9^{o}C in the naturally infected group was

significantly associated with shedding strength. Previously, using data from all naturally infected influenza cases who met case criteria (including H1N1, H3N2, and B infections) we reported count as the only symptom associated with fine aerosol shedding strength (Yan et al., 2018). We also reported an association between upper respiratory symptoms and viral shedding into nasopharyngeal swabs but not aerosols, concluding that "the head airways made a negligible contribution to viral aerosol generation and that viral aerosols represent infection in the lung." In the Hong Kong household transmission cohorts, viral RNA copies detected in combined nose and throat swabs were 1-2 $\log_{10}$ higher in symptomatic compared with asymptomatic or paucisymptomatic (i.e., no more than 1 symptom reported per day) infection, which may be driven by a portion of individuals presenting with more upper as opposed to lower respiratory symptoms (Ip et al., 2017). Further analysis of the Hong Kong data showed that the presence of respiratory symptoms was not associated with transmission probability except in the case of child-to-child transmission and cough or phlegm is detected (Wardell et al., 2017), suggesting a level of independence between the presence of symptoms and transmission probability among symptomatic, adult index cases. This would be consistent with the notion that fine aerosol shedding strength, independent of symptom presentation in primary cases, plays a role in driving transmission.

In the current study, when assessing symptoms as predictors of viral shedding above the detection limit (***Table S3.1***), we show that lower respiratory symptom score, cough score, and cough count were positively associated with fine aerosol shedding

in both experimental and naturally infected groups, however upper respiratory symptom score and nasopharyngeal swab Ct value were associated, positively and negatively, respectively, with fine aerosol shedding only for experimentally infected cases. Taken together these findings may suggest that, among minimally symptomatic influenza A cases initiated by intranasal challenge, upper respiratory viral replication drives illness with a low probability of lower respiratory replication required for fine particle aerosol shedding. These data should be interpreted with caution given a lack of heterogeneity in symptom severity, with mild illness characteristic of the experimental cases and moderate to severe illness characteristic of the naturally infected population. It may be for this reason that other studies have given mixed results with respect to observing associations between symptomatology and nose/throat viral load (Lau et al., 2013, 2010).

Age was not associated with probability or strength of fine aerosol shedding in either the experimental or naturally infected study populations (***Tables 3.4, S3.1***). This finding is expected given that both study populations consisted of healthy, young adults. Despite the mean age different in years was about 8 years (***Table 3.1***), seasonal epidemic influenza subtypes generally do not pose heterogeneous infection risk across the young adult ages in the studies. Only males shed into aerosols in the experimentally infected group. This finding might be explained by the low probability of shedding into aerosols (28%) on top of the low number of females in the study (N=11). This difference could be worrisome for the generalizability of the challenge model used in EMIT. There may be immunological explanations for this phenomenon

that would call for further investigation. There is preliminary evidence from studies of vaccine-associated immunity that TLR7 is involved in adaptive immune response to influenza virus through B cell activation (Onodera et al., 2016). This could provide women with an immune system advantage given TLR7 encoding on the X-chromosome and incomplete inactivation of the second allele (Berghöfer et al., 2006; Fischinger et al., 2019). The uncertainty surrounding sex-related immunology against influenza infection warrants future work.

Given the associations between symptoms and shedding observed in the experimental and naturally infected study populations we attempted to adjust for these symptoms to understand the direct effect of experimental versus natural infection as a proxy for infection mode on the viral load in fine particle aerosols on the maximum day of shedding for each study volunteer or participant. The DAG describing the relationships between the variables is described in ***Figure S3.5***. Propensity score modelling failed to balance the distribution of covariates in the experimental and naturally infected case groups and we concluded that the groups were simply too different to achieve an unbiased estimate of the main effect of group membership on shedding strength. Interactions terms and upper level terms were not included in propensity score models because of a lack of a priori rationale. Given the large standardized differences in the populations across numerous models it is unlikely that alternative model specifications would improve balance. If this, or other propensity score adjustments were to be considered for making group comparisons, further prerequisite assessment of the balance of propensity scores themselves, based on

Donald Rubin's Rules would also warn against their use (***Appendix 3.4***). Thus, we are left with unadjusted shedding comparisons (***Table 3.2***) that do not avoid bias introduced with the selection bias of symptomatic naturally-acquired infections. Thus, assuming minimal contribution of potential confounders on the pathway between mode of inoculation and study population membership (i.e., age, sex, host immunity, virus pathogenicity, dose) we cannot conclude that the unadjusted differences in symptomatology and shedding are a result of mode of inoculation, or simply the result of the differences inherent in recruitment and enrollment procedures and potentially unobserved confounders in the absence of a randomized controlled design.

There is growing evidence that airborne transmission plays an important role in the population spread of influenza (Cowling et al., 2013b; Nguyen-Van-Tam et al., 2019; Tellier, 2009; Tellier et al., 2019). Humans experimentally challenged to influenza virus by airborne particles were had a 50% risk of infection to a 0.6-3.5 $TCID_{50}$ dose and exhibited increased propensity for moderate to severe illness with fever and cough compared with others experimentally challenged by nasal droplets (Alford et al., 1966; Little et al., 1979). The term anisotropic has been used to describe such infections where inoculation mode determines illness presentation (Milton, 2012). A population of cases with naturally-acquired infections would be expected to demonstrate a higher proportion of moderate-severe influenza-like illness compared with a population of cases exclusively infected by exposure to the nasal mucosa. We observed illnesses in experimentally infected cases mostly characterized by upper respiratory symptoms with minimal lower respiratory and systemic symptom scores.

Naturally infected cases presented with strong lower respiratory and systemic symptom scores, especially when compared with those of experimentally infected cases (***Figures 3.1, 3.3***). Compared with other symptoms, systemic scores declines more rapidly following day 1 post symptom onset, consistent with previously reported findings (Ip et al., 2016) and suggestive of the immune system clearing systemic infection. These findings suggest that natural infections observed here may be more likely to result in lung and systemic infection initiated by an airborne dose, whereas experimentally infected cases with nasal mucosal exposure had illness localized to the upper respiratory tract.

Identifying naturally infected reference groups that represent the true distribution of symptom severity presents a challenge. Although a substantial proportion of cases are asymptomatic, symptomatic community cases are prone for inclusion in epidemiologic studies upon seeking medical attention (Carrat et al., 2002). Multi-year sero-surveillance of large cohorts in the UK shows influenza infections presented asymptomatically at a rate of 77 per 100 person-seasons (Hayward et al., 2014). While noting the influence of study design, a meta-analysis of longitudinal studies using serological evidence of infection and controlling for background illness reported a 65%-85% asymptomatic fraction (Leung et al., 2015). The household transmission design, as conducted in Hong Kong, represents a powerful strategy to observe secondary cases before, during, and after exposure to a potentially infectious primary household case (Cowling et al., 2009). Still, considerations regarding generalizability aside, this design may be unable to detect short or mild infections

because nose and throat swab collection to confirm infection by RT-PCR occurred every several days and not daily. Additionally, the household design has so far not collected exhaled breath aerosols from primary or secondary cases. New studies with comprehensive surveillance of naturally-acquired influenza infection would be useful for addressing questions related to infectious potential in asymptomatic, and mild, moderate, severe infections.

The infectious dose for airborne influenza, and the infectious potential of cases infected by various modes is largely unknown. If the typical fine aerosol shedding rate from influenza cases is important for driving airborne transmission, then our findings would indicate that nasal mucosal exposure in the experimental challenge model produces cases with airborne infectious potential similar to cases infected naturally by contact, large droplets, or fine aerosols. If above average shedders are important for driving airborne transmission (i.e., superspreader hypothesis), then infections acquired through nasal mucosa may not pose as much airborne infectious potential.

If we assume that the symptomatic naturally infected UMD cases represent the upper 1% of symptom severity and shedding strength in the overall population, and if we also assume that the experimental cases are representative of total community infections, the chances of an experimental case reaching the level of fine aerosol shedding observed in the naturally infected group would be .39% (1% of 39 experimental cases). If shedders in the upper percentiles of shedding rate are

responsible for driving transmission, then it would take many more experimental cases to adequately simulate transmission events in a human transmission challenge trial model. This introduces logistical challenges and motivates work to identify, among naturally infected shedders, characteristics predictive of aerosols (and mucosal) shedding. It is plausible that symptomatic cases with observed high levels of aerosol shedding could be placed in a controlled exposure setting where recipients would receive exposure to just these symptomatic cases, however such a design would be resource intensive.

We cannot make conclusive comparisons between the experimentally and naturally infected populations given the selection bias in the recruitment of the naturally infected comparison group. If we assume that virus used in the challenge model was appropriately pathogenic (i.e. representative of real wildtype virus with the dose, environmental, and host conditions required for infection), our observations are suggestive that the population of influenza infections naturally-acquired by any mode: a) present with a symptom profile suggestive of airborne infection, b) are more likely to shed virus into fine particle aerosols, and c) shed 2-3 $\log_{10}$ more viral RNA at the upper end of the shedding distribution. Future work should examine the relationships between inoculation mode, dose, environmental conditions, and host immunity across different age groups. In particular, immune responses to influenza virus by and across modes may vary between children and adults, with implications for subsequent infectivity (Lau et al., 2013; Ranjeva et al., 2019; Viboud et al., 2004; Wardell et al., 2017).

Tables

Table 3.1. Demographics and symptomatology of influenza A Cases

	Experimental	Natural	p value
N-Participants	39	83	
Breath collection visits	84	146	
Age			< 0.001
Mean (SD)	29.9 (7.0)	22.3 (7.6)	
Range	20.0 - 45.0	15.0 - 63.0	
Sex			0.003
Female	11 (28.2%)	47 (56.6%)	
Male	28 (71.8%)	36 (43.4%)	
Frequency fever > 37.9ºC (%)	6 (15.4%)	17 (20.5%)	0.502
Temperature (C)*			< 0.001
N-Missing	2	1	
Mean (SD)	36.6 (0.6)	37.3 (0.6)	
Range	35.3 - 38.4	36.3 - 39.7	
Upper respiratory symptom score			< 0.001
Mean (SD)	1.4 (1.9)	7.0 (3.0)	
Range	0.0 - 6.0	0.0 - 15.0	
Lower respiratory symptom score			< 0.001
Mean (SD)	0.2 (0.4)	3.2 (1.5)	
Range	0.0 - 1.0	0.0 - 6.0	
Systemic symptom score			< 0.001
Mean (SD)	0.7 (1.2)	5.4 (2.4)	
Range	0.0 - 5.0	0.0 - 9.0	
Total symptom score			< 0.001
Mean (SD)	2.2 (2.9)	15.5 (5.5)	
Range	0.0 - 11.0	4.0 - 29.0	
Cough symptom score**			< 0.001
Mean (SD)	0.2 (0.4)	2.2 (0.8)	
Range	0.0 - 1.0	0.0 - 3.0	
Cough count***			< 0.001
Mean (SD)	1.7 (4.8)	26.7 (32.5)	
Range	0.0 - 35.0	0.0 - 265.0	
Nasopharyngeal swab Ct value			< 0.001
N-Missing	20	3	
Mean (SD)	27.1 (5.0)	22.6 (5.6)	
Range	17.0 – 36.3	13.1 – 38.1	

Symptom scores, body temperature, and observed cough counts are reported per visit, with multiple visits per person. Ten symptoms were rated from 0 to 3 with maximum possible composite score of 15 for upper respiratory, 6 for lower respiratory, and 9 for systemic symptoms. ANOVA (t-tests with equal variances) and chi-squared tests were used for continuous and categorical variables, respectively.

* Tympanic temperature for experimental and oral for naturally infected cases. It is known that tympanic temperature is between 0.3 and 0.6 degrees C higher than oral temperatures. ** Cough symptom score is included as part of the composite lower respiratory score. *** Cough count per half hour exhaled breath collection.

Table 3.2. Viral shedding into exhaled breath aerosols

All experimental and natural infections						
	Experimental		Natural			
	(39 subjects; 84 GII obs.)		(83 subjects; 146 GII obs.)		p value**	
	Coarse	Fine	Coarse	Fine	Coarse	Fine
No. positive subjects (%)	6 (15)	11 (28)	45 (54)	71 (86)	<0.001	<0.001
No. positive samples (%)	6 (7)	14 (17)	66 (45)	111 (76)	<0.001	<0.001
GM (GSD)*	2.7E+3 (3.26)	5.1E+3 (4.72)	1.8E+4 (13.91)	3.9E+4 (15.12)	<0.001	<0.001
RNA copies by percentile						
25th	ND	ND	ND	1.3E+3		
Median	ND	ND	ND	8.8E+3	<0.001	<0.001
75th	ND	ND	8.8E+3	9.8E+4		
90th	ND	2.5E+3	8.2E+4	1.3E+6		
95th	1.3E+3	7.9E+3	9.7E+5	6.6E+6		
Maximum	3.4E+4	1.3E+5	4.9E+8	4.9E+7		
Maximum shedding observations for experimental and natural infections						
	Experimental		Natural			
	(11 subjects; 11 GII obs.)		(71 subjects; 71 GII obs.)		p value***	
	Coarse	Fine	Coarse	Fine	Coarse	Fine
RNA copies by percentile						
25th percentile	0.0E+	0.0E+	0.E+	3.0E+3		
Median	0.0E+	0.0E+	1.7E+3	1.3E+4	<0.001	<0.001
75th percentile	0.0E+	1.1E+3	1.0E+4	1.4E+5		
90th percentile	1.4E+3	3.1E+3	4.2E+5	3.3E+6		
95th percentile	2.2E+3	6.4E+4	9.8E+5	1.2E+7		
Maximum	2.8E+4	8.0E+4	4.3E+8	4.4E+7		

Samples collected Days 1-4 post inoculation in the experimentally infected and Days 1-3 post symptom onset in the naturally infected. Shedding given per half hour sample.

*GM, geometric mean. GSD, geometric standard deviation (only positive samples were included in computation of GM and GSD. Tobit regression was used to impute RNA copies for samples where there were replicates below detection limit); ND, not detected. **Fishers exact tests were used to compare binomial proportions between experimental and natural cases for fine and coarse shedding subjects and samples. Welsh's t-test for unequal variance was used to compare GM. Wilcoxon rank sum test was used to compare medians. When restricting analysis to samples with detectable RNA quantities, the Wilcoxon rank sum test gave p-values of 0.0316 and 0.00275 for coarse and fine comparisons, respectively. *** When restricting analysis to samples with detectable RNA quantities, the Wilcoxon rank sum test gave p-values of 0.0245 and 0. 00315 for coarse and fine comparisons, respectively.

Table 3.3. Covariates in experimental and naturally infected cases from fine aerosol shedders on day of maximum shedding

Variables	Experimental	Natural	Standardized Difference %	P value (parametric)*	P value (non-parametric)**
Age	31.09 (8.01)	21.82 (6.70)	-123.0	<0.001	<0.001
Frequency ever febrile (%)	4.95 (45)	28.40 (40)	-18.5	0.599	1.000
Temperature (ºC)	36.76 (0.66)	37.46 (0.67)	99.9	0.001	<0.001
Upper respiratory score	3.64 (1.80)	7.01 (2.75)	117.4	<0.001	0.002
Lower respiratory score	0.46 (0.52)	3.37 (1.40)	176.7	<0.001	<0.001
Systemic symptom score	1.18 (1.25)	5.86 (2.10)	182.4	<0.001	<0.001
Total symptom score	5.27 (2.61)	16.24 (4.70)	187.8	<0.001	<0.001
Cough score	0.46 (0.52)	2.32 (0.75)	193.6	<0.001	<0.001
Cough count	4.00 (6.42)	28.48 (28.10)	88.9	<0.001	0.002
Nasopharyngeal swab Ct value	23.18 (2.84)	22.40 (6.02)	-13.6	0.479	0.048
Propensity score	0.44 (0.32)	0.93 (0.14)	204.3	0.000	<0.001
Linear propensity score	-0.85 (2.74)	4.78 (3.05)	157.8	0.000	0.000

Reporting mean (standard deviation) for each variable except for frequency ever febrile, from N=11 experimental and N=71 naturally infected cases. The mean and max absolute value standardized differences were 130.3% and 204.3%, respectively. Kolmogorov-Smirnov test for the mean standardized difference was 0.686 (p<0.001).Sex was removed because no females shed into fine aerosols in the experimental group.

* t-tests; ** Kolmogorov-Smirnov tests

Table 3.4. Unadjusted changes in RNA copies shed into fine aerosols

Predictor	Experimental Estimate (CI)	Natural Estimate (CI)	Combined Estimate (CI)
Age	4.20E+2 (-2.59E+3, 3.43E+3)	5.62E+4 (-1.80E+5, 2.93E+5)	-1.68E+3 (-1.84E+5, 1.81E+5)
Sex	-	8.19E+5 (-2.33E+6, 3.97E+6)	1.87E+5 (-2.56E+6, 2.93E+6)
Fever >37.9ºC	1.00E+4 (-4.13E+4, 6.13E+4)	**4.51E+6 (7.05E+5, 8.32E+6)**	**3.66E+6 (3.81E+5, 6.93E+6)**
Body temperature	1.39E+4 (-2.12E+4, 4.90E+4)	2.21E+6 (-1.14E+5, 4.53E+6)	**2.06E+6 (1.60E+5, 3.96E+6)**
Upper respiratory score	-1.72E+3 (-1.51E+4, 1.16E+4)	-1.26E+5 (-7.03E+5, 4.50E+5)	5.90E+2 (-4.78E+5, 4.79E+5)
Lower respiratory score	1.84E+4 (-2.58E+4, 6.26E+4)	-1.32E+5 (-1.27E+6, 1.00E+6)	1.82E+5 (-6.52E+5, 1.02E+6)
Systemic symptom score	-6.40E+3 (-2.51E+4, 1.24E+4)	-4.03E+5 (-1.15E+6, 3.46E+5)	-5.90E+4 (-5.95E+5, 4.77E+5)
Total symptom score	-1.55E+3 (-1.07E+4, 7.64E+3)	-1.35E+5 (-4.71E+5, 2.01E+5)	3.24E+3 (-2.32E+5, 2.39E+5)
Cough symptom score (as continuous)	1.84E+4 (-2.58E+4, 6.26E+4)	1.41E+6 (-6.69E+5, 3.50E+6)	1.23E+6 (-1.64E+5, 2.63E+6)
Cough symptom score (as factor)			
No symptom	REF	REF	REF
Mild	1.84E+4 (-2.58E+4, 6.26E+4)	1.02E+6 (-1.30E+7, 1.50E+7)	6.58E+5 (-5.02E+6, 6.33E+6)
Moderate	-	9.92E+5 (-1.25E+7, 1.45E+7)	9.87E+5 (-4.21E+6, 6.19E+6)
Severe	-	3.34E+6 (-1.01E+7, 1.68E+7)	3.33E+6 (-1.76E+6, 8.42E+6)
Cough count	2.37E+3 (-9.56E+2, 5.69E+3)	2.12E+4 (-3.51E+4, 7.74E+4)	2.70E+4 (-2.26E+4, 7.67E+4)
Nasopharyngeal swab Ct value	-3.39E+3 (-1.15E+4, 4.75E+3)	-1.32E+5 (-3.94E+5, 1.30E+5)	-1.34E+5 (-3.74E+5, 1.06E+5)

Effect of a single unit increase in temperature or symptom scores. Effect of febrile compares ever febrile >37.9ºC to afebrile. Effect of sex compares male to female. Bolded values are significant at p=0.05. Only males shed into aerosols in the experimental group. Cough scores of 2 or 3 were never observed in the experimental group. Observations from the maximum fine aerosol shedding day for each subject were used (11 experimental, 71 natural, 82 combined).

Table 3.5. Covariates with propensity score ATE weighted adjustment

Variables	Experimental	Natural	Standardized Difference %	P value (parametric)*	P value (non-parametric)**
Age	27.55 (7.11)	21.78 (6.00)	-85.2	0.018	0.015
Frequency febrile (%)	2.42 (45)	(33)	-24.9	0.640	1.000
Temperature (C)	37.21 (0.67)	37.32 (0.66)	16.2	0.708	0.858
Upper respiratory score	3.991 (1.24)	6.37 (2.76)	90.0	0.000	0.242
Lower respiratory score	0.27 (0.47)	3.11 (1.37)	162.2	0.000	0.000
Systemic symptom score	1.20 (1.18)	5.04 (2.63)	132.8	0.000	0.008
Total symptom score	5.46 (1.98)	14.52 (5.46)	144.7	0.000	0.000
Cough score	0.27 (0.47)	2.26 (0.71)	179.1	0.000	0.001
Cough count	2.15 (4.73)	27.62 (25.47)	103.7	0.000	0.008
Nasopharyngeal swab Ct value	22.46 (2.01)	22.87 (5.54)	8.5	0.613	0.454
Propensity score	0.69 (0.29)	0.78 (0.34)	27.2	0.571	0.044
Linear propensity score	0.90 (2.12)	3.39 (3.89)	68.6	0.051	0.044

Reporting mean (standard deviation) for each variable except for frequency febrile, with weighted ATE adjustment used data from 5.38 experimental and 25.37 naturally infected cases. The mean and max absolute value standardized differences were 86.9 % and 179.1%, respectively. Kolmogorov-Smirnov test for the mean standardized difference was 0.609 ($p<0.001$). Sex was removed because no females shed into aerosols in the experimental group.

* t-tests; ** Kolmogorov-Smirnov tests

Figures

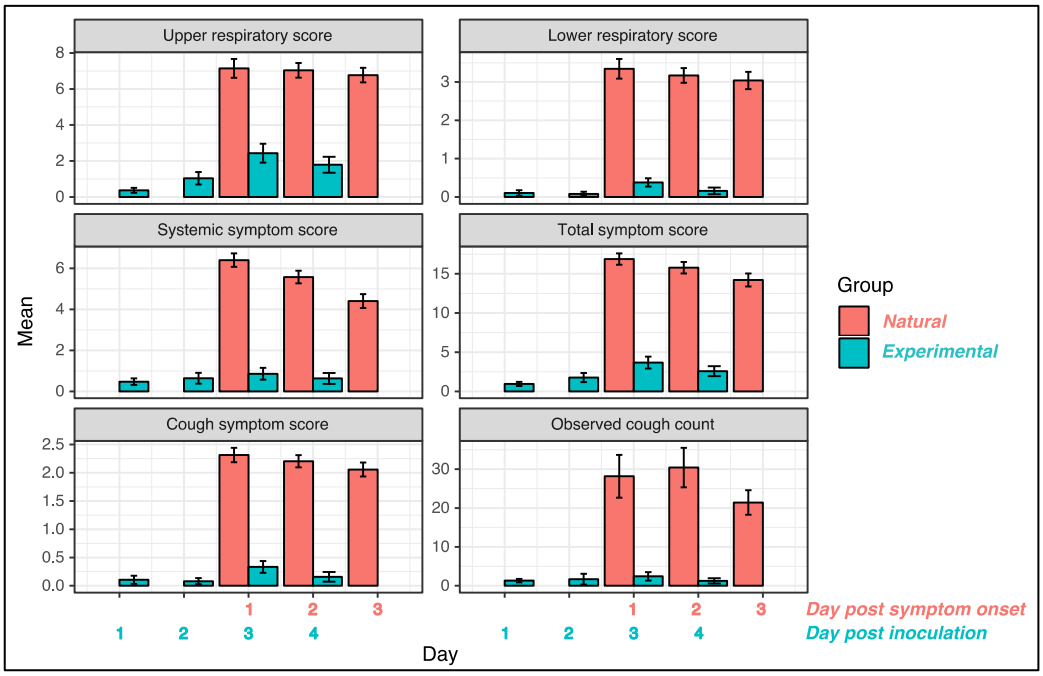

Figure 3.1. Mean symptom scores and observed cough counts over time. Day 3 post inoculation is aligned with day 3 post symptom onset. Upper respiratory score (sum of runny nose, stuffy nose, sneezing, sore throat, earache, score range 0-15). Lower respiratory score (sum of shortness of breath, and cough, range 0-6). Systemic symptom score (sum of malaise, headache, muscle/join ache, range 0-9). Total symptom score (sum of all symptom scores, range 0-30). Symptoms scores were measured once, on each day of sample collection for natural infections, and three times per day for experimental infections. For experimentally infected cases, the symptom score measurement that was taken at the time closest to exhaled breath collection was used as the symptom for each day post inoculation. Observed cough counts were those recorded during half-hour exhaled breath collection. Bars represent the standard error around the mean.

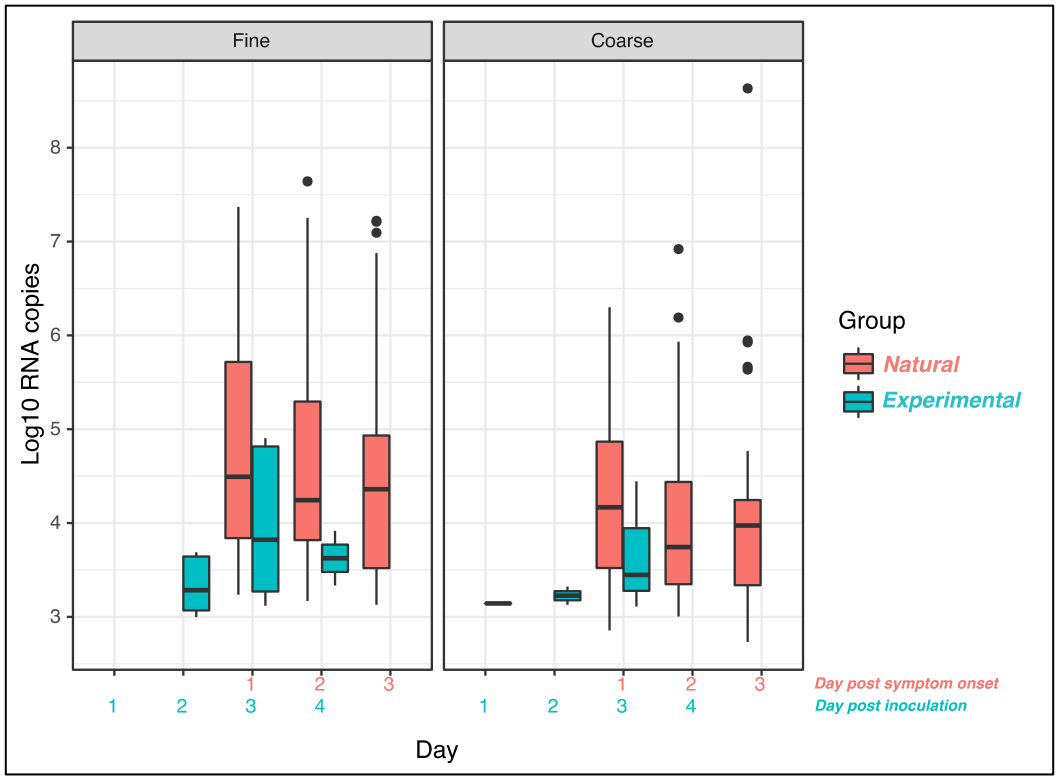

Figure 3.2. Fine and coarse aerosol shedding over time. Includes all shedding observations from 84 (experimentally infected cases) and 146 subject-days (naturally infected cases). Day 3 post inoculation was aligned with day 1 post symptom onset. Detectable aerosol shedding in $\log_{10}$ aerosol copies, with boxes showing the inner-quartile range (IQR) with a band to indicate the median, and whiskers extending to the highest and lowest data points within 1.5 IQR.

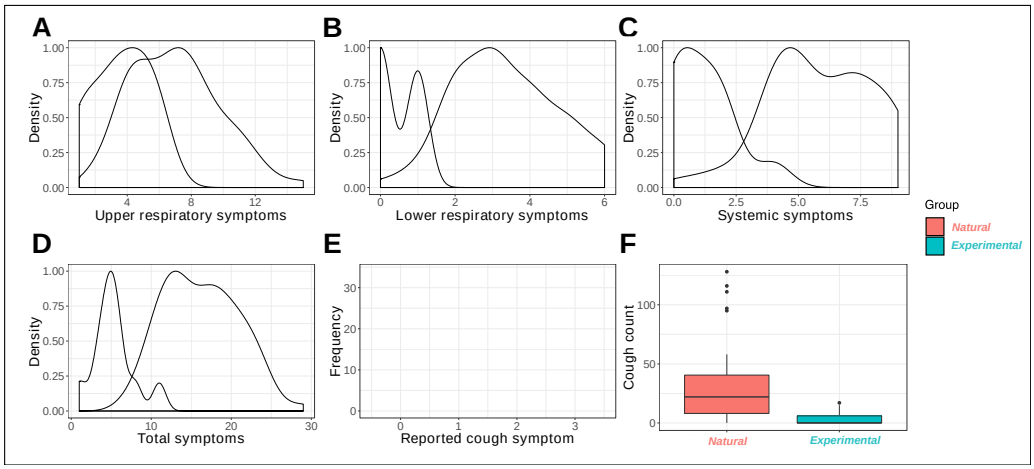

Figure 3.3. Comparison of self-reported symptoms and observed coughs from maximum fine aerosol shedding day observations. Includes data from 11 experimental, 71 natural observations. Density plots, scaled so that the highest value for a single moment is equal to one, compare (**A**) upper respiratory symptoms (runny nose, stuffy nose, sneezing, sore throat, and earache, score range 0-15), (**B**) lower respiratory symptoms (shortness of breath, and cough, score range 0-6), and (**C**) systemic symptoms (malaise, headache, muscle/joint ache, score range 0-9). (**D**) Total symptom score (range 0-30). (**E**) Cough symptom score (range 0-3). (**F**) Observed cough counts with boxes showing the inner-quartile range (IQR) with a band to indicate the median, and whiskers extending to the highest and lowest data points within 1.5 IQR.

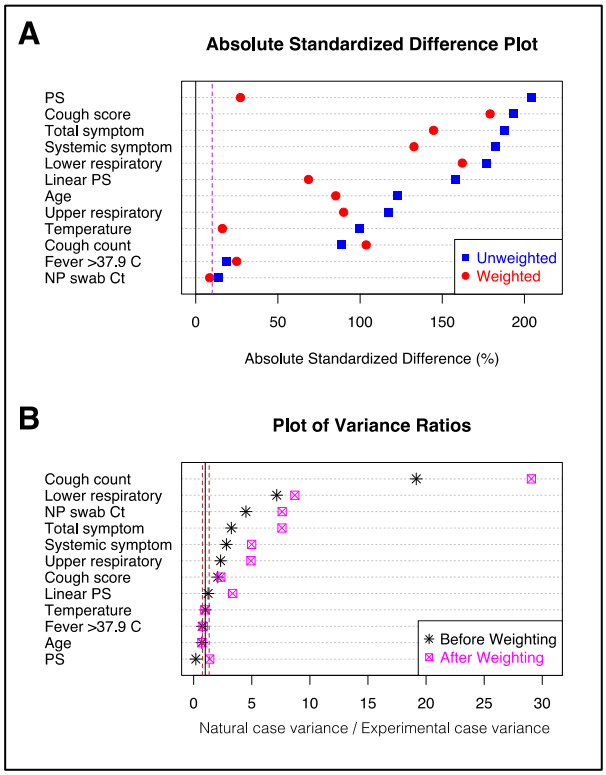

Figure 3.4. Balance diagnostics for propensity score adjustment by ATE weighting. ATE: Average treatment effect approach, where the naturally infected cases are considered "treatment." Each naturally infected cases is weighted 1/(propensity score) and each experimentally infected case is weighted as 1/(1 – propensity score). Plots were done using the propensity score model that led to the lowest mean standardized difference across all covariates (**A**) Absolute standardized differences between experimental and naturally infected case covariates plotted for each covariate, the propensity score (PS) and the linear PS. The dotted line represents 10%. Balanced populations should have absolute standardized differences close to zero and not exceeding 10%. (**B**) Variance ratios for naturally infected cases to experimental cases, plotted for each covariates, PS, and linear PS. Dotted lines represent 0.5 and 2, the range for which balanced populations generally do not exceed.

CHAPTER IV

ESTIMATING THE AIRBORNE INFLUENZA QUANTUM GENERATION RATE FROM A HUMAN TRANSMISSION TRIAL WITH A CONTROLLED ENVIRONMENT

Abstract

Quantifying influenza transmission risk by airborne, contact, and large droplet spray transmission modes informs the strategic use of prevention strategies to reduce the burden of seasonal epidemics, and the threat of pandemics. We used data from the largest human influenza challenge-transmission trial (Evaluating Modes of Influenza Transmission, ClinicalTrials.gov number NCT01710111) to estimate the average generation rate of airborne infectious doses sufficient to infect 63% of exposed susceptibles (Well's quantum of airborne infection). We quantified influenza A viral RNA exhaled into fine particle aerosols (≤ 5μm) from experimentally infected Donors and used the rebreathed-air equation to estimate the airborne quantum generation rate *q* and its relationship to RNA shedding. Out of 42 infected influenza Donors, 11 shed detectable levels of influenza RNA into fine particle aerosols with adjusted geometric mean 4.7E+3, geometric standard deviation 6.0, and range 2.6E+2 - 1.6E+5, accounting for observations below detection limit and where no exhaled breath sample was collected. The exposure room where the single transmission event occurred had one of the three highest inhalation exposures. The average quantum generation rates for infected Donors (N = 42) and aerosol shedding Donors (N = 11) were 0.029 (0.027, 0.03) and 0.11

(95% CI 0.088, 0.12) per hour, respectively. There were 1.4E+5 (1.0E+5, 1.8E+5) RNA copies shed into fine particle exhaled breath aerosols per quantum. We present methodology for estimating influenza airborne infectious dose to facilitate the prediction of secondary attack rates given measured or estimated infectious airborne viral source strength and indoor and outdoor CO_2 concentrations. The estimate quantum dose generation rate appears reasonable and consistent with the limited scientific literature available for comparison. Further validation of these results under a variety of scenarios and with higher attack rates is needed.

Introduction

The substantial, annual global disease burden attributed to seasonal influenza and the threat of influenza pandemics demand increased preparedness. Yet efforts to improve vaccines, engineering controls, and other population prevention strategies are hindered by a lack of understanding about the competing risk contributions of contact, large droplet, and droplet nuclei (i.e., airborne) transmission modes. There is evidence that airborne transmission via virus contained in exhaled breath droplet nuclei likely plays a role in epidemics, and that influenza infections initiated this way lead to illnesses of greater severity (Henle et al., 1943; Knight et al., 1965; Alford et al., 1966; Couch et al., 1970; Little et al., 1979; Tellier, 2009; Hayden, 2012; Cowling et al., 2013a). Quantifying the risk posed by airborne transmission is widely accepted as a major goal for translational public health practice. To this end mathematical modelling techniques applied to droplet nuclei transmission have developed over the last century.

Wells postulated an airborne quantum as an infectious dose generated by an infected individual during exposure with a susceptible (Wells, 1955). The Wells-Riley equation for estimating the probability of indoor airborne transmission requires assumptions of well-mixed air space and steady-state conditions and is defined as:

$$P = \frac{D}{S} = 1 - \exp(-\frac{Ipqt}{Q}) \quad (1)$$

with *P* probability of infection for *S* exposed susceptibles, *D* secondary infections, *I* infectors in their infectious stage (i.e., when they are emitting virus), *p* breathing rate per indoor occupant, *q* quantum generation rate from each *I*, *t* exposure time, and *Q* outdoor air supply rate (Riley et al., 1978). Rudnick and Milton have described the *q* term as the "average infectious source strength of infected individuals." They emphasize that a) *q* is not an organism but rather a dose that reflects the stochasticity of airborne contagion, and b) an infectious dose may not be greater than a single organism that reaches a vulnerable locus (Rudnick and Milton, 2003a).

Rudnick and Milton's rebreathed-air version of the Wells-Riley equation uses indoor and outdoor CO_2 levels to estimate indoor occupant exposure to exhaled breath, based on the facts: a) droplet nuclei are emitted through the exhaled breath of infectious individuals and b) CO_2 contained in exhaled breath is constant at 38,000 ppm and is the predominant source of CO_2 in buildings. Assuming a well-mixed space, the rebreathed-air equation uses measured CO_2 levels to directly estimate exposure to exhaled breath that may be contaminated with a quantifiable level of infectious particles. This approach enables exposure assessment under non-steady state conditions representing an advantage for practical exposure

assessment compared with the Wells-Riley equation. The rebreathed-air equation is defined as:

$$P = \frac{D}{S} = 1 - \exp\left(-\frac{\overline{f}Iqt}{n}\right) \quad (2)$$

where $\overline{f}$ is the time-weighted average fraction of indoor air that is exhaled breath with n individuals in the room contributing CO_2. Thus, $\frac{I}{n}$ equals the fraction of the $\overline{f}$, or the "rebreathed fraction," that is from an infectious individual.

Solving the rebreathed-air equation for q requires measurement or estimation of the other variables and assurance that the exposure between infectious cases and susceptibles resulted in transmission to secondary cases, D. Such data could be derived from an experimental human transmission model, or intensive epidemiologic surveillance with accurate quantification of viral exposure by transmission mode. These study designs have so far been challenging to operationalize, and few have been carried out, however a 2013 US CDC-funded influenza transmission-challenge trial provides an appropriate dataset (EMIT; ClinicalTrials.gov number NCT01710111; (Nguyen-Van-Tam et al., 2019)). One transmission event was observed yielding an overall secondary attack rate (SAR) of 1/75 = 1.33% and Nguyen-Van-Tam and colleagues suggest a role for airborne transmission when discussing the findings in context. We use this trial data and apply the rebreathed-air equation to examine the relationship between airborne exposure and infection risk, to estimate an airborne infectious dose 63% (ID_{63}) generation rate, q, for influenza, and to estimate the RNA copies in fine particle exhaled breath aerosols per quantum, σ.

Methods

The EMIT challenge-transmission trial methods are described elsewhere (Nguyen-Van-Tam et al., 2019). In short, seronegative volunteers were randomised to viral 'Donor' (N=52), 'Intervention Recipient' (N=40) and 'Control Recipient' (N=35) groups. Donors were inoculated with 0.5ml per nostril of a suspension containing $5.5\log_{10}TCID_{50}$/ml of influenza H3/Wisconsin/67/2005 manufactured under current good manufacturing practices. Recipients were exposed to Donors for four consecutive days and assessed for evidence of infection. Continuous CO_2 monitoring was conducted in exposure rooms where mechanical ventilation controlled indoor CO2 concentrations, relative humidity, and temperature to produce what were considered as favorable conditions for influenza transmission, while balancing the thermal comfort of volunteers, and the capacity of the building's mechanical ventilation system to attain comparable conditions in exposure rooms throughout the study. Viral shedding into exhaled breath aerosols was collected from Donors with a Gesundheit-II (McDevitt et al., 2013; Yan et al., 2018).

Data were cleaned and analyzed in R Studio (Rv3.5.1 R Development Core Team, Vienna, Austria) and SAS Studio (Release 3.7 (Enterprise Edition), v9.4M6, Cary, NC). The development of new equations to evaluate the relationship between q and aerosolized RNA copies is described in Results. Empirical bootstraps with 10,000 samples were used (base R) to produce 95% confidence intervals for q and σ.

The rate of Donor viral shedding into exhaled breath aerosols was computed from samples with detectable viral RNA in one or both qRT-PCR duplicates with values imputed for samples where at least one duplicate was below detection limit. Imputed values were generated from Tobit regression (SAS Proc NLMIXED) (Twisk and Rijmen, 2009) with fixed effects of self-reported cough symptom and study day, and random effect of person, using 100 quadrature points. Tobit regression parameter coefficients were taken from generalized linear models (SAS Proc GENMOD) with fixed effects of self-reported cough symptom and study day. Self-reported cough symptoms were collected thrice daily on an ordinal scale 0-3 (3 most severe) and daily averages were used in regression models.

For infected Donors who shed into aerosols with at least one detectable qRT-PCR replicate ("ever-aerosol-shedders") on at least one study day, aerosol shedding was assumed to exist at levels below the detection limit in samples where one or no qRT-PCR replicates had detectable RNA and on days where no sample was collected. No Donors demonstrated detectable RNA in fine particle aerosols on day 1 of exposure so the fine aerosol shedding period was assumed to be study days 2-4. Tobit regression was used as described before using all symptom scores and exhaled breath sample data from ever-aerosol-shedders during study days 2-4. Parameter estimates for fixed effects for cough, day, and random effect of person were then used to estimate aerosol shedding rates for ever-aerosol-shedders on study days 2-4 with no exhaled breath collection.

Laboratory evaluation of biological specimens by qRT-PCR was done alongside those described by Yan et al., 2018 and the assay's limit of quantification was 2000 RNA copies per half-hour sampling period, representative of the "most dilute sample that gave a positive result in all replicates". University of Maryland dormitory room CO_2 surveillance and calibration is reported in Jenkins, 2018. Sensitivity of indoor CO_2 level on q and σ was performed by modulating indoor CO_2 concentrations upwards and downwards by 10% intervals to +/-50%. Scripts to reproduce analyses are available on GitLab.

Results

Linking q with measurable airborne virus

We applied the rebreathed-air equation to the EMIT transmission trial data to estimate an airborne influenza infectious dose generation rate, q, to give rise to 1.33% SAR. Because of the controlled environment dictated by the experimental design, the single, secondary infection was assumed to have resulted from exposure to viral Donors. Based on the discussion in Nguyen-Van-Tam et al., 2019, we assume for this analysis that the transmission event occurred via the airborne mode. Evidence described later supports this assumption.

The transmission trial was carried out over the course of three, quarantine periods during which exposure events occurred in up to five exposure rooms over four days, where exposure between Donors and Recipients ranged from approximately 13 to 16 hours per day. Quarantines 1, 2, and 3 used five, three, and five exposure rooms, respectively for a total of 13 exposure rooms. Recipients were assigned to

exposure groups (EGs) on day 1 and switched rooms each day with their group. Donors assigned to EGs on day 1 were reallocated on day 2 to new EGs where they remained through the end of exposure. Donor EG reallocation was done according to clinical presentation in an attempt to evenly distribute viral source strength. Donors never shed detectable influenza RNA into fine particle aerosols on study day 1 and airborne exposure on this day was considered negligible. Three Recipients were withdrawn from exposure at different time points due to symptom presentation in order to prevent a second generation of transmission; None tested positive for influenza by Sofia rapid test. Each EG had a defined airborne exposure as a function of the level of rebreathed air and rate of shedding into exhaled breath aerosols. The single transmission event occurred in quarantine 2 EG C.

The relationship between q and the observed rate of RNA copy shedding into fine particle exhaled breath aerosols per hour, $\mathbb{V}$, is defined by:

$$q = \frac{\mathbb{V}}{\sigma} \quad (3)$$

where σ is the number of RNA copies per ID_{63} and represents the difference between estimated RNA copy airborne exposure, and the viral RNA quantity that reaches a vulnerable locus in the respiratory tract and evades the host immune system. Using Equation 3 to substitute for q in Equation 2 gives:

$$P = \frac{D}{S} = 1 - \exp\left(-\frac{\overline{f}I\mathbb{V}t}{n\sigma}\right) \quad (4)$$

Exposure to exhaled breath from infectious case

The integrated exposure to exhaled breath over time in an indoor space, $\overline{f}$, was computed for each EG by integrating over the CO_2 concentrations observed in the room over the four exposure days (i.e., study days 1-4) after subtracting background CO_2 levels and dividing by the constant CO_2 concentration in exhaled breath, 3.8E+4. This fraction is described as the "rebreathed fraction" by Rudnick and Milton. ***Figure 4.1*** plots observed CO_2 concentrations in each exposure room during 5-minute intervals throughout each quarantine experiment. Background levels were computed as the average CO_2 concentrations observed between 02:00 and 03:00 hours in each exposure room during the four nights following daytime exposure events. Their arithmetic means (standard deviations) were 418.30 (23.13), 434.55 (22.16), and 422.31 ppm (12.15) for quarantines 1, 2, and 3, respectively. During nights, viral Donors and Recipients were housed outside exposure rooms. No study staff occupied exposure rooms during this time either. Thus, the nighttime CO_2 concentrations are good proxies for outdoor CO_2.

The fraction of air in the EGs that is the exhaled breath from viral shedders, $\frac{\overline{f}_I}{n}$, is displayed in ***Figure 4.2a***. Three EGs had no Donors who shed into fine particle aerosols (quarantine 1 EGs B and D, and quarantine 2 EG A). EG 4 in quarantine 2 had a substantially higher $\frac{\overline{f}_I}{n}$ because there were two shedding Donors compared with a maximum of one in every other exposure room. Otherwise, EGs across all quarantines had relatively similar exposure to exhaled breath from Donors.

<u>Viral RNA shed into exhaled breath aerosols from infectious donors</u>

Measured exhaled breath fine aerosol shedding rates enables translation of Donor exhaled breath exposure to viral inhalation exposure. Of the 52 inoculated donors, N=4, 41, 4, and 3 gave G-II samples on one, two, three, and four days, respectively for a total of 110 sampling instances. There were a total of 25, 31, 30, and 24 G-II samples collected on study days 1, 2, 3, and 4, respectively. Among inoculated donors, 42 were determined to have been infected with influenza A by serology, or by two days of positive qRT-PCR tests on nasopharyngeal swabs between days one and six after inoculation.

Among the 42 infected Donors, Influenza A viral RNA was detected in 14 fine aerosol exhaled breath samples from 11 Donors, and in six coarse aerosol samples from six Donors. All who shed into coarse aerosol also shed into fine aerosols. A Donor deemed uninfected but with evidence of airborne shedding was excluded (***Appendix 1***). Out of the 14 positive fine aerosol samples, four had one out of two qRT-PCR replicates below detection limit. Imputing for these samples to account for uncertainty of replicate values below detection limit, the geometric mean (GM) of the 14 positive fine aerosol samples, was 1.0E+4 RNA copies per hour, the geometric standard deviation (GSD) was 4.7, and the range was 2.0E+3 – 1.6E+5. We assumed the 11 Donors who shed virus into fine aerosols had some positive quantity of viral shedding below the detection limit on study days 2-4 where no RNA copies were detected, or no exhaled breath samples were collected. Study day 1 was excluded because fine aerosol shedding was never observed on this day.

For each infected Donor who ever shed into fine aerosols (i.e., at least 1 fine aerosol sample qRT-PCR replicate positive) *i,* on each study day *j,* the rate of RNA copy shedding into fine aerosols per hour is defined by V_{ij}. Imputed values of V_{ij}, given by $\widehat{V}_{ij}$, for days without measurements (N=14) and samples with one or both non-detectable qRT-PCR duplicates, assumed to exist below the limit of detection (N=9 samples) were estimated using Tobit regression with fixed effects of cough symptom and study day, defined by equation 5.

$$\widehat{V}_{ij} \sim \beta_0 + \beta_1 * cough_{ij} + \beta_2 * study\ day_{ij} + b_0 + b_1 * i \quad (5)$$

For samples where both qRT-PCR duplicates were above the limit of detection (N=10), a duplicate mean was taken directly from measured values. This yielded a total 33 RNA copy shedding rate person-day observations for 11 positive Donors, adjusted GM (GSD) of 4.7E+3 (6.0) and range 2.6E+2 – 1.6E+5. ***Table 4.1*** describes V_{jk} and V_k, ***Figure 4.2b*** illustrates V_{jk} and ***Figure S4.1*** shows the model performance compared with observed values. For comparison, ***Table S4.1*** reports the fine aerosol shedding RNA copy numbers where one or both qRT-PCR duplicates were above the limit of detection (N=14 samples) and Tobit estimation was used to estimate sample RNA quantities where only one duplicate was detected. ***Figure S4.2*** presents the fine aerosol shedding rates by study day. Tobit regression diagnostics and parameters are presented in ***Appendix 4.2***.

While fine particle aerosols are involved in airborne exposure, coarse particle aerosols (≥5μm) represent larger droplets that may be emitted during speaking or coughing, and could potentially initiate infection should they land directly on a mucosal membrane of a susceptible or contaminate a fomite that is handled by a susceptible. They settle to the ground relatively quickly. In total, six Donors shed

into coarse aerosols, all of whom also shed into fine aerosols. There were only two coarse exhaled breath aerosol samples with both detectable replicates and their replicate averages were 5.6E+4 and 4.2E+3 RNA copies shed per hour, from Donors in quarantine 1 EG E and quarantine 3 EG B, respectively. There were four other positive coarse aerosol sample replicates that ranged from 2.6E+3 to 6.8E+4 RNA copies per hour. Virus contained in coarse aerosols was assumed to not contribute to transmission risk.

Using 75 discrete exposure events to compute q

Because the transmission trial represents a discrete level of exposure to each of the 75 susceptibles, there are a total 75 exposure scenarios one led to infection. By summing the probability of infection, P for each Recipient, we solve for q for the trial as a whole. Riley, Murphy, and Riley (1978) used a similar approach to sum risk of transmission across multiple exposure periods between school children during a measles outbreak. Because two Recipients were withdrawn before the end of study day 4, we adjusted for their absence in their respective EGs from the moment of their withdrawal. The withdrawal of a Recipient terminates the exposure for the withdrawn Recipient and partitions the exposure in the EG for the remaining Recipients into l partitions within k EG, on j study day, for Recipient i, described by equation 6.

$$R_{total} - R_{infected} = \sum_{ijkl} \exp\left(-\frac{\bar{f} t_{ijkl} I_{ijk} q}{n_{ijkl}}\right) \quad (6)$$

where R_{total} is 75, the total number of Recipients in the study, and $R_{infected}$ is one, the total number of secondary cases in the study. Solving Equation 6 by minimizing the difference between the sides of the equation with I as the number of Donors ever observed during the exposure period to have shed into fine

aerosols results in q=0.11 (95% CI 0.088, 0.12) quanta generated per hour. Solving for q with I as the number of infected donors results in q=0.029 (0.027, 0.03). The sensitivity of the q values with respect to indoor air CO_2 levels is reported in ***Table S4.2*** and ***Figure S4.3***.

Using 75 discrete exposure events to compute σ

Riley, Murphy, and Riley summarized airborne viral exposure with an r term, which we adapt here using the rebreathed air equation as:

$$r = \frac{\overline{f}IVt}{n} \quad (7)$$

Substituting r into Equation 4 yields a simpler form of the rebreathed air equation given by Equation 8 that shows the relationship between the exposure to exhaled breath containing viral RNA and σ, the number of RNA copies per ID_{63}.

$$P = \frac{D}{S} = 1 - \exp(-\frac{r}{\sigma}) \quad (8)$$

The viral exposure term per Recipient r_i is a cumulative exposure term over all study days, EGs and Recipient withdrawal partitions. It is defined as:

$$r_i = \sum_{(jkl)_i} \frac{\bar{f}t_{(jkl)_i}V_{(jk)_i}}{n_{(jkl)_i}} \quad (9)$$

After accounting for withdrawal partitions, ***Figure 4.2c*** and ***Figure 4.2d*** plot r_{jk} and r_k, respectively. The EG where the transmission event occurred (quarantine 2, EG C), indicated by the red bar in ***Figure 4.2d*** had among the highest exposure to viral RNA (***Table 4.2***). Taking the same approach used for computation of q, we use Equation 10 to solve for σ.

$$R_{total} - R_{infected} = \sum_i \exp(-\frac{r_i}{\sigma}) \quad (10)$$

Solving equation 10 by minimizing the difference between the sides of the equation gives σ=1.4E+5 RNA copies/ID_{63} (95% CI 1.0E+5, 1.8E+5). The sensitivity of the σ values with respect to indoor air CO_2 levels is reported in ***Table S4.2*** and ***Figure S4.3***. Applying the ratio of RNA copies to fluorescent focus units for influenza virus of approximately 1.0E+3, from Yan et al., 2018, translates σ to 1.4E+2 fluorescent focus units, representative of infectious particles per ID_{63}. We note that Yan and colleagues reported a correlation between quantitative culture and fine aerosols ($r=0.34$, $p<0.0001$).

Application of q and σ to airborne exposure scenarios

Applying q to influenza challenge transmission 'proof-of-concept' study

A proof-of-concept study prior to the EMIT trial demonstrated the feasibility of human transmission following nasal inoculation of seronegative volunteers (Killingley et al., 2012). Nine viral Donors were inoculated (with the identical virus, mode, and dose used in the EMIT trial). Six Donors were used in three exposure rooms, two per room. Five of these donors were confirmed by serology and qRT-PCR tests, to have been infected, all of whom met ILI as defined by Killingley and colleagues. Five susceptible Recipients were placed in each of the three exposure rooms four were considered to be seronegative and susceptible to infection. We applied the Well's Riley equation (Equation 1) given an 8.3% SAR (1/12 seronegative Recipients), and assumed infected Donors generated q at the same rate as in the EMIT trial (for all infected Donors: 0.029 per hour or 4.8E-4 per minute), a standard pulmonary ventilation rate of 8 l/min, to estimate the ventilation rate in the exposure rooms (Equation 11). There was no knowledge of rate of RNA copy shedding into fine aerosols in the proof-of-concept study.

$$R_{total_{seronegative}} - R_{infected} = \sum_{i_{seronegative}k} \exp(-\frac{I_{i_{seronegative}k} qpt}{Q}) \qquad (11)$$

Solving Equation 11 gave Q=112 L/min. This is probably a fairly low estimate given that exposure rooms with attached bathrooms had bathroom exhaust of roughly 1.4E+3 L/min (based on standards for bathrooms of size 50 square feet and smaller) with operation of the bathroom exhaust (which turned on with the light switch during bathroom use) likely about 10-20% of the exposure time. Thus, mechanical ventilation rate in the attached bathrooms would be estimated at 140-280 L/min. However, if some of the makeup air comes from the bathroom (e.g., leaks in plumbing chase), then a lower ventilation rate could be expected in the exposure space outside the bathroom, and thus the calculated rate of 112 L/min may be reasonable.

If instead we use the EMIT q computed from the fine aerosol shedding Donors of 0.11 quanta/hour (1.8E-3 quanta/minute) and apply this to Equation 11, we get a ventilation rate of 395 L/minute. It would be reasonable to estimate the q for the proof-of-concept study to be somewhere in the range between the EMIT quanta generation rate using infected Donors and shedding donors. Thus, applying the EMIT trial q to the proof-of-concept study yields estimated ventilation rates within a reasonable range of 112 – 395 L/minute.

Estimating the q for symptomatic, naturally infected cases presented by Yan et al., 2018

Yan et al., 2018 report the influenza viral shedding (RNA copies and quantitative fluorescent focus units) on 218 half-hour exhaled breath samples from 142 symptomatic individuals from a population of mostly young adults in the

University of Maryland community. Taking into account samples assumed to contain RNA in quantities below the limit of detection, the adjusted geometric mean RNA copies recovered from exhaled breath fine particle aerosols was 2.4E+4 (95% CI 1.4E+4, 2.8E+4) per hour. Applying Equation 3 and the σ of 1.4E+5 RNA copies/ID_{63}, a q computed with the data presented by Yan and colleagues is 0.17 ID_{63} per hour (95% CI 0.10, 0.27). We note that the influenza cases in the University of Maryland population were selected from symptomatic individuals who presented to the University health center or directly to the study within the first 3 days of illness and were febrile >37.8 ^{o}C with cough or sore throat or had a positive QuickVue rapid test. This population may not be representative of the viral shedding that might be expected from a larger population of influenza cases given that many cases are asymptomatic or mildly symptomatic. If symptom severity is positively correlated with shedding strength, then the q computed for the Yan et al., 2018 study may over-estimate the q for the greater influenza infected population.

Comparing EMIT trial q with Moser et al., 1979

Moser et al., 1979 reported on an influenza outbreak in a Boeing 737 attributed to exposure to an intensely ill passenger during a 4.5-hour delay with no mechanical ventilation. Given the SAR of 72% among 54 people on board, well above the average reproduction ratio for influenza, it is plausible that the individual on board was a super shedder. The maximum RNA copies detected in exhaled breath fine aerosols by Yan et al., 2018 was 8.8E+7 per hour. If we assume that the super shedder on the Boeing 737 was shedding at the same rate, then we can apply the σ of 1.4E+5 and Equation 3 to compute a q for the airplane scenario of 630. Using

their non-steady-state version of the Wells-Riley equation Rudnick and Milton (2003) computed a q of 79 or 128, under outdoor air exchange rates of 0.1 and 0.5/h, respectively. Their estimate is within a single log10 of the estimated value obtained using the maximum fine aerosol shedding rate observed in Yan et al., 2018.

Estimating risk of airborne transmission between dormitory roommates

The computed σ can be used to estimate probability of airborne transmission in a variety of non-experimental settings using the Wells-Riley of rebreathed-air equations (Equations 1 and 2). Viral shedding rates into aerosols from symptomatic, influenza cases during the 2012-13 influenza season in the University of Maryland campus community has been characterized by G-II (Yan et al., 2018). For this naturally infected population, the geometric mean shedding rate into fine aerosols, adjusted for samples below detection limit, was 2.4E+4 RNA (95% CI 1.4E+4, 2.8E+4) copies per hour. Calibrated, continuous dormitory room CO_2 concentration has been measured over several semesters at the University of Maryland. Nighttime indoor CO_2 concentration for a typical room in one dormitory has been measured as 1.1E+3 ppm (GSD 453) and typical nighttime outdoor CO_2 concentration was 450ppm. Thus, for a hypothetical 8-hour exposure period during the night while two roommates are sleeping, if one roommate is an average aerosol shedding, shedding 2.4E+4 RNA copies per hour into fine aerosols, then the risk of airborne transmission to a susceptible roommate would be 1.2%. In a different dormitory with a typical nighttime indoor CO_2 room concentration measured at 1.7E+3 ppm (GSD 796 ppm), the risk of airborne transmission to the susceptible roommate increases to 2.3%. This risk increases to

3.4% if the exposure time increases from 8 to 12 hours. ***Figure 3*** shows the probability of infection as a function of indoor CO_2 concentration in the two dormitory rooms, and fine aerosol shedding rates for positive samples only, reported in Table 2 in Yan et al., 2018. Probability of infection in the dormitory rooms is low until an infector is shedding at one GSD above the GM and exposed to a higher rebreathed fraction.

Discussion

We applied the rebreathed-air equation and computed an airborne influenza quanta generation rate, q, and the influenza viral RNA copy number per ID_{63} from a human challenge-transmission trial. We also presented a framework for these computations using the rebreathed-air equation with measured viral shedding and CO_2 concentrations. The infectious dose generation rates (95% CI) were q=0.11 (0.088, 0.12) and q=0.029 (0.027, 0.030) doses/hr for aerosol shedders and infectious Donors, respectively, are relatively low, consistent with a typically low reproductive number for influenza of 1.5-2 and prolonged exposure associated with larger outbreaks (Boelle et al., 2011; Moser et al., 1979b). Compared with the computed σ of 1.4E+5 (95% CI 1.0E+5, 1.8E+5) RNA copies per quantum, the fine aerosol viral shedding rate per hour from the 26% infected Donors with detectable fine aerosol shedding was small, with GM 4.7E+3 and range 2.6E+2 – 1.6E+5. The maximum fine aerosol shedder among the experimentally infected Donors barely produced a single quantum per hour into aerosols, while a Donor shedding at the GM generated 0.03 quanta per hour. Based on the aerosol shedding strength observed in a study of symptomatic, naturally infected influenza

cases in an H3 predominant season (Yan et al., 2018), a typical case generated 0.17 quanta per hour (95% CI 0.10, 0.27). Meanwhile, a symptomatic, naturally infected case shedding the maximum quantity of RNA into fine aerosols produced, 630 quanta per hour, suggesting a role for supershedders in airborne influenza transmission.

It appears reasonable to assume airborne transmission in the single, observed transmission event. The transmission trial resulted in 1.3% SAR, although a proof-of-concept experimental human influenza transmission trial using half the exposure time and fewer than half the infectious Donors gave SAR 8.3%, using the infection criteria of the former (Killingley et al., 2012). Compared with proof-of-concept, after increasing the magnitude and duration of exposure, the follow-on transmission trial was expected to produce a 16% SAR. Thus, the observed SAR of 1.3% was much lower than expected under identical study conditions ($p<0.001$) (Nguyen-Van-Tam et al., 2019). As detailed in Nguyen-Van-Tam and colleagues, the main difference between these studies was likely the ventilation. The proof-of-concept study was carried out in hotel rooms, with what was likely to be relatively little ventilation compared with the follow-on trial in a controlled environment. That the SAR did not increase between the proof-of-concept and follow-on trials, yet the magnitude and duration of direct and indirect contact between infectious and susceptible volunteers more than doubled, and the air exchange rate likely increased – which would promote dilution of infectious airborne particles – supports the interpretation that airborne particles and not contact or large droplets drove transmission in this model. The finding that the single transmission event occurred in a Recipient with one of the highest levels of airborne exposure and

that volunteers with no viral aerosol exposure were not infected further supports the interpretation that transmission was via fine aerosols. Coarse aerosols are less likely to contribute to airborne transmission because they settle quickly. Coarse aerosol shedding was a couple of logs lower among naturally infected aerosol shedders, supporting the hypothesis that coarse aerosols contribute lower risk relative to fine aerosols.

In this study, the two main factors contributing to transmission risk were the rate of fine aerosol shedding from infectious cases, and the level of rebreathed air in the indoor exposure space governed by the air exchange rate. The estimated SARs in the modelled University of Maryland dormitory room (***Figure 4.3***) were similar to those estimated in studies of influenza transmission in households. The airborne SARs ranging from 1.2% to 3.4% for a single night of exposure (up to 10.2% for 3 nights of exposure) between one infected and one susceptible roommate in a dormitory room is similar to reported household SARs of 8% and 21% (Cowling et al., 2009; Simmerman et al., 2011). Analysis of these household trials – which used hand hygiene and facemask interventions to control for transmission model – has reported that airborne influenza could be responsible for about half of influenza transmission events and that interventions to interrupt contact and large droplet modes may not reduce overall risk, but rather shift transmission mode (Cowling et al., 2013a). Thus, accounting for the SAR due to airborne risk alone in the household trials makes the SAR comparison between the household transmission studies and theoretical dormitory example more similar.

An analysis of a separate household cohort found that among 52 sample pairs between primary and potential secondary household transmission cases with sequence data of sufficient quality, 47 (90%) were considered phylogenetically supported transmission events (McCrone et al., 2018). This lends credence to the assumption that household transmission events in the aforementioned household studies were between household contacts. Despite this, it may be a minority of infections that are acquired from household contacts in the residential setting. Reanalysis of household transmission data described in McCrone et al., 2018 assuming one case in each household came from an outside source, shows 72% of influenza cases originated from sources outside the household. This is consistent with literature on TB transmission in high-burden settings. Risk attributable to non-household resident sources have been estimated as 81% in suburbs of Cape Town, South Africa (Verver et al., 2004), >75% in a periurban township outside of Cape Town (Wood et al., 2010), 77% in rural Vietnam (Buu et al., 2010), and >65% in Lima, Peru (Brooks-Pollock et al., 2011), pointing toward shorter-term shared air exposure to supershedders as important for TB transmission. There may also be a similar role for supershedders in airborne influenza transmission.

Using the rebreathed-air equation to estimate airborne transmission risk between roommates in University of Maryland dormitory rooms with measured CO_2 concentrations provides insight on the behavior of transmission probability as a function of the rebreathed fraction and the rate of infectious airborne particles containing influenza virus (***Figure 4.3***). If a roommate is shedding virus at one GSD above the GM observed in a population of symptomatic influenza cases observed in the University of Maryland campus community (Yan et al., 2018),

then the rebreathed fraction in the room is very influential in determining infection risk in a susceptible roommate, ranging in risk of about 10% for an indoor air CO2 level one GSD below the GM in a well ventilated dorm, to about 90% at two GSDs above the GM in a poorly ventilated dorm. When the rate of shedding approaches the highest percentiles the probability of infection becomes quite high regardless of rebreathed fraction. This suggests that influenza transmission could be driven by poorly ventilated environments inhabited by average viral shedders or the highest viral shedders (i.e., supershedders) regardless of ventilation level. Phylogenetic studies could evaluate the theory that a minority of viral shedders are responsible for the bulk of transmission. An analytical framework to explore this hypothesis has been described (Colijn and Gardy, 2014). Studies that can refine predictors of high-level aerosol shedding, as done by Yan and colleagues, or can refine predictors of transmission related to indoor environments are of great importance to population level disease prevention programs.

The Wells-Riley equation has been used in numerous studies to estimate transmission risk for Tuberculosis (Riley et al., 1978). The rebreathed-air equation adapts the Wells-Riley equation by directly estimating inhalation exposure to concentrations of airborne contaminants in exhaled breath by using CO_2 to estimate exhaled breath concentration (Rudnick and Milton, 2003a). In the current EMIT trial analysis, we assumed the pulmonary ventilation rates of Donors and Recipients (and study monitors who also spent time in the rooms) were relatively similar. Given that volunteers were participating in similar activities, were not participating in heavy physical activities, and never experienced severe illness, the

main differences in the contribution to exhaled breath in the room would be related to baseline respiratory function, which was not likely to be substantially different between healthy, young adult volunteers. To test the assumption that the exposure rooms were well mixed spaces, tracer gas studies were conducted in one of the exposure rooms. CO_2 sensors in the corners and center of the room followed similar patterns in CO_2 concentration levels that reflected CO_2 releases into the rooms. These finding were robust to the opening and closing of the door (***Appendix 3.3***).

This study provides the beginnings of a scientific basis for specifying indoor ventilation rates sufficient to prevent transmission from average infectious influenza cases. Despite the inability to compute confidence bounds for q due to the low SAR, given the single transmission event in the trial, the computed q and σ estimate lower bounds from which transmission probability in various scenarios can be projected. Although the computed q was found to be reasonable after application to the proof-of-concept transmission study ventilation conditions (Killingley et al., 2012), replication of these findings in other settings is needed to translate these findings into control measures that can be incorporated into building design or and operation and maintenance requirements. Additional discussion about q and the connection to viral exposure and SIR modelling can be found in ***Appendix 3.4***.

As required by the nature of the human challenge model, volunteers were all young adults above age 18. Other variables in the challenge model were selected to maximize the transmission potential to Recipients. Volunteers were selected

with low levels of preexisting antibodies to influenza H3 virus. Volunteer psychosocial stress levels were not observed despite its importance in infection susceptibility following exposure (Cohen et al., 1991). The temperate temperature and humidity were selected to optimize environmental conditions favorable for influenza transmission (Lowen and Steel, 2014; Shaman et al., 2010). Comparison of wildtype reference virus to the laboratory prepared A/Wisconsin/67/2005 (H3N2) used for inoculation showed partial adaptation to laboratory culture environments yet conservation of a fixed variant in the HA gene, suggesting that the laboratory prepared virus was not likely to be the cause of the low SAR (Nguyen-Van-Tam et al., 2019; Sobel Leonard et al., 2016). Thus, although the current challenge model provided a platform to carefully control, examine and quantify transmission, heterogeneity in host immunity, viral, coinfection, contact exposure networks, and environmental factors related to transmission risk were not observed in this model. Addressing how additional variation in these factors influences transmission risk by airborne and other modes is required to increase generalizability and translate findings into actionable public health strategies aimed at promoting healthy built environments. To this end, a hybrid challenge study approach could be explored with recruitment of naturally infected cases as Donors and a demographically and immunologically diverse population as Recipients, however the feasibility of conducting such a study would pose a challenge. The isolation of H1N1 variants unique to lower respiratory tract compared with the nasal mucosa points toward the possibility of transmission mode tracing through sequencing samples from community exposure networks (Piralla et al., 2011).

Given our limited data on transmission in the EMIT trial, we have presented what appear to be reasonable estimates for q and σ. We also presented a powerful and feasible methodology for estimating influenza airborne infectious dose and predicting transmission risk given measurements of the source strength of virus shed into exhaled breath and CO_2. The airborne infectious dose generation rate for experimentally infected Donors with A/WI virus in the controlled challenge environment was low, consistent with expectations. Typical experimentally infected aerosol shedders and naturally infected community cases generate few infectious doses per hour, however observed cases that shed the most virus generate several hundred infectious doses per hour. Airborne risk in the presence of an average shedder could be substantially mitigated by increased ventilation, but not in the presence of a supershedder. Future work is needed to explore the role of supershedders and refine risk attributable to the airborne mode while addressing heterogeneity in host immunity, virus, coinfection, contact exposure networks, and environmental factors related to transmission risk. In addition to providing a scientific foundation for promoting built environments that reduce transmission, this work builds toward enabling the public health community to gain the capacity to rapidly quantify viral shedding from early cases in an outbreak, characterize the probability of transmission through the airborne mode and the implications for population epidemiology, and mount effective responses.

Tables

Table 4.1. Fine particle aerosol shedding strength from detected and estimated samples

Quar.	Exposure Group	Day 2	Day 3	Day 4	Daily Average***
1	A	8.8E+3 (1, 2)	1.6E+5 (1, 2)	1.3E+4 (0, 2)	1.8E+5 (2, 6)
	B*	ND (0, 2)	ND (0, 1)	ND (0, 2)	ND (0, 5)
	C	1.2E+3 (0, 3)	1.3E+4 (1, 2)	1.3E+3 (0, 1)	1.6E+4 (1, 6)
	D*	ND (0, 2)	ND (0, 2)	ND (0, 2)	ND (0, 6)
	E	1.4E+4 (0, 2)	1.3E+5 (1, 3)	1.6E+4 (1, 3)	1.6E+5 (2, 8)
2	A*	ND (0, 2)	ND (0, 4)	ND (0, 0)	ND (0, 6)
	B	2.7E+3 (1, 4)	2.7E+4 (1, 2)	2.9E+3 (0, 1)	3.3E+4 (2, 7)
	C**	9.8E+3 (1, 4)	1.3E+5 (1, 4)	1.2E+4 (0, 3)	1.5E+5 (2, 11)
3	A	4.1E+3 (0, 2)	4.0E+4 (0, 2)	4.3E+3 (1, 2)	4.9E+4 (1, 6)
	B	2.0E+3 (1, 2)	2.0E+4 (0, 1)	2.1E+3 (0, 2)	2.4E+4 (1, 5)
	C	2.6E+2 (0, 2)	2.6E+3 (1, 2)	2.8E+2 (0, 2)	3.2E+3 (1, 6)
	D	3.9E+3 (1, 2)	2.5E+4 (0, 2)	2.7E+3 (0, 2)	3.2E+4 (1, 6)
	E	3.4E+2 (0, 2)	3.9E+3 (1, 3)	4.1E+2 (0, 2)	4.6E+3 (1, 7)

RNA copies shed into fine particle exhaled breath aerosols per hour by day-EG, V_{jk}, by EG, V_k from observed and imputed samples (number samples with at least 1 detectable qRT-PCR replicate, number samples tested).

* EGs with no Donors observed to shed any fine aerosols with at least one qRT-PCR replicate positive. ** EG with the transmission event. *** Not time weighted.

Table 4.2. Total fine particle aerosol viral exposure

Quarantine	Exposure Group	Total aerosol viral exposure (log10 RNA)
1	A	3.8
	B*	0.0
	C	2.9
	D*	0.0
	E	3.9
2	A*	0.0
	B	3.3
	C**	3.8
3	A	3.3
	B	3.1
	C	2.3
	D	3.2
	E	2.3

* EGs with no Donors observed to shed any fine aerosols with at least one qRT-PCR replicate positive.
** EG with the transmission event.

Figures

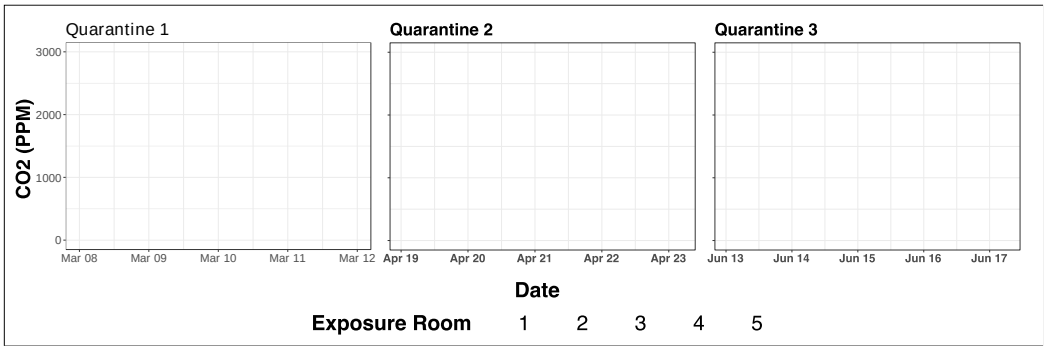

Figure 4.1. Observed CO_2. Concentrations measured at 5-minute intervals over the entire course of the four-day exposure period.

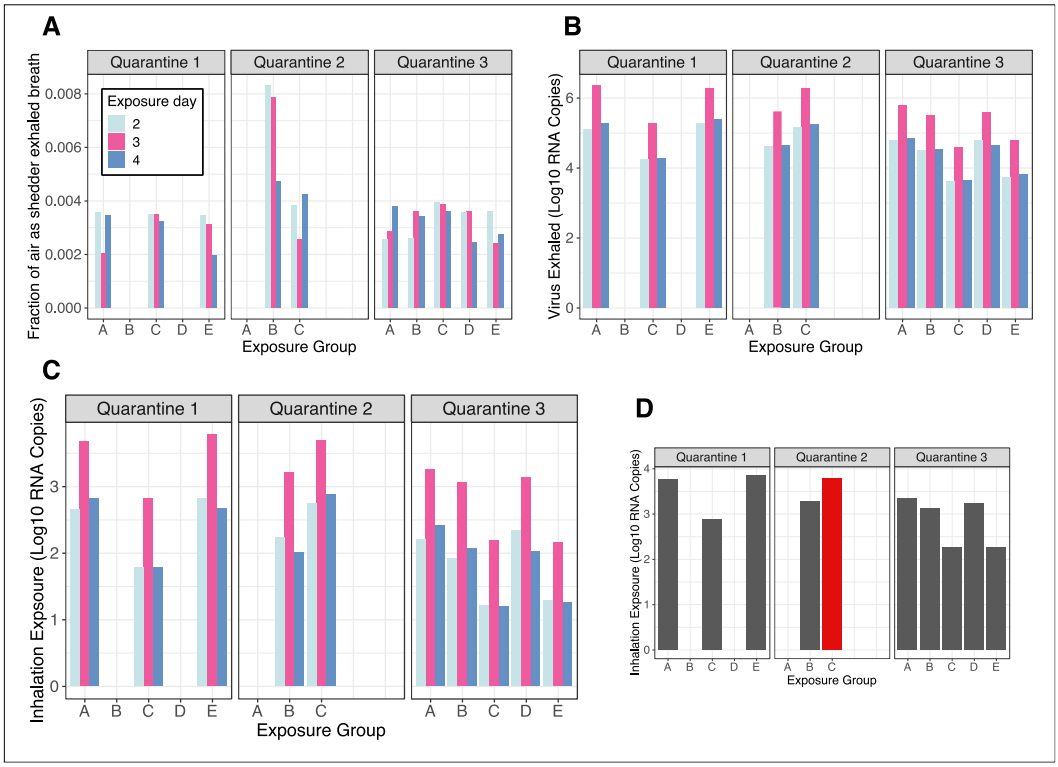

Figure 4.2. Exposure related to transmission risk. **A** shows, for each Recipient in each exposure group (EG), the fraction of inhaled air containing exhaled breath from Donors who shed into fine aerosols. **B** shows Donor shedding in each EG by day, and **C** and **D** show Recipient exposure to viral RNA aerosols in each EG by day, and cumulatively, respectively. The single transmission event occurred in Quarantine 2 EG C (red bar in **D**).

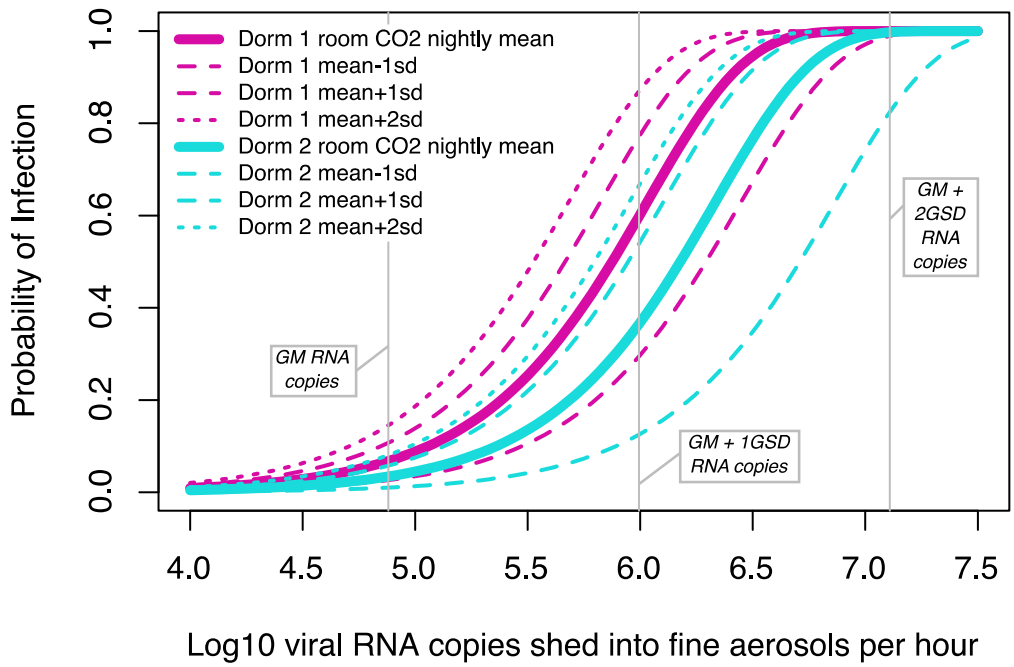

Figure 4.3. Probability of infection in dormitory rooms with different rebreathed fractions. The grey lines indicates GM, GM + 1GSD, and GM + 2GSD shedding rates, reported in Yan et al., 2018, transformed to per hour. Dormitory room CO_2 measured during the 2017-2018 academic year at the University of Maryland (reported in Jenkins et al., 2018).

CHAPTER V

SUMMARY AND CONCLUSION

Summary of key findings

This dissertation used data from the EMIT human challenge-transmission trial to address three hypotheses:

1. The fraction of secondary cases attributable to airborne transmission will be greater than those attributable to contact and large droplet spray.
2. The fine aerosol shedding profiles of natural, community-acquired influenza cases are well approximated by artificial infection initiated by nasal instillation of virus.
3. The infectious quantum generation rate for influenza is estimated as a function of the quantity of infectious aerosols exhaled by infectious cases, and the rate of airborne virus removal mainly driven by ventilation, given the susceptible immune status of the human trial volunteers.

Assessment of hypotheses has generated three main findings:

i. Comparison of a proof of concept human influenza trial with a larger, follow-on trial, with the main difference being ventilation levels, suggests a minimal role in contact and large droplet spray transmission and a possible role for airborne transmission.

ii. Comparison of experimentally inoculated infections with symptomatic, naturally infected cases suggests that the probability of the artificial nasal

inoculation resulting in the highest levels of symptom severity and viral shedding observed in the naturally infected group is low.

iii. The airborne quantum generation rate (95% CI) for influenza in the controlled human transmission trial environment among infected Donors and airborne viral shedding Donors is at most 0.029 (0.027, 0.03) and 0.11 (0.088, 0.12) per hour, respectively. The number of RNA copies per infectious quantum was 1.4E+5 (95% CI 1.0E+5, 1.8E+5). Given this quantum generation rate, and levels of viral shedding in a college campus community in dormitory rooms evaluated for exhaled breath exposure, the typical viral shedder presents low risk of transmission to a susceptible roommate during a nighttime of exposure in a well-ventilated dormitory but a moderate risk in a poorly ventilated dormitory. Supershedders at the 95th percentile of fine aerosol shedding present high risk regardless of indoor levels of ventilation (***Figure 5.1)***.

The computed infectious quantum generation rate (q, described in Chapter IV) enables the comparison between estimated exposure to influenza virus and infection risk. Thus, given levels of exhaled breath aerosol viral shedding and ventilation rates for indoor shared air spaces, the Wells-Riley equation can be applied to estimate infection risk. Of course, this assumes that the assumptions inherent in the computation of the q in the EMIT human challenge-transmission trial can be generalized to other transmission scenarios. The population of susceptible volunteers had low HAI and MN titres, representing above average susceptibility than the general population, suggesting q may be overestimated. The computed q must also be interpreted with caution because it represents a point estimate, with confidence bounds generated by empirical bootstrap, given that it is

derived from a single transmission event. The q for influenza is relatively low compared with that estimated for other respiratory infections. Few studies have estimated q, but some estimations exist for influenza and other infections known to be transmissible by the airborne mode.

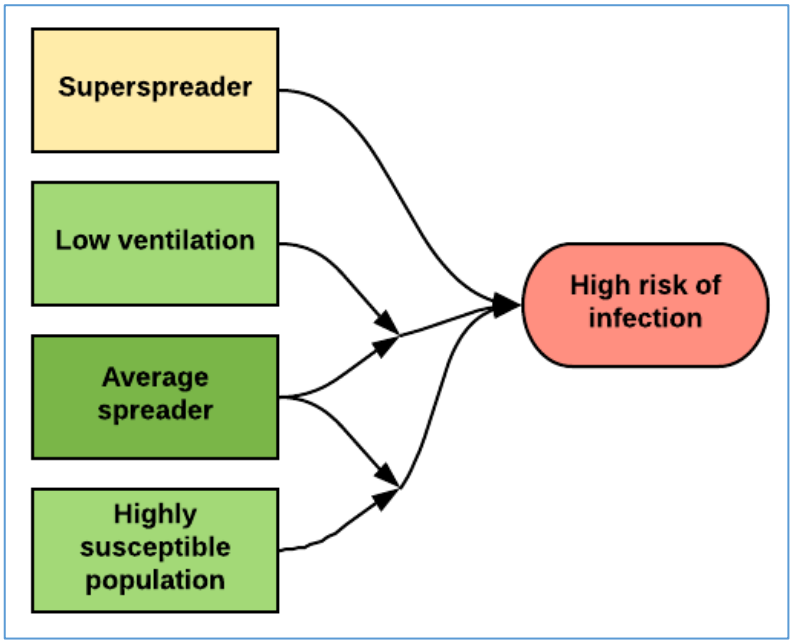

Figure 5.1. Risk of infection as a function of aerosol shedder, ventilation, and immunity.

Limitations and questions for future research

The EMIT challenge-transmission trial, like Alford's challenge study with aerosol viral exposure, used a population with low pre-existing antibodies to the challenge virus subtype. Thus, these studies are useful for demonstrating transmission dynamics with susceptible secondary cases, but lack generalizability to the general population with varying levels of immunity. Additional issues with generalizability are explored in Chapter 3. That only one transmission event was

observed in a Control Recipient represents a major limitation, as the mode of transmission cannot be ascertained with certainty and the risk ratio represents the lower bound for infection risk and lends uncertainty to the confidence bounds. Nonetheless, the analyses in this dissertation attempted to a) learn what was possible about influenza transmission given that EMIT was unique in its design and the largest human-transmission trial conducted to date, and b) fully assess the limitations of the study design to inform future investigations. Numerous questions exist to drive future studies aiming to refine risk assessment and optimize population prevention strategies. Such questions include:

a) To what extent do temperature, humidity, latitude, subtype, and engineering controls such as ventilation, air flow, and UVGI effect transmission risk?
b) To what extent do social contact networks of direct contact exposure predict observed transmission risk?
c) What is the optimal set of social contact network and indoor air quality variables to predict observed transmission events in a contained community setting (i.e., dormitories, military barracks, boarding schools, nursing homes, hospitals, schools, occupational settings, etc.)?
d) Evaluate the influence of engineering control strategies – ventilation, airflow dynamics, filtration – on influenza risk reduction, while accounting for variability in human susceptibility to illness, and the concurrent deployment of administrative and behavioral interventions.
e) To what extent does infection mode influence the immune response and subsequent viral shedding peak, temporal trend, and virion infectiousness,

and to what extent are age, sex, prior infection, vaccination, and immune status modify these effects?

f) Could viral load by site (lung produced aerosols versus upper respiratory tract produced mucosa) be a biomarker of mode of infection?

g) How do symptoms correlate with shedding from lung versus upper respiratory mucosa across age, sex, socio-behavioral factors, immune status, and subtype? What does this mean related to the subset of the population that is being sampled in studies that recruit medical care seeking respiratory infection cases? There is limited data about the extent of shedding as a function of symptom profile. Asymptomatic individuals have been shown to shed 1-2 $\log_{10}$ RNA copies fewer into nasal mucosa than symptomatic cases (Ip et al., 2017). If symptomatic cases are more likely the result of airborne transmissions, then asymptomatic infections may be more representative of population infected by upper respiratory mucosal exposure.

h) Is an epidemiologic framework that could identify exposure networks and confirm transmission events, potentially by infection mode, feasible given the current state of the science?

i) To what extent is aerosol shedding a function of viral concentration in the respiratory fluid of the distal airways versus expiratory volume, cough, and other drivers of expiratory particle generation?

Lessons learned for future study design

We would like to see if findings from the experimental challenge-transmission model are borne out in real-world epidemiology and population transmission dynamics. This way we can assess a range of other important variables including heterogeneity in immunity by age, sex, prior infection, coinfection, immunization, coinfections, shedding dynamics by age, sex, and immune status, a range of socio-behavioral variables related to human-human transmission including psychological stress (Cohen et al., 1991), sleep, physical activity, diet, overall well-being, and the physical built environment including temperature, humidity, ventilation, and the importance of other particulates and exposures (mixtures). The advantage of the experimental trial in a controlled environment is that a relationship can be drawn between strength of viral shedding and subsequent secondary attack rate, giving a dose response relationship. However recent advances in genomic sequencing and bioinformatics are beginning to show a path forward for using molecular markers, in combination with epidemiological contact and exposure surveillance, to confirm who transmitted to whom (Campbell et al., 2019; Volz et al., 2009; Volz and Frost, 2013). Preliminary data shows that transmission chains may be able to give information about mode of transmission if it is true that viral communities evolve distinctly in the lung versus the upper respiratory mucosa.

There is evidence that influenza may manifest as compartmentalized infections in the lung and nasopharynx (Yan et al., 2018). Preliminary sequence data on a few aerosol-nasopharyngeal swab paired samples from the study conducted by Yan and colleagues shows distinct variants evolved in these compartments. Deep sequencing with an average read depth of 15,000X (range 12,000X-20,000X) per

sample was conducted on three pairs of nasopharyngeal (NP) swabs and aerosol samples from qRT-PCR confirmed influenza A cases. Single nucleotide variants were identified after trimming reads with FLASH (ver. 1.2.11), assembling de novo using SPAdes (ver. 3.10.1), and mapping assembled to contigs with bowtie 2 (ver. 2.3.2). There were no shared variants between NP swabs and aerosol samples, and 20-147 variants unique to either NP or aerosol samples per pair, giving a Jaccard similarity coefficient of 0. Airborne transmission likely involves viral communities produced in the lung, while contact transmission likely involves nasal communities, thus enabling a path to identify infection route that requires characterization. Considering the nasopharynx and lung as separate entities that carry the ability to infect independently, reconstruction of transmission chains in observed contact networks can be achieved by analyzing shared variants (Worby et al., 2017). Bayesian approaches can be used to infer transmission events for outbreaks that are not completely sampled and/or are ongoing (Didelot et al., 2017).

Relevant ongoing research at University of Maryland

Current work at the University of Maryland (Characterizing and Tracking College Health, the "CATCH the virus study") has been employing an epidemiologic, observational approach to understand transmission risk and modes of influenza and other respiratory pathogens on the university campus community. Three years of surveillance of a healthy cohort spanned assessment of a wide range of health-related data including on sleep and stress, and upon infection, symptom assessment, collection of specimens for quantification of mucosal and exhaled

breath viral load, viral community, and immune biomarkers. Comprehensive environmental monitoring to assess exposure to exhaled breath (e.g., with CO_2 measurement and sampling for airborne viral RNA) has been carried out in dormitories and other campus buildings. Contacts with potentially high levels of exposure to infectious cases have been followed prospectively for evidence of infection yielding rich data on temporal trends in symptoms, viral shedding, and biomarkers indicative of impending infection and shedding. Contact and exposure networks are based on knowledge of dormitory room location, class schedules, and a location tracking application.

Such a study design enables the investigation of associations between indoor air environment, exposure networks, and sociobehavioral variables related to exposure and immunity. This model, while focusing mostly on a narrow population range of young adults can be expanded to a pediatric community on campus, and older adults in the campus and surrounding communities, representing a microcosm of a healthy, age-inclusive community.

Implications for public health practice

Although new studies are needed to refine estimates of transmission risk by various modes to understand relationships between infection mode, dose, age, sex, immunity, environment, symptoms, and human and viral infectivity, our findings are substantial enough to begin supporting the scientific underpinnings of public health interventions aimed at reducing transmission and population epidemics through targeted exposure control strategies. Finding suggest that ventilation and

airflow controls, to reduce exposure to contaminated exhaled breath, could have major impact on preventing disease in shared air spaces. Preventive measures that are precautionary in nature could take these findings into consideration.

In the case of influenza, it may be that the infectious generation rate of the average infectious aerosol shedder is low enough to pose only mild risk under well ventilated conditions but may pose moderate to severe risk under less ventilated conditions (***Figure 5.1***). Fine particle aerosol supershedders may pose substantial risk regardless of indoor ventilation. However, supershedders may be quite rare in the population. These findings are described in more detail in Chapter 4.

Understanding exactly how much risk is attributable to airborne transmission, and the extent to which risk can be attenuated by engineering controls, as opposed to behavioral and administrative controls, opens the door for well-informed exploration of building design and operation and other strategies to minimize transmission. Results from this proposed research respond to the Surgeon General's Call to Action to Promote Healthy Homes by driving an area of transdisciplinary research to launch "public health actions that will have a significant impact on health [through] a more holistic understanding of how housing affect's people's health" (Office of the Surgeon General (US), 2009). Results from this research directly respond to the Surgeon General's notion of using a "broad approach involving many disciplines," by providing an integrative framework for improving health indoors that involves engineers, epidemiologists, exposure scientists, behavioral scientists, and policy makers.

Figure 5.2 provides a basic representation of the form disease prevention recommendations could take given the achievement of improved risk quantification for airborne particles with the goal of suppressing the reproductive ratio for ARIs below one. The top right cloud shows that there is likely a threshold at which environmental controls alone cannot contain an outbreak, but it is unlikely that they will ever be used exclusively. Here we underscore that, as demonstrated by Nardell et al., 1991 in the case of TB, there exist potential limits to the extent that engineering controls alone can control transmission risk in shared air environments. Given that the extent of strategies to prevent the spread of one pathogen may not be the same for all pathogens it is important to quantify risk dynamics in indoor settings for a variety of pathogens. Measles, for instance, is highly contagious. Infected cases have been estimated to shed over on average 500 quanta per hour (Rudnick and Milton, 2003b). Based on this estimation, if the typical measles case were dropped in the University of Maryland dormitory roommate transmission scenario, they would infect a susceptible roommate at a similar probability as the maximum fine particle influenza shedder from Yan et al., 2018, in which case engineering-based controls may not provide much protection if any at all.

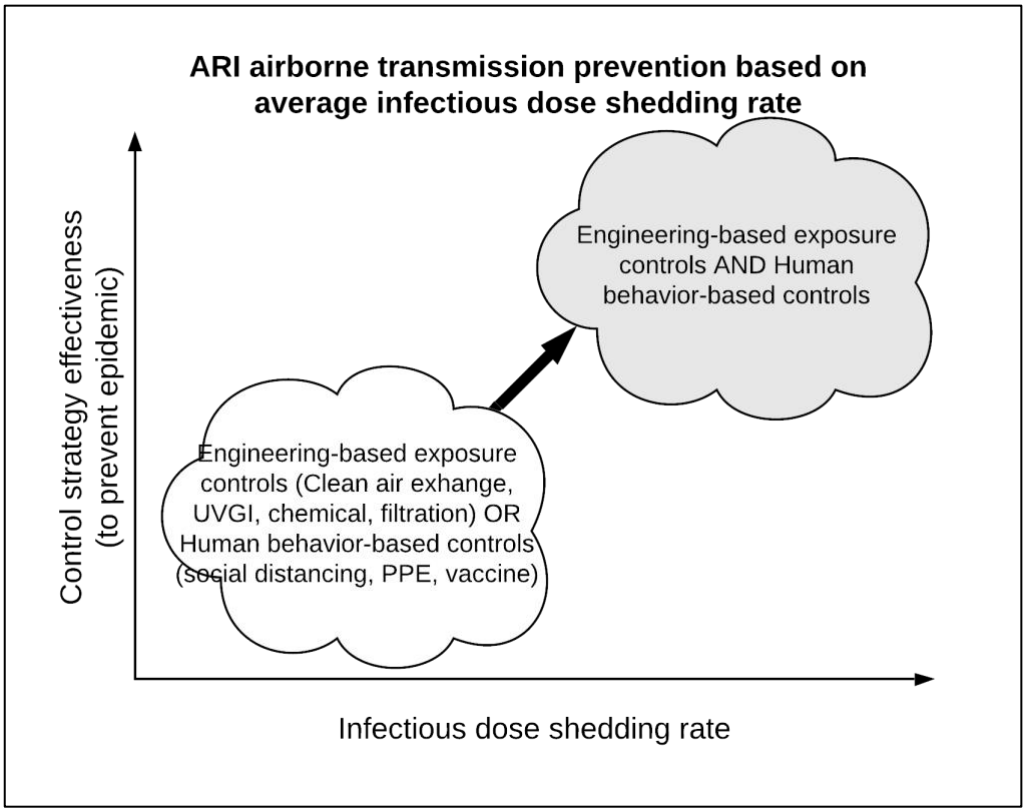

Figure 5.2. Population prevention strategies with increasing airborne transmission risk

Conclusions

The population health burden posed by influenza and other respiratory infections is expansive. The risk of emerging infectious diseases to initiate pandemics is greater than ever. This dissertation begins to fill a major knowledge gap and advances the field through improving understanding of airborne transmission risk. The long-term goal of this work is to increase the validity of quantum generation rate estimates, enable prediction of infection dynamics immunologically heterogeneous populations, and test the effectiveness of various strategies to minimize infections. With pandemics in mind, the idea is for the public health

community to gain the capacity to rapidly quantify viral shedding from early cases in an outbreak and characterize the probability of transmission through the airborne mode and mount and effective response. This is especially necessary in hospital setting with high exposure. PPE can be better recommended and enforced in cases where building design and airflow, ventilation, filtration, and other techniques are known to be inadequate in reducing risk to acceptable levels.

Completion of this work motivates studies to refine parameters of infection transmission and to strengthen methods to observe and understand the implications of viral shedding into exhaled breath aerosols. This proposal sets up future work to test the effectiveness of indoor air environmental controls on transmission, an area where little is known. Modelling studies on airflow and ventilation strategies to mitigate airborne pathogens (e.g., Gao et al., 2016) benefit from new information relating airborne exposure to risk that informs model parameters. Other future work will focus on the influence of vaccines, human immunity, and coinfections on susceptibility to infection and propensity for contagiousness.

Results from this dissertation show that CO_2 measurements can be effectively used in a risk assessment framework. This framework can be used in a variety of settings. In the long-term, CO_2 monitoring could promote a citizen science approach to tracking airborne exposures and risk across communities everywhere. It forms the basis for environmental justice work where indoor exposures may disproportionately affect some workplaces, housing developments, and communities. Future studies that examine the interaction between chemical

airborne particulate exposure and infectious disease exposure via the airborne mode could yield increasingly meaningful exposure models for predicting health outcomes. Particulates, volatile organic compounds, semi-volatile organic compounds, as well as thermal and psychological comfort are important considerations in buildings to prevent diseases and optimize cognitive function (Allen et al., 2016; Milton et al., 2000; Myatt et al., 2002).

It is becoming increasingly clear that the indoor environment has a major influence on health and well-being. New research is needed to better understand the design and operation standards to optimize human wellness in these indoor spaces. This body of future research is bound together by its translational nature in that it builds toward informing the improved design and remediation of indoor spaces, where humans spend over 90% of their time, to promote well-being, and to hamper preventable infections. This path of investigation inevitably links with fields of research promoting energy sustainability in built environments and research related to dual goals of optimizing ventilation for public health and reducing energy expenditures are not mutually exclusive (SeppĘnen, 2008).

APPENDICES

CHAPTER II SUPPLEMENTARY INFORMATION

EMIT Team Members

EMIT team members were: Walt Adamson, Blanca Beato-Arribas, Werner Bischoff, William Booth, Simon Cauchemez, Sheryl Ehrman, Joanne Enstone, Neil Ferguson, John Forni, Anthony Gilbert, Michael Grantham, Lisa Grohskopf, Andrew Hayward, Michael Hewitt, Ashley Kang, Ben Killingley, Robert Lambkin-Williams, Alex Mann, Donald Milton, Jonathan Nguyen-Van-Tam, Catherine Noakes, John Oxford, Massimo Palmarini, Jovan Pantelic, and Jennifer Wang. The Scientific Advisory Board members were: Allan Bennett, Ben Cowling, Arnold Monto, and Raymond Tellier.

SI.2 Appendices

Appendix 2.1. Efficacy of a Face Shield to Reduce Transmission of Influenza Virus in Large Droplets

Study Objective

The objective was to determine the efficacy of a face shield to selectively reduce transmission of large droplets containing viable influenza viruses without impeding droplet nuclei transfer in a mannequin model. The results of this study defined the feasibility of this intervention in selectively blocking such particles in a subsequent human-to-human influenza transmission study (EMIT).

Rationale

Large particle (> 10μm) behave as ballistic particles and will be stopped by a face shield while small particles (<5μm) can float over an extended period of time and distance and will be less effected by a face shield. It remains unknown how particles between 5 and 10μm will behave. Therefore, this study focused on the efficacy of a face shield in selectively blocking large particles from reaching the upper respiratory tract of human subjects while allowing small particles to enter.

Methods

Established human aerosol dispersal patterns were used to evaluate the effect of a face shield in filtering out the large droplet fraction carrying influenza. For this purpose, we produced a range of particles sizes (<1 to >100μm) of a live Influenza virus (H1N1 Influenza virus A/WS/33) using an airbrush system. The carrier

particle size was assessed in real time by an aerodynamic particle sizer (APS) for the particle range <1 to 20μm. Airborne virus was recovered by a six stage Andersen sampler with a styrofoam anatomical head placed on top allowing air to flow through a hose connecting the mouth opening to the sampler. The Styrofoam head allowed the anatomically correct positioning of the face shield to the mouth opening (Fisherbrand Full Face shield, Thermo Fisher Scientific Inc., Waltham, MA). Plaque forming units were counted by tissue culture plates (MDCK) for each sampler stage. The effect of a face shield was tested under the following conditions: absolute humidity (6·9 g/m3 [20°C, 40%RH]), air spray direction to face shield (straight, 90°), and air flow (none, 110ft/min). The face shield was modified during the trial to optimise small particle penetration while blocking large droplets. In addition to the virus exposure we also used latex beads of defined sizes (1, 5, 10, 15, 20, and 50μm) to conclusively determine the collection efficacy of our mannequin model. Beads were detected by flow cytometry (BD Accuri C6 system). Results are expressed in total counts and percent reduction of the viral/bead recovery load.

Endpoint

The endpoint was the percent reduction in viral air load through a face shield by <20% for small particles <5μm (droplet nuclei) and >90% for large particles > 10 μm (droplets). This was tested under the following conditions: air flow directions (straight vs. 90° turn, ***Figure S2.1***) and air velocities (no air movement vs. ~2·4 km/hour (Force 1 [Beaufort Scale description: light air] directed, turbulent airflow).

Results

Wearing a face shield led to a 98·8% (straight; ***Figure S2.2***) and 97·6% (90° rotated; ***Figure S2.3***) reduction in large particles >4·7μm ($p<0·05$) compared with not wearing a face shield and facing straight toward the source. Small particles <4·7μm were not significantly affected (0·7% reduction [straight, ***Figure S2.4***], 10·6% reduction [90° rotated, ***Figure S2.5***]) ($p>0·05$) compared with not wearing a face shield and facing straight toward the source. Generating a directional air flow reduced large particles by 68.0% (straight, ***Figure S2.2***) and 99·4% (90° turn, ***Figure S2.3***) without face shield, and 98·7% (straight, ***Figure S2.2***) and 99·5% (90° turn, ***Figure S2.3***) with face shield ($p<0·05$). With directional airflow, small particles were reduced by 73·0% (straight, ***Figure S2.4***) and 54·6% (90° turn, ***Figure S2.5***) without face shield, and 83·9% (straight, ***Figure S2.4***) and 84·7% (90° turn, ***Figure S2.5***) with face shield.

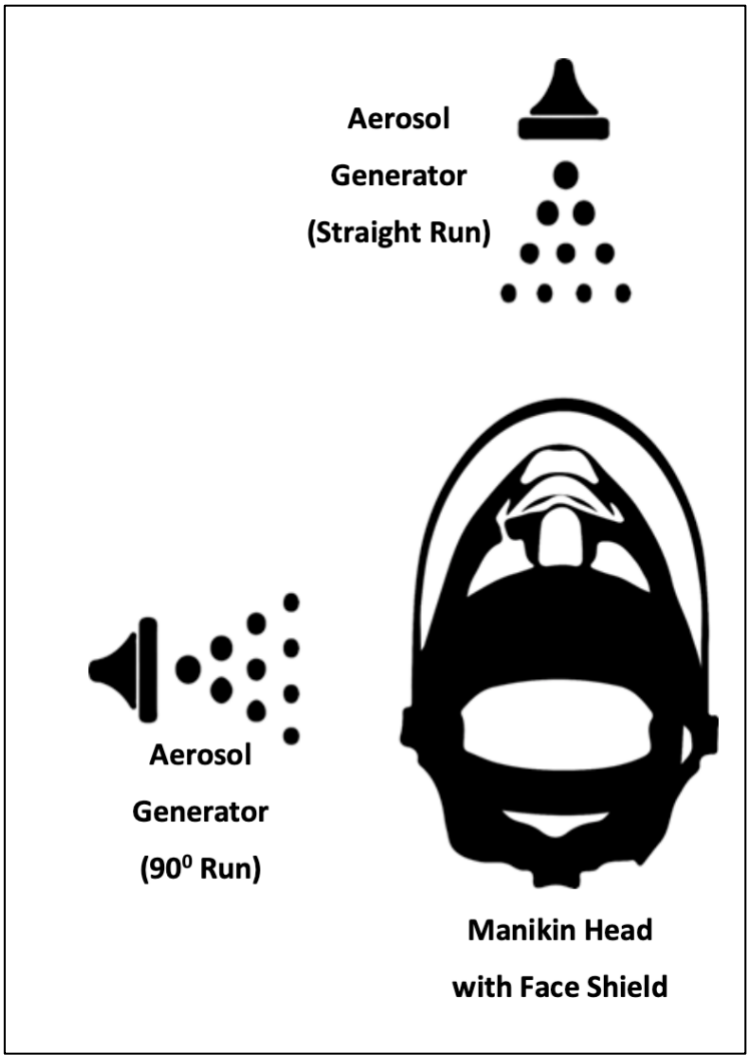

Figure S2.1. Straight and 90^{o} turn test conditions

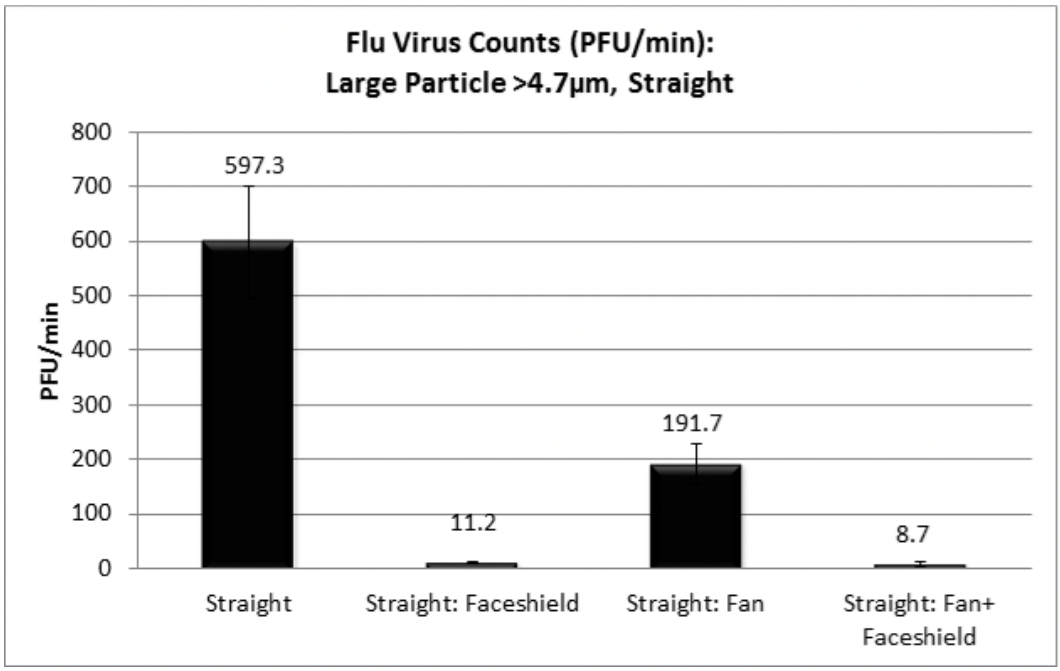

Figure S2.2. Effect of Face Shield on Virus Transmission - Large Particle >4·7µm, error bars = standard deviation

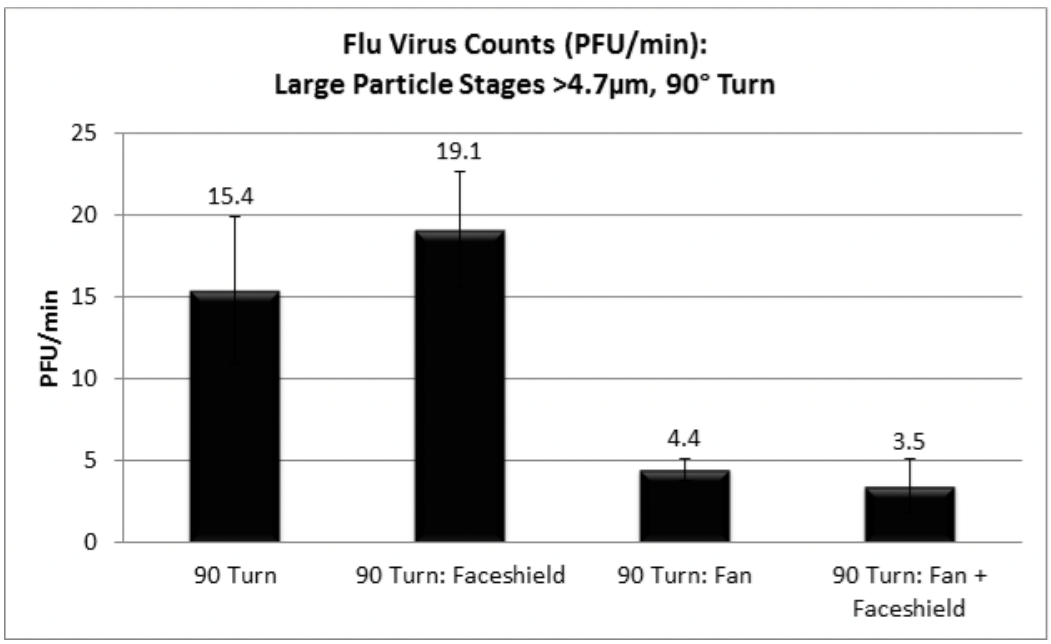

Figure S2.3. Effect of Face Shield on Virus Transmission - Large Particles >4·7µm 90° Turn, error bars = standard deviation

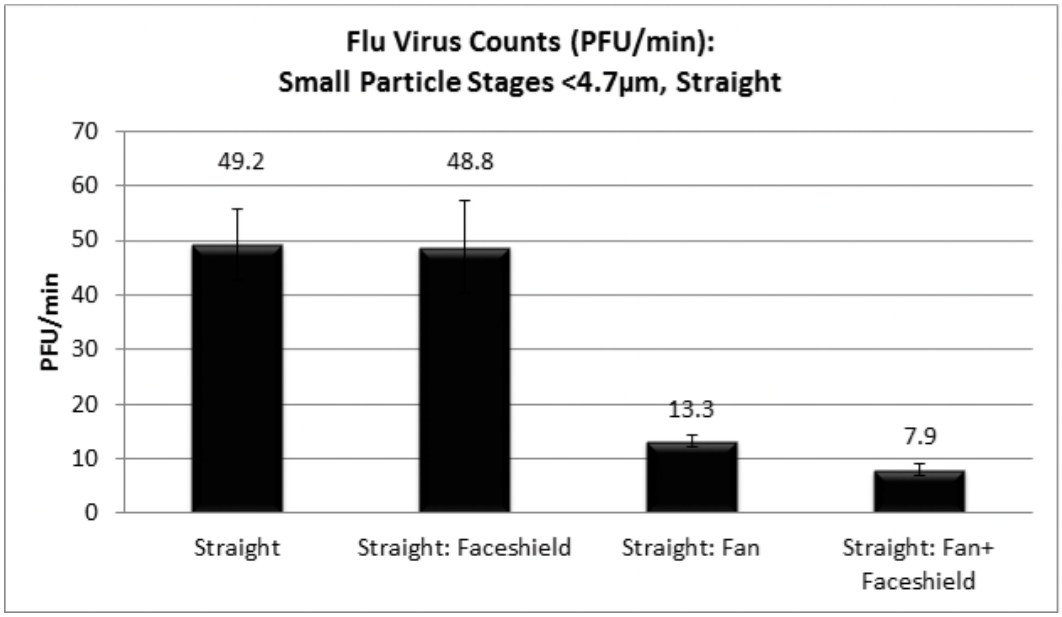

Figure S2.4. Effect of Face Shield on Virus Transmission - Small Particles < 4·7µm Straight Airflow, error bars = standard deviation

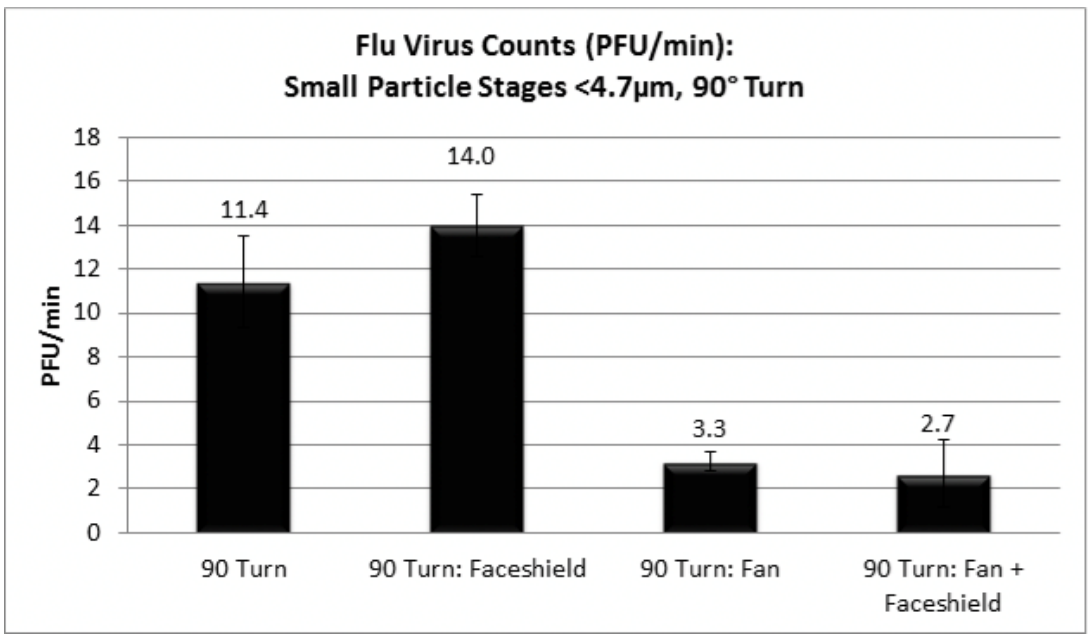

Figure S2.5. Effect of Face Shield on Virus Transmission - Small Particles <4·7µm 90° Turn, error bars = standard deviation

The collection of beads was broken down by bead size and detection in the Andersen sampler stages for small particle <4·7μm and large particle stages >4·7μm. The face shield reduced 1 μm beads by 11·4% (straight) and 43·3% (90° turn) in the small particle stages and by 99·6% (straight) and 37·9% (90° turn) in the large particle stages. Directional airflow increased bead recovery by 185·4% in the small particle stages and reduced collection by 32·7% in the 90° head position. An overall reduction of 1μm beads was noted in the large particle stages (-98·3% [straight], -28·2% (90° turn). Only less than seven 5 μm beads per run were detected in the small particle stages as expected. In the large particle stages the face shield reduced 5μm bead collection by 7·9% (straight) and 77·1% (90° turn). Airflow led to a reduction by 12·5% (straight) and an increase of 17·8% (90° turn). Based on the expected absence of 5 μm bead findings in the smaller particle stages only the results of the large particle stages are reported for the 10, 15, 20, and 50μm bead sizes. In summary, the face shield successfully reduced beads by 95·2 to 100% (straight) and 23·3 to 87·7% (90° turn). Directional airflow led to a recovery reduction by 97·9-98·5% (straight) and 53·2-100% (90° turn).

Conclusions

The face shield successfully blocked large particles >4·7μm from reaching the mouth and nose of a mannequin head while allowing passage of particles <4·7μm in a head-on air flow pattern in both virus and bead runs. Turning the head (90° rotation) significantly decreased the total virus detection compared to a head-on airflow pattern to very low concentrations (78.0-97·4%). Addition of a face shield while turned slightly increased the virus detection with face shield for both small

and large particles (22-24%), while bead counts >4·7μm decreased (23-86%). The effects were not significant indicating negligible changes due to the face shield at the low recovery level. Increase of the air flow (turbulent) led to a decrease in virus detection in both small and large particles (straight and 90° rotated). With a head-on airflow 1 μm beads increased, however larger beads decreased (>90% for 10-50 μm beads). Combined with a 90° turn 1 to 50 μm beads decreased.

The modified face shield met the endpoint by reducing virus particles >10 μm by more than 90% while maintaining exposure to particles <5μm (<20% reduction). Turning the head perpendicular to the exposure source alone led to a substantial reduction of the overall virus recovery negating any significant effects of the face shield. The method of blocking selected particle sizes from reaching the human respiratory tract through a face shield is feasible and can be used to study virus transmission routes in human exposure studies.

Appendix 2.2. Full inclusion and exclusion criteria

Inclusion

- Age 18 to 45 years, inclusive.
- In good health with no history of major medical conditions from medical history, physical examination, and routine laboratory tests as determined by the Investigator by a screening evaluation.
- A total body weight ≥50 kg and a body mass index (BMI) >18 (if BMI is >32, a body fat percentage within WHO and NIH range for gender and age). BMI [kg/m^2] = Body weight [kg] ÷ Height^2 [m^2].
- Non-sterilised males must agree to refrain from fathering a child from the point of entering Quarantine until the day 28 follow up visit by using an effective method of contraception.
- Sexually active females of child-bearing potential must agree to use 2 effective methods of avoiding pregnancy that are deemed to be effective from the point of entry into the Quarantine unit until the day 28 follow up visit.
- An informed consent document signed and dated by the subject and investigator.
- HAI titre ≤10 against challenge virus

Exclusion

- Subjects who have a significant history of any tobacco use at any time (≥ total 10 pack
- year history, e.g. one pack a day for 10 years).
- Subjects who are pregnant or nursing, or who have a positive pregnancy test at any point in the study.

- Presence of any significant acute or chronic, uncontrolled medical illness (full list available on request), that in the view of the Investigator(s), is associated with increased risk of complications of respiratory viral illness.
- Abnormal pulmonary function in the opinion of the investigator as evidenced by clinically significant abnormalities in spirometry.
- History or evidence of autoimmune disease or known immunocompromise of any cause.
- Subjects with any history of asthma, COPD, pulmonary hypertension, reactive airway disease, or any chronic lung condition of any aetiology. The history of childhood asthma until and including the age of 12 is acceptable.
- Positive human immunodeficiency virus (HIV), hepatitis B (HBV), or hepatitis C (HCV) screen.
- Any significant abnormality altering the anatomy of the nose or nasopharynx.
- Any clinically significant history of epistaxis (nose bleeds).
- Any nasal or sinus surgery within 6 months of inoculation.
- Recent (within the last 3 years of the screening visit) and/or recurrent history of clinically significant autonomic dysfunction (e.g. recurrent episodes of fainting, palpitations, etc.).
- Any laboratory test or ECG which is abnormal and deemed by the investigator(s) to be clinically significant.
- Confirmed positive test for class A drugs or alcohol that cannot be satisfactorily explained (e.g. recent use of codeine tablets).
- Venous access deemed inadequate for the phlebotomy (and IV infusion) demands of the study.

- Subjects symptomatic with hayfever on admission into the unit for a quarantine session or prior to inoculation will be excluded.
- Any known allergies to the excipients in the challenge virus inoculums.
- Health care workers (including doctors, nurses, medical students and allied healthcare professionals) anticipated to have patient contact within two weeks of human viral challenge. Healthcare workers should not work with patients until 14 days after challenge or until their symptoms are fully resolved (whichever is the longer). In particular, any health care workers who work in units housing elderly, disabled or severely immunocompromised patients (e.g. bone marrow transplant units) will be excluded from participating in the study.
- Presence of household member or close contact (for an additional 2 weeks after discharge from the isolation facility) who: is less than 3 years of age; has known immunodeficiency; is receiving immunosuppressant medication; is undergoing or soon to undergo cancer chemotherapy within 28 days of viral inoculation; has been diagnosed with emphysema or chronic obstructive pulmonary disease (COPD), is elderly and resides in a nursing home, or who has severe lung disease or another significant medical; has received a bone marrow or solid organ transplant
- Intending to travel within the next 3 months (to countries for which travel vaccinations are recommended).
- Those employed or immediate relatives of those employed at RVL or staff and students working directly in or for any of the units in which the Chief Investigator works.
- Receipt of blood or blood products, or loss (including blood donations) of 450 mL or more of blood, during the 3 months prior to inoculations.

- Acute use i.e. within 7 days prior to human viral challenge of any medication or other product (prescription or over-the-counter), for symptoms of hayfever, rhinitis, nasal congestion or respiratory tract infection.
- Receipt of any investigational drug within 3 months prior inoculation
- Receipt of more than 4 investigational drugs within the previous 12 months
- Prior participation in a clinical trial with the same strain of respiratory virus.
- Participation in any other respiratory virus challenge within 1 year prior to challenge.
- Receipt of systemic glucocorticoids, antiviral drugs, and immunoglobulins or any other cytotoxic or immunosuppressive drug within 6 months prior to dosing. Receipt of any systemic chemotherapy agent at any time.
- Presence of significant respiratory symptoms existing on the day of challenge or between admission for challenge and challenge with / exposure to virus.
- History suggestive of respiratory infection within 14 days prior to admission for challenge / exposure.
- Any other finding in the medical interview, physical exam, or screening investigations that, in the opinion of the investigator, GP or sponsor, deem the subject unsuitable for the study.

Power Calculation

Having achieved a secondary attack rate (SAR) of 25% in the 'proof-of-concept' study,(Killingley et al., 2012) we assumed that with increased numbers of donors per room, improved environmental control (temperature, humidity, ventilation rate), and a longer exposure time (increased from 2 days in the proof-of-concept study to 4 days) we would achieve an SAR of 40%. Based on a predicted SAR of

40% in CR and to detect a reduction of 50% (the magnitude of difference specified by the funder) in the IR group (i.e. a modified SAR of 20%), the statistical power of the overall experiment was estimated by conducting a computer simulation.

Handling of Breath Samples

Concentration of fine aerosol samples and extraction of coarse aerosol samples were performed at the quarantine site. All samples were stored at -80˚C, shipped to the University of Maryland on dry ice, and stored at -80˚C until analysis.

Outcome Definitions

Symptoms 'lasting ≥24 hours', were considered present if reported on 3/3 symptom observations within a single day, or over two consecutive days at any frequency (i.e., occurring ≥1 out of 3 symptom observations on 2 consecutive days). Fever was defined as temperature >37·9 ºC.

Appendix 2.3. Baseline Characteristics

Table S2.1 shows the baseline characteristics of the study volunteers, which were randomized as viral Donors (D), Intervention Recipients (IR), and Control Recipients (CR).

Table S2.1. Baseline Characteristics

	D (N=52)	IR (N=40)	CR (N=35)
Gender			
Female	15 (28.8%)	13 (32.5%)	12 (34.3%)
Male	37 (71.2%)	27 (67.5%)	23 (65.7%)
Age			
Median (Q1, Q3)	30 (25, 38)	28 (24, 34)	27 (25, 36)

Appendix 2.4. Trial profile

Figure S2.6 gives a summary of the screening and randomisation of the trial groups.

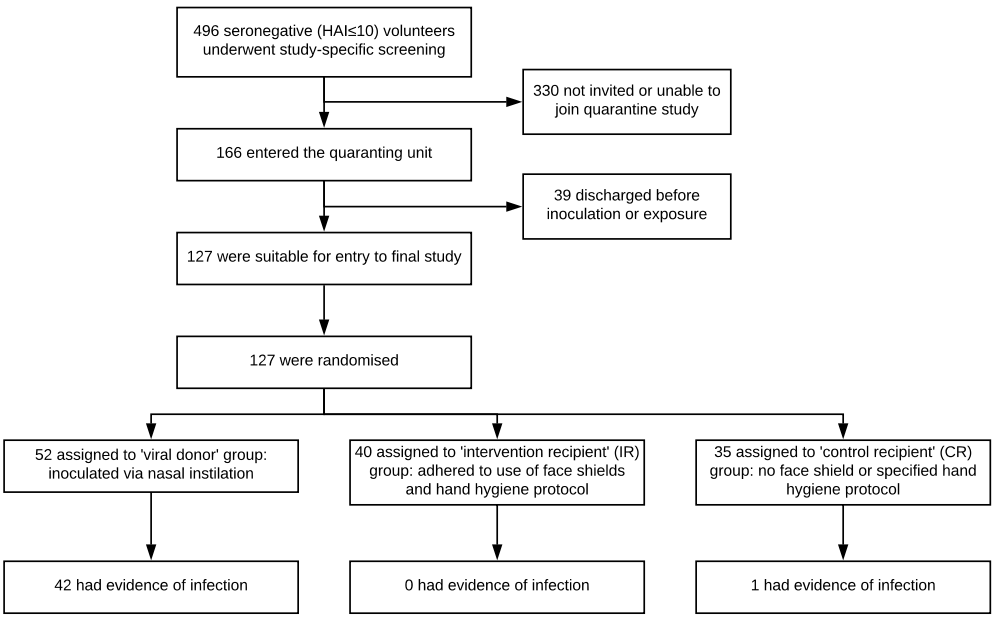

Figure S2.6. Trial profile

Appendix 2.5. Comparing the Current Study and Proof-of-Concept Study Using Current Outcome Criteria and Applying Infection Criteria from The Proof of Concept Study

As shown in Results, the observed SAR in the current study was significantly below the expected 16% SAR that would have resulted from a doubling of the proof-of-concept SAR in response to design changes including doubling the number of Donors per Recipient and doubling the number of days of Recipient exposure to Donors. The observed SAR was also lower, but not significantly different from the 8·3% (1/12) observed in the proof of concept study, applying the main study infection criteria to the proof of concept study data (proof-of-concept v overall p = 0·26, proof-of-concept v CR p = 0·45, and proof-of-concept v IR p = 0·23).

The proof of concept study published by Killingley and colleagues (2012) used less stringent qRT-PCR-based infection classification criteria. Whereas the current study required two days of qRT-PCR positive nasopharyngeal swabs, the proof of concept study required just a single day of PCR or culture positive nasal wash or throat swab. Seroconversion criteria for infection was the same for both studies. None of the recipients from the proof of concept study were culture positive, two had a single day each of PCR positive nasal wash, and one had evidence of seroconversion. The recipients with single PCR positive washes did not seroconvert and the seroconversion did not have a positive wash. The PCR criteria were tightened because a single positive PCR, especially with high Ct values and

without concomitant seroconversion, could represent random laboratory errors and because it is not clear that they represent true infection.

If we were to apply the proof-of-concept study's infection classification criteria to the main quarantine transmission study, we would have observed 2 more infected donors and 2 more infected CR. ***Tables S2.2*** and ***S2.3*** reproduce ***Tables 2.1*** and **2.*3*** from the manuscript main text (Donor and Recipient status, respectively), but apply the infection criteria used in the proof of concept study.

Table S2.2. Donor Status using infection criteria from proof of concept study

		Clinical Illness (% of Infected)			Laboratory Confirmed Infection Criteria (% of Infected)		
Quarantine #	Infected/Inoculated (%)	Symptomatic	Febrile	ILI	PCR Confirmed Infection	PCR Confirmed Infection and Seroconversion	Seroconversion by HAI : MN : Either
1	15/20 (75)	11 (73)	4 (27)	8 (53)	13 (87)	12 (80)	12 : 14 : 14
2	11/12 (92)	7 (64)	0 (0)	5 (45)	11 (100)	9 (82)	9 : 7 : 9
3	18/20 (90)	16 (89)	2 (11)	14 (78)	17 (94)	13 (72)	14 : 11 : 14
Total	44/52 (85)	34 (77)	6 (14)	27 (61)	41 (93)	34 (77)	35 : 32 : 37

Table S2.3. Recipient Status using infection criteria from proof of concept study

			Clinical Illness (% of Exposed)			Laboratory Confirmed Infection Criteria (% of Exposed)		
Quarantine #	Recipient Classification	Infected/ Exposed (%)	Symptomatic	Febrile	ILI	PCR Confirmed Infection	PCR Confirmed Infection and Seroconversion	Seroconversion by HAI : MN : Either
1	Control (CR)	0/11 (0)	4 (36)	0 (0)	3 (27)	0 (0)	0 (0)	0 : 0 : 0
	Intervention (IR)	0/10 (0)	2 (20)	0 (0)	1 (10)	0 (0)	0 (0)	0 : 0 : 0
2	Control (CR)	3/9 (33)	2 (22)	0 (0)	2 (22)	2 (22)	0 (0)	1 : 1 : 1
	Intervention (IR)	0/10 (0)	3 (30)	0 (0)	2 (20)	0 (0)	0 (0)	0 : 0 : 0
3	Control (CR)	0/15 (0)	6 (40)	0 (0)	4 (27)	0 (0)	0 (0)	0 : 0 : 0
	Intervention (IR)	0/20 (0)	6 (30)	0 (0)	2 (10)	0 (0)	0 (0)	0 : 0 : 0
Total	Control (CR)	3/35 (9)	12 (34)	0 (0)	9 (26)	2 (6)	0 (0)	1 : 1 : 1
	Intervention (IR)	0/40 (0)	11 (28)	0 (0)	5 (12)	0 (0)	0 (0)	0 : 0 : 0

The original proof of concept reported an SAR of 25% (3/12). If we were to apply the less stringent, proof of concept infection criteria to the main study, we would observe an overall SAR of 4%, with three infections among CR and zero among IR. This represents a significant difference between the proof-of-concept and the main study overall ($p = 0{\cdot}03$), in contrast to the non-significant difference between studies using the more stringent outcome criteria. The difference between the proof-of-concept and the CR group ($p = 0{\cdot}16$ would continue to fall short of being statistically significant. However, the main study was designed to more than double the exposure and thus the expected SAR. Thus, in comparison with an expected SAR of 50%, the observed SAR was significantly lower (4% overall, $p < 0{\cdot}0001$; and 9% among CR, $p < 0{\cdot}0001$). The observed is similarly statistically significantly lower than the more conservative expected SAR of 40% used in the power calculations.

These alternate approaches to the outcome criteria produced similar results. Using the less stringent criteria increased the level of statistical significance showing that the difference between the larger challenge-transmission experiment and the proof-of-concept experiment was not driven by choice of outcome criteria.

CHAPTER III SUPPLEMENTARY INFORMATION

SI.3 Tables

Table S3.1. Unadjusted odds ratios on shedding into fine aerosols above LOD

Predictor	Experimental OR (95% CI)	Natural OR (95% CI)	Combined Groups OR (95% CI)
Age	1.05 (0.92-1.19)	0.98 (0.93-1.04)	**0.9 (0.85-0.95)**
Sex	-	2.22 (0.99-4.97)	1.19 (0.62-2.29)
Study day*			
Day 1	-	REF	-
Day 2	REF	0.25 (0.06-1.03)	-
Day 3	50.89 (0.07-36,036.30)	**0.17 (0.04-0.73)**	-
Day 4	0 (0-7.51)	-	-
Febrile >37.9ºC	4.51 (0.48-42.28)	0.87 (0.35-2.18)	1.64 (0.72-3.71)
Temperature (C)	4.77 (0.94-24.17)	1.88 (0.87-4.06)	**6.11 (3.11-12)**
Upper respiratory symptom score	**2.24 (1.07-4.69)**	1.07 (0.93-1.22)	**1.42 (1.26-1.61)**
Lower respiratory symptom score	**6.49 (1.14-37.09)**	**1.35 (1.04-1.76)**	**2.12 (1.67-2.69)**
Systemic symptom score	1.73 (0.94-3.16)	1.15 (0.97-1.36)	**1.56 (1.34-1.82)**
Total symptom score	**1.64 (1.09-2.47)**	1.07 (0.99-1.15)	**1.21 (1.13-1.29)**
Cough score (as continuous)	**7.49 (1.28-43.91)**	**1.9 (1.2-2.99)**	**3.44 (2.32-5.09)**
Cough (as factor)			
No symptom	REF	REF	REF
Mild	**7.49 (1.28-43.91)**	8.5 (0.81-88.85)	**10.54 (4.1-27.11)**
Moderate	-	**12.92 (1.32-126.08)**	**23.69 (9.31-60.28)**
Severe	-	**20.4 (2.06-202.21)**	**37.4 (14.15-98.84)**
Cough count	**1.29 (1.02-1.62)**	**1.02 (1-1.04)**	**1.07 (1.04-1.09)**
Nasopharyngeal swab Ct value	**0.74 (0.6-0.92)**	0.98 (0.91-1.05)	**0.89 (0.84-0.94)**

* Study day refers to day post nasal inoculation for experimentally infected cases with a range of 1-4. For naturally infected cases, study day refers to day post symptom onset with a range of 1-3. No fine aerosol shedding was observed on day 1 post inoculation for experimentally infected cases. Because of differences in meaning for the study day variable between groups, combined estimates are not given.

Using all exhaled breath observations for the 39 experimental and 83 natural infections (N=84, 146, respectively and 230 combined). Effect of a single unit increase in temperature or symptom scores. Effect of febrile compares ever febrile>37.9ºC to afebrile. Effect of sex compares male to female. Bolded values are significant at p=0.05. Only males shed into aerosols in the experimental group.

Predictor	Experimental OR (95% CI)	Natural OR (95% CI)	Combined Groups OR (95% CI)

Cough scores of 2 or 3 were never observed in the experimental group. Limit of detection (LOD) for influenza A aerosols was 500. Per Yan et al., 2018, LOD represents "the most dilute sample that gave a positive result in any replicate."

Table S3.2 (part 1/3). Quality of covariate balance after propensity score adjustment

	Model 1*		Model 2		Model 3		Model 4		Model 5	
Approach	**Stand. Dif.**	**Var. Rat.**	**Stand. Dif.**	**Var. Rat.**	**Stand. Dif.**	**Var. Rat.**	**Stand. Dif.**	**Var. Rat.**	**Stand. Dif.**	**Var. Rat.**
No adjustment	(-125.6, 288.9)	(0.7, 19.2)	(-125.6, 288.9)	(0.7, 19.2)	(-125.6, 288.9)	(0.7, 19.2)	(-125.6, 288.9)	(0.7, 19.2)	(-125.6, 288.9)	(0.7, 19.2)
1:1 Propensity Matching **	(-305.3, 130.6)	(0.4, 8.0)	(-312.6, 129.5)	(0.1, 8.2)	(-305.3, 130.6)	(0.4, 8.0)	(-312.6, 127.2)	(0.2, 9.6)	(-312.6, 129.5)	(0.1, 8.2)
Propensity subclassification by stratification***										
Sextile 1	(-128.2, 425.6)	(0.0, 6.4)	(-128.2, 425.6)	(0.0, 6.4)	(-138.2, 425.6)	(0.0, 6.4)	(-128.2, 425.6)	(0.0, 6.4)	(-128.2, 425.6)	(0.0, 6.4)
Quintile 1	(-156.4, 362.0)	(0.2, 3.0)	(-156.4, 364.4)	(0.2, 6.7)	(-156.4, 362.0)	(0.2, 7.2)	(-156.4, 362.0)	(0.0, 6.4)	(-156.4, 364.4)	(0.0, 6.7)
Quartile 1	(-175.5, 335.4)	(0.1, 2.8)	(-170.7, 237.8)	(0.1, 2.1)	(-175.5, 335.4)	(0.1, 8.0)	(-167.6, 246.4)	(0.1, 6.2)	(-170.7, 237.8)	(0.1, 7.8)
Tertile 1	(-180.5, 260.0)	(0.1, 5.1)	(-177.4, 245.6)	(0.1, 2.7)	(-180.5, 257.0)	(0.1, 5.1)	(-177.4, 261.3)	(0.1, 5.5)	(-178.4, 252.4)	(0.1, 5.9)
Propensity Weighting, ATT****	(-165.7, 237.3)	(1.1, 16.7)	(-195.2, 221.1)	(4.8, 14.7)	(-164.6, 237.6)	(1.1, 16.8)	(-125.2, 243.4)	(0.6, 24.3)	(-193.0, 222.5)	(2.6, 14.6)
Propensity Weighting, ATE*****	(-139.3, 190.6) Mean:105.2	(1.0, 12.4)	(-139.8, 185.5) Mean: 113.7	(1.9, 12.7)	(-138.9, 190.4) Mean: 105.2	(1.0, 12.5)	(-125.6, 185.4) Mean: 111.4	(0.6, 15.9)	(-139.0, 185.5) Mean: 113.9	(1.2, 12.9)

* Range across all covariates (not only covariates in the propensity score model)

** Greedy match: experimentally infected were selected randomly, one by one and matched with the observation in the naturally infected group that had the nearest linear propensity score.

*** Bottom quantiles reported only: Only bottom quantiles for stratification by sextiles, quintiles, quartiles, and tertiles had enough samples in both groups to take standardized differences and variance ratios for all covariates.

**** ATT. Average treatment effect for the treated (where naturally infected cases are considered "treated")

***** Propensity weighting by ATE (average treatment effect approach, where naturally infected cases are considered "treated") consistently provided the best balance between groups. For this reason, mean absolute standardized differences are given to provide an additional indicator of balance beyond standardized difference ranges.

Model 1 covariates: lower respiratory score, cough score, cough count
Model 2 covariates: lower respiratory score, cough score, cough count, upper respiratory score
Model 3 covariates: lower respiratory score, cough score, cough count, NP swab ct value
Model 4 covariates: lower respiratory score, cough score, cough count, body temperature
Model 5 covariates: lower respiratory score, cough score, cough count, upper respiratory score, nasopharyngeal swab Ct value

Table S3.2 (part 2/3). Quality of covariate balance after propensity score adjustment

	Model 6		Model 7		Model 8		Model 9		Model 10	
Approach	**Stand. Dif.**	**Var. Rat.**	**Stand. Dif.**	**Var. Rat.**	**Stand. Dif.**	**Var. Rat.**	**Stand. Dif.**	**Var. Rat.**	**Stand. Dif.**	**Var. Rat.**
No adjustment	(-125.6, 288.9)	(0.7, 19.2)	(-125.6, 288.9)	(0.7, 19.2)	(-125.6, 288.9)	(0.7, 19.2)	(-125.6, 288.9)	(0.7, 19.2)	(-125.6, 288.9)	(0.7, 19.2)
1:1 Propensity Matching	(-278.5, 126.0)	(0.3, 8.4)	(-287.8, 126.0)	(0.3, 8.4)	(-385.5, 132.9)	(0.2, 8.4)	(-557.0, 124.9)	(0.2, 7.4)	(-421.7, 132.9)	(Inf, 8.4)
Propensity subclassification by stratification										
Sextile 1	(-128.2, 425.6)	(0.0, 1.2)	(-128.2, 425.6)	(0.0, 1.2)	(-166.9, 319.8)	(0.0, 5.2)	(-129.3, 505.3)	(0.0, 3.4)	(-147.3, 406.5)	(0.0, 5.9)
Quintile 1	(-153.7, 218.9)	(0.1, 3.3)	(-156.4, 364.4)	(0.0, 2.4)	(-151.9, 341.6)	(0.0, 3.7)	(-144.0, 401.8)	(0.0, 10.1)	(-167.0, 435.9)	(0.0, 7.9)
Quartile 1	(-166.0, 237.8)	(0.1, 3.0)	(-166.0, 237.8)	(0.3, 3.1)	(-174.4, 334.2)	(0.0, 4.3)	(-158.7, 364.1)	(0.0, 9.7)	(-174.4, 348.0)	(0.0, 6.1)
Tertile 1	(-177.4, 250.2)	(0.1, 2.5)	(-175.6, 242.1)	(0.1, 3.2)	(-185.3, 335.6)	(0.1, 6.4)	(-174.4, 361.4)	(0.0, 8.7)	(-186.1, 276.2)	(0.1, 6.4)
Propensity Weighting, ATT	(-163.3, 232.8)	(0.4, 23.5)	(-157.8, 133.8)	(0.6, 56.1)	(-164.8, 233.4)	(0.7, 15.8)	(-107.8, 240.4)	(0.3, 18.5)	Only 1 experimental case used	Only 1 experimental case used
Propensity Weighting, ATE	(-130.5, 184.4) Mean:121.8	(1.0, 14.9)	(-128.5, 179.0) Mean: 123.1	(0.9, 17.2)	(-136.3, 177.6) Mean: 104.1	(1.0, 12.3)	(-101.1, 169.3) Mean: 101.4	(1.1, 17.1)	(-117.6, 179.4) Mean: 104.0	(0.9, 21.2)

Model 6 covariates: lower respiratory score, cough score, cough count, upper respiratory score, body temperature
Model 7 covariates: lower respiratory score, cough score, cough count, upper respiratory score, NP swab ct value , body temperature
Model 8 covariates: cough and cough count
Model 9 covariates: cough count and body temperature
Model 10 covariates: cough, cough count and body temperature

Table S3.2 (part 3/3). Quality of covariate balance after propensity score adjustment

	Model 11		Model 12		Model 13		Model 14	
Approach	**Stand. Dif.**	**Var. Rat.**	**Stand. Dif.**	**Var. Rat.**	**Stand. Dif.**	**Var. Rat.**	**Stand. Dif.**	**Var. Rat.**
No adjustment	(-125.6, 288.9)	(0.7, 19.2)	(-125.6, 288.9)	(0.7, 19.2)	(-125.6, 288.9)	(0.7, 19.2)	(-125.6, 288.9)	(0.7, 19.2)
1:1 Propensity Matching	(-363.5, 132.9)	(0.23, 8.4)	(-574.5, -9.2)	(0.1, 8)	(-417.8, 129.5)	(0.2, 9.4)	(-295.9, 110.1)	(0.3, 11.2)
Propensity subclassification by sextiles								
Sextile 1	(-158.1, 329.9)	(0.00, 4.9)	(-212.1, 369.6)	(0.0, 5.8)	(-224.1, 235.2)	(0.0, 5.6)	(-200.1, 240.5)	(0.0, 9.1)
Quintile 1	(-171.4, 350.9)	(0.00, 4.3)	(-174.6, 358.2)	(0.3, 4.8)	(-194.8, 232.4)	(0.2, 4.3)	(-161, 236.2)	(0.2, 3.4)
Quartile 1	(-175.8, 256.4)	(0.13, 4.7)	(-174.6, 358.2)	(0.3, 4.8)	(-199.6, 226.9)	(0.4, 6.6)	(-174.2, 213.4)	(0.1, 4.4)
Tertile 1	(-152.5, 233.0)	(.23, 5.1)	(-184.9, 331.2)	(0.1, 9.0)	(-141.3, 219.3)	(0.3, 7.3)	(-140.5, 228.6)	(0.3, 4.3)
Propensity Weighting, ATT	(-164.2, 182.8)	(1.2, 59.1)	(-78.9, 263.5)	(0.6, 22.1)	(-80.8, 284.2)	(0.6, 67.9)	(-41.5, 187.3)	(1.7, 537.4)
Propensity Weighting, ATE	(-131.1, 176.6) Mean: 99.4	(0.9, 24.0)	(-87.9, 162.2) Mean: 90.1	(1.2, 19.3)	(-85.2, 179.1) Mean: 86.9	(1.0, 29.1)	(-83.7, 157.6) Mean: 105.1	(1.0, 30.8)

Model 11 original covariates: lower respiratory score, age, cough, cough count, upper respiratory score, systemic symptom score, NP ct value, body temperature (Algorithm did not converge, so chose new model 11 covariates.)

Model 11 new covariates: cough score, body temperature (Variables were dropped from the original model 11 specification one by one, in order of lowest effect strength to highest; algorithm failed to converge until I arrived at the new model 11 specification.)

Model 12 covariates: fever and body temperature

Model 13 covariates: fever, body temperature, and upper respiratory symptom score

Model 14 covariates: febrile, body temperature, and total symptom score

Note: Adding cough count to model 14 did not improve the population balance after ATE weighting.

SI.3 Figures

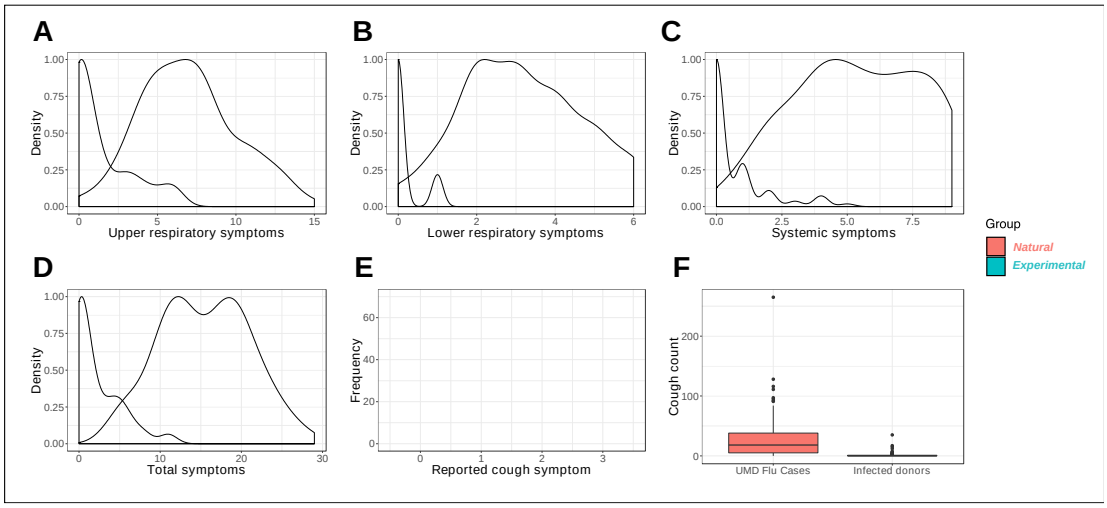

Figure S3.1. Comparison of self-reported symptoms and observed cough counts with all observations. From N=84 experimental, and N=146 natural infection sample days where aerosols were also collected. Density plots, scaled so that the highest value for a single moment is equal to one, compare (**A**) upper respiratory symptoms (runny nose, stuffy nose, sneezing, sore throat, and earache, score range 0-15), (**B**) lower respiratory symptoms (shortness of breath, and cough, score range 0-6), and (**C**) systemic symptoms (malaise, headache, muscle/joint ache, score range 0-9). (**D**) Total symptom score (range 0-30). (**E**) Cough symptom score (range 0-3). (**F**) Observed cough counts with boxes showing the inner-quartile range (IQR) with a band to indicate the median, and whiskers extending to the highest and lowest data points within 1.5 IQR.

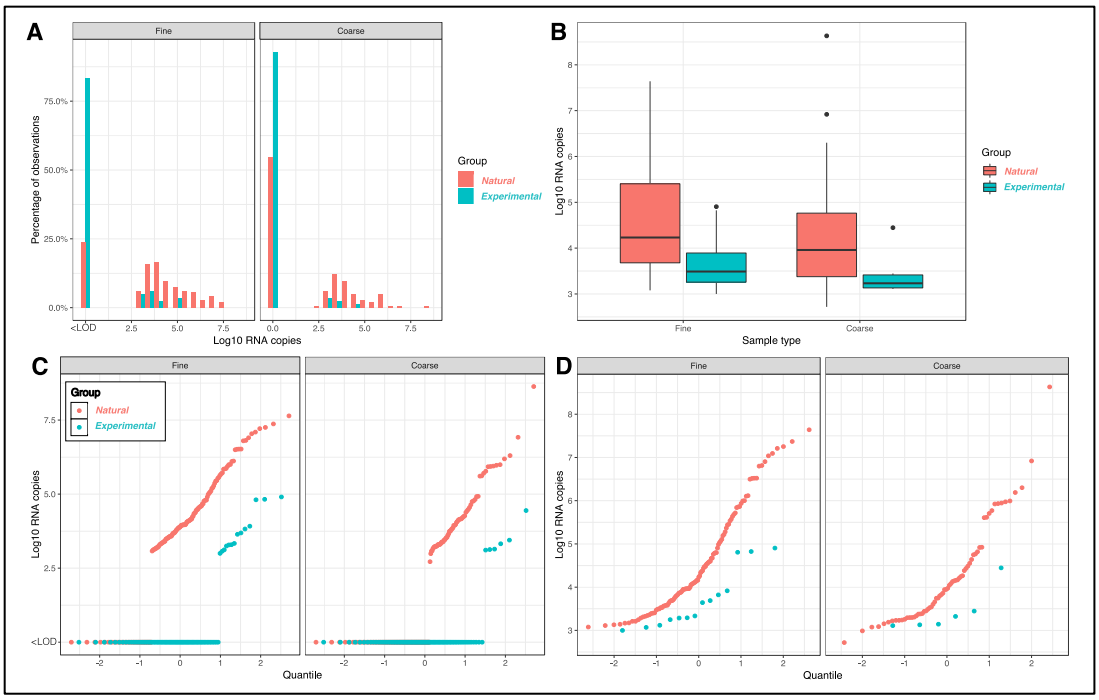

Figure S3.2. Comparison of natural and experimental RNA copy shedding into fine and coarse aerosols. (**A**) Histogram of RNA copies shed into fine and coarse aerosols. (**B**) Boxplot comparison by group and aerosol fraction includes all positive samples. Scatter plots of log10 RNA copies in ascending order (along x-axis) of shed into aerosols over quantiles (relative to experimental or naturally infected group, with normal distribution assumed): (**C**) samples below LOD plotted as zero; (**D**) plotted after deletion of samples below LOD.

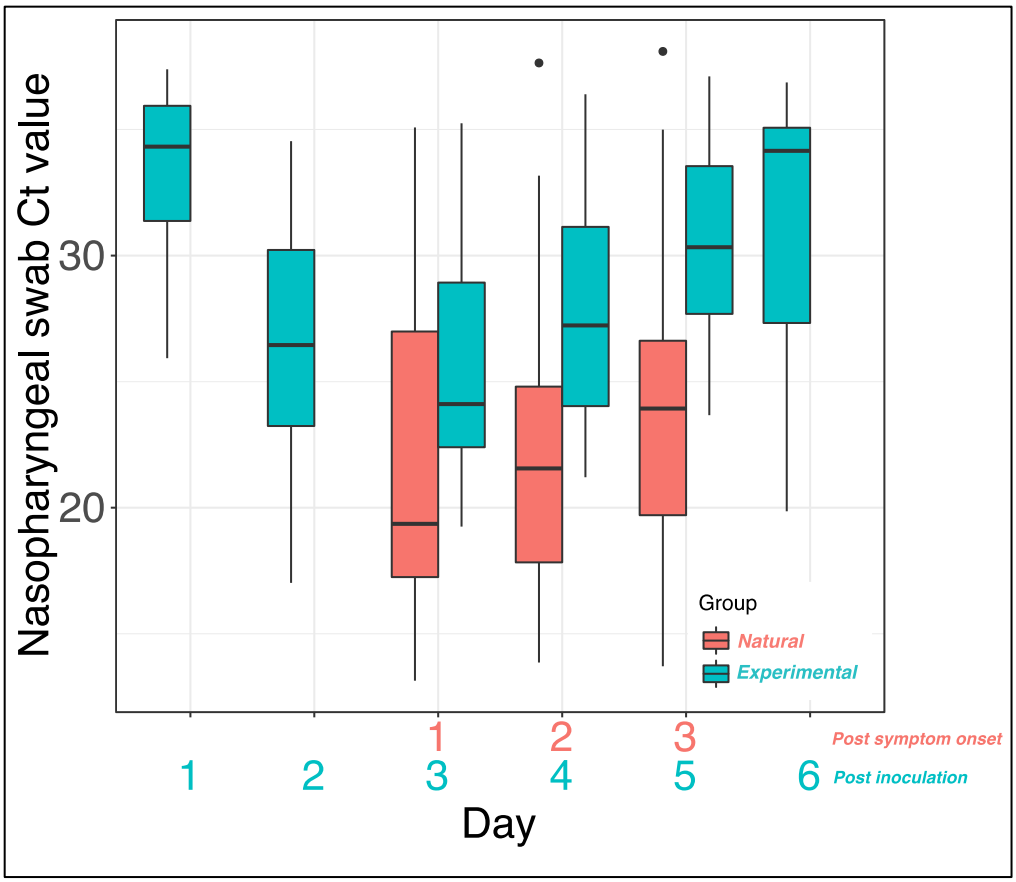

Figure S3.3. Nasopharyngeal swab Ct values over time. Includes all qRT-PCR detectable nasopharyngeal swab samples during days 1-6 post-inoculation, and days 1-3 post symptom onset for experimental and naturally infected cases, respectively. Boxes show the inner-quartile range (IQR) with a band to indicate the median, and whiskers extending to the highest and lowest data points within 1.5 IQR.

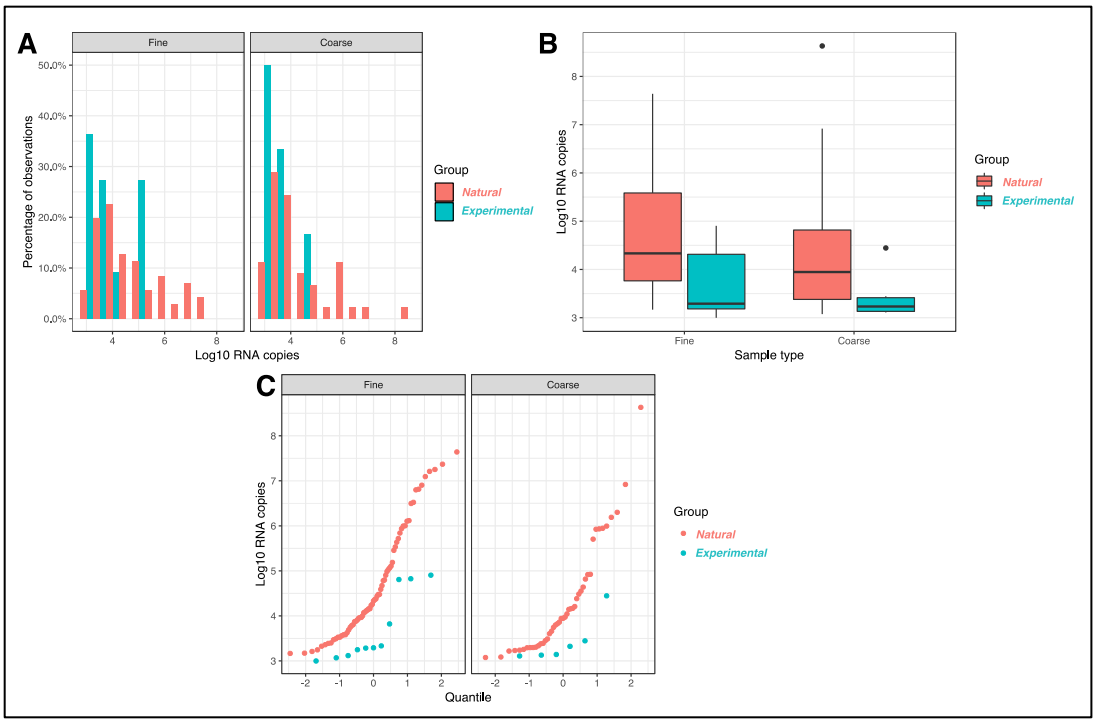

Figure S3.4. Maximum fine and coarse aerosol shedding, limited to samples above LOD, (**A**) histogram of RNA copies shed into fine and coarse aerosols, (**B**) RNA shedding comparison by group and aerosol fraction, (**C**) RNA shedding quantity of samples by quantile for each group and aerosol fraction.

SI.3 Appendices

Appendix 3.1. Selection of naturally infected cases for analysis from larger population of naturally infected community cases collected at University of Maryland

The set of data from the community cases observed in the University of Maryland campus community are different from that of the "complete data" used in the analyses of Yan et al., 2018. The data in the current manuscript come from the set of 158 qRT-PCR confirmed influenza cases with exclusion of all breath collection visits from four dual influenza infections, breath collection visits on days 0 and >3 post symptom onset, as well as those with incomplete qRT-PCR data, and those that were not H3 infections confirmed by qRT-PCR of nasopharyngeal swab. Cough counts from three exhaled breath sampling visits that were missing and thus excluded by Yan and colleagues, were imputed for this analysis. ***Table S3.3*** provides a summary of cases and exhaled breath collection visits selected for analysis from 178 enrolled community cases.

Table S3.3. Community case exclusion and inclusion to achieve analytical dataset

	Exclusions					Inclusions	
Reason for exclusion	**Number subjects with all breath collection excluded**	**Number breath collection visits excluded from subjects with all breath collection visits excluded**	**Number subjects with at least 1 but not all breath collection visits excluded**	**Number breath collection visits excluded from subjects with at least 1 but not all breath collection visits excluded**	**Total breath collection visits excluded (sum of the 3rd and 5th columns)**	**Running count of subjects**	**Running count of breath collection visits**
Total screened	-	-	-	-	-	355	276
Case inclusion criteria*	177	0	0	0	0	178	276
Not confirmed by qRT-PCR	20	26	0	0	26	158	250
Day 0, >3 post symptom onset	9	8	9	10	18	149	232
Incomplete qRT-PCR data**	5	6	1	1	7	144	225
Dual infection***	3	4	0	0	4	141	221
Non H3 infection	58	75	0	0	75	83	146
Overall	**95**	**119**	**10**	**11**	**130**	**83**	**146**

* Positive Quidel QuickVue rapid influenza test, or oral temperature >37.8 °C, plus cough or sore throat, and (ii) presented within the first 3 d of symptom
onset.

** Description of the incomplete PCR data:

- Drop subject 333 1 and only G-II visit because lost coarse aerosol sample (although good data exists for the NP and the fine aerosol)
- Drop subject 52 because false positive (this makes 52 a negative case and thus we exclude all sampling instances)
- Drop subject 58 because false positive (58 only had 1 G-II sampling instance so this was excluded)
- Drop subject 182 2nd G-II visit because bad inter-run calibrator on the PCR (there is still a 1st G-II visit for 182 so this subject is not excluded entirely)
- Drop subject 322 because bad inter-run calibrator on the PCR (this was the only G-II sampling instance, so this subject is excluded entirely)

- Drop subject 337 because bad inter-run calibrator on the PCR (this was the only G-II sampling instance, so this subject is excluded entirely)

*** Dual infections:

- 1 instance: H3N2 and Pandemic H1
- 1 instance: B and unsubtypable A
- 1 instance: B and H3N2

Appendix 3.2. Propensity score workflow

Table S4. Codebook of the data frame used in propensity score analyses

Variable	Type of Variable	Description
subject.id	Subject ID # (numeric, integer variable)	ID numbers below 400 are UMD Flu Cases. ID numbers above 400 are Infected Donors.
Group	Factor with two levels, 0 and 1 (the "Group" variable is actually numeric and uses 0 and 1 as the only possible options: 0 for Infected donors and 1 for UMD flu cases; but the "Group_factor" variable is the factor variable and uses the text "Infected donors" and "UMD Flu Cases" as the levels.	Coded as 0 = Infected donors; 1 = UMD flu cases
Group_factor	Factor with two levels 0 and 1	Coded as 0 = Infected donors; 1 = UMD flu cases (the levels of the variable are written as "Infected donors" and "UMD Flu Cases"
Age	Numeric, integer variable	Age in years
Sex	Factor with two levels, 0 and 1 (although technically this "sex" variable is coded as numeric with possible levels 0 and 1 and the sex_factor variable is the one that is factor with levels "female" and "male")	0 = female, 1 = male
Sex_factor	Factor with two levels	"female" and "male" (with female coded as 0 and male as 1 in the "sex" variable)
Upper_resp	Numeric, discrete	Sum of the ordinal (4-level from 0-3 with 0=none and 3=severe symptom) for the following symptoms: runny nose, stuffy nose, sneezing, sore throat, and earache, score range 0–15.
Lower_resp	Numeric, discrete	Sum of the ordinal (4-level from 0-3 with 0=none and 3=severe symptom) for the following symptoms: shortness of breath, and cough, score range 0–6
Systemic_sx	Numeric, discrete	Sum of the ordinal (4-level from 0-3 with 0=none and 3=severe symptom) for the following symptoms: malaise, headache, muscle/joint ache, score range 0–9
Total_sx	Numeric, discrete	Sum of the ordinal (4-level from 0-3 with 0=none and 3=severe symptom) for the following symptoms: runny nose, stuffy nose, sneezing, sore throat, earache, shortness of breath, cough, malaise, headache, muscle/joint ache: score range 0–30.

Cough	Numeric, discrete (factor with 4 levels)	4 levels for symptoms severity with 0 as no symptom to 3 as most severe symptom
Cough_factor	Factor, 4 levels	"0-none", "1-mild", "2-moderate", "3-severe" coded for cough self-reported symptom scores of 0, 1, 2, and 3, respectively.
cough_count_full	Numeric, discrete.	Number of times coughed during 30-minute sample collection in the g-ii machine. Included 2 instances of missing cough in the Infected donor group
Body_temp	Continuous (1 decimal place)	
Ever_febrile	Numeric, discrete (factor with 2 levels)	1 = had fever > 37.9 degrees C on any of the days of observations (1-4 days post inoculation for donors and 1-3 day post symptom onset for UMD Flu Cases). 0 = temperature reading was below the study threshold for "febrile illness"
Ever_febrile_factor	Factor (2 levels)	Coded as "yes" = 1 (yes, was febrile at some point during observation), "no" = 0 (no, was never observed to reach the body temperature threshold for febrile).
NP_ct	Continuous (2 decimal places)	CT value on the qRT-PCR assay for influenza A viral RNA.
sample_mean_copies	Continuous outcome	RNA copies – the mean of replicates for samples with detectable virus (have not used tobit to impute for samples where there was not at least 1 replicate above detection limit).
Variables in dataframe but not used		
study.day	Character variable with 4 levels.	The 4 levels represent the possible study days. For UMD Flu Cases the study day refers to the three days post symptom onset and for Infected donors the study day refers to the four days post inoculation.
sample.type	Character variable with 2 possible levels	For this df this variable is always "Condensate" because the fineflu data frame has been filtered to included only the condensate samples and their associated clinical evaluation data.
Date	Character	Date of the data collection for the associated observation.
Nose_run	Numeric, discrete (factor with 4 levels)	4 levels for symptoms severity with 0 as no symptom to 3 as most severe
Nose_stuf	Numeric, discrete (factor with 4 levels)	4 levels for symptoms severity with 0 as no symptom to 3 as most severe
Sneeze	Numeric, discrete (factor with 4 levels)	4 levels for symptoms severity with 0 as no symptom to 3 as most severe
Throat_sr	Numeric, discrete (factor with 4 levels)	4 levels for symptoms severity with 0 as no symptom to 3 as most severe
Earache	Numeric, discrete (factor with 4 levels)	4 levels for symptoms severity with 0 as no symptom to 3 as most severe

Malaise	Numeric, discrete (factor with 4 levels)	4 levels for symptoms severity with 0 as no symptom to 3 as most severe
Sob	Numeric, discrete (factor with 4 levels)	4 levels for symptoms severity with 0 as no symptom to 3 as most severe
Headache	Numeric, discrete (factor with 4 levels)	4 levels for symptoms severity with 0 as no symptom to 3 as most severe
Mj_ache	Numeric, discrete (factor with 4 levels)	4 levels for symptoms severity with 0 as no symptom to 3 as most severe
Febrile_day	Numeric, discrete (factor with 2 levels)	1 = had fever > 37.9 degrees C on the associated day of data collection. 0 = temperature reading was below the study threshold for "febrile illness"
Cough_number	Numeric, discrete.	Number of times coughed during 30-minute sample collection in the g-ii machine. Included 2 instances of missing cough in the Infected donor group

This table describes data that has been restricted to the maximum day observation of shedding for those who shed into fine aerosols. There are 71 observations for UMD Flu Cases and 11 for Infected donors. Each observation corresponds to the day with the highest observed RNA copy number (average of replicates) shed into fine aerosol for each subject. Note that there were a total of 83 UMD flu cases (flu A) and 39 Infected donors so we can already see that only 28% of the Infected Donors shed into fine particle aerosols, while 86% of UMD Flu A Cases shed into fine particle aerosols. Analysis with the outcome of the odds of shedding into fine aerosols will also be done.

Propensity work with outcome as continuous shedding

Specifying the propensity score model

The propensity score model is a logistic regression model. It regresses the logit of the study population (natural versus experimental infection) on a set of covariates. Comparison groups conditioned on an appropriately specified propensity score should have similar means and variances, with standardized differences of close to 0 and variance ratios of close to 1 (Austin, 2009). Propensity score models that achieved comparison group balance after conditioning on propensity score were considered for use in estimating the effect of comparison group membership on the outcomes of interest. Propensity score model specifications that achieved balanced population means were also tested against Donald Rubin's propensity score balancing criteria.

Rubin's criteria assesses the degree of overlap between propensity scores in each group. Correctly specified propensity score models that also have enough overlap in propensity scores sufficiently minimize bias introduced by lack of group randomization, with the acknowledgement that unmeasured confounders may still introduce bias. None of the 14 propensity score models tested achieved enough covariate balance between naturally and experimentally infected study populations, even after truncating the sampling frame from both groups. Thus, we conclude that the populations are too different to make support valid comparisons between groups with respect to the outcome, even if covariate adjustment should be used.

In the initial propensity score model, predictors of experimental or natural infection group were selected on the basis of their relationship with the outcome of observed shedding into fine aerosols above the detection limit. The lower respiratory symptom score, cough symptom score, and the cough count observed during half-hour exhaled breath collection all had positive, statistically significant effects on the odds of viral shedding into fine aerosols. Since the cough symptom score makes up 50% of the lower respiratory score and likely drives the effect seen in the lower respiratory score, the cough score and not the lower respiratory symptom score was included. Thus, the initial propensity score model included only cough symptom score and observed cough count as predictors. Overlap in propensity scores between study population groups decreased when including lower respiratory scores, affirming this decision.

Propensity score model specifications need not be concerned with multicollinearity because the estimated propensity scores and not the variances are of main interest. Age was associated with study population, however published literature assessing propensity score model specification have warned against including variables that are associated with group membership but not the outcome of interest because of the risk of increasing variance in the estimated effect without reducing bias (Austin et al., 2007; Brookhart et al., 2006).

Donald Rubin's rules for assessing propensity score balance were used to evaluate propensity score model specifications (Rubin, 2001) (add citation: 2001 paper from Rubin about using propensity scores to design studies – Rubin DB 2001 Using Propensity Scores to Help Design Observational Studies: Application to the Tobacco Litigation. *Health Services & Outcomes Research Methodology* 2: 169-188). Failure of balance between covariates in the two study populations indicates the need for adjustment using three propensity score balancing methods: matching, subclassification, inverse probability weighting. Valid of the effect of natural infection compared with experimental infection, in our specific studies, can be carried out after improving balance to an acceptable range.

- First rule: The absolute value of the standardized difference of the linear propensity score should be close to 0 and definitely less than 50.
- Second rule: The ratio of variances of the linear propensity score between the comparison groups (i.e., natural to experimental infection). This should be close to 1 and definitely between ½ and 2.

- Third rule: After regressing the residuals for each covariate specified in the propensity score model on the linear propensity score, the ratio of variance of residuals between comparison groups (i.e., natural to experimental infection) close to 1.

Appendix 3.3. Description of comparison analysis and profile of studies that generated data

Figure S3.5 shows the enrollment profiles of the two studies and DAG (directed acyclic graph) used for making comparisons between experimentally and naturally infected influenza A/H3 cases. The main outcomes of interest are the probability of shedding virus into aerosols and the rate of viral shedding in aerosols. Given their role in transmission, fine particle aerosols are of particular interest. These outcomes are illustrated in the DAG (***Figure S3.5***). Other comparisons of interest are the temporal dynamics of illness, the temporal dynamics of aerosol shedding, and the overlap of symptoms with strength and duration of shedding.

The main independent variable of interest is the mode of inoculation, with the experimentally challenged infections representing contact transmission via exposure to nasal mucosa, and the naturally infected cases representing transmission by any plausible mode (the red rectangle in the DAG). Other differences may exist in the two study populations related to the conditions of infection initiation including systematic differences in age, sex, immunity, and dose. Although these potential confounders may not be completely controlled for by study design, they are not likely to play a major role in confounding the interpretation that experimentally infected cases represent contact or large droplet spray transmission to the upper respiratory tract and naturally infected cases represent transmission by any plausible mode. Brief discussion follows about each of these potential confounders.

The source population for the observational study and the inclusion criteria for the challenge study favored recruitment of healthy, young adults. The age of the young adults was several years higher but unlikely to drive differences in susceptibility. Susceptibility is likely to be higher for young children or elderly populations. Male and female were well balanced in study population of naturally infected cases; however, this distribution was skewed in the trial study with a majority male infections. Epidemiological evidence from various influenza seasons, and illnesses in various age groups suggests that males may have elevated risk hospitalization, suggesting a potential role for sex in influenza pathogenesis (Gabriel and Arck, 2014). It is uncertain to what extent sex may influence susceptibility to infection, but it is acknowledged as a potential confounder in the relationship between study population membership and infection initiation for members of the studies. Virally challenged volunteers were screened for low levels of pre-existing antibodies (HAI $\leq$10), while the naturally infected population was not. The symptomatic, naturally acquired infections were likely to have had less immunity compared with the total source population because they were infected. But, a small subset of naturally infected cases had been immunized for influenza for the current and/or previous influenza seasons, pointing toward a range of pre-existing antibodies above the exclusion threshold of the trial study (Yan et al., 2018). Thus, pre-existing antibodies were unmeasured in the naturally infected study population and could be a confounding factor related to the infection conditions between the study populations. The laboratory prepared virus used for human challenge could have been attenuated

compared with wildtype, but virologic investigation of this virus suggests that the HA variant matches other wildtype viruses and may not be a major source of difference (Nguyen-Van-Tam et al., 2019; Sobel Leonard et al., 2016). Finally, the dose leading to infection may have been different between the two study populations and could also be a confounding variable. Volunteers received an intranasal dose of 5.5 $\log_{10}$ $TCID_{50}$, however the dose leading to infection in the naturally infected populations was unmeasured. It has been shown that low doses of aerosolized virus can initiate infection (Alford et al., 1966). In naturally infected cases not infected by aerosols (i.e., infected similarly to infected volunteers, via contact exposure to upper airway mucosa), they may have been exposed to a range of doses and correlations between dose and viral shedding peak and duration have been reported in volunteers challenged with influenza virus (Keitel et al., 1990). Overall, potential confounding factors between transmission mode – the main independent variable of interest – and the initiation of infection that may not have been fully controlled for in the designs of the experimental and observational studies were age, sex, host immunity, viral pathogenicity, and dose. Assessment of these potential confounders leads us to believe that they are not likely to have a substantial effect in obscuring the main effect of mode on the conditions of infection in the study populations.

Covariates are illustrated as confounders because there is reported evidence and/or biological plausibility for considering them so based on their expected effects on the independent variable (study population membership) and the dependent variables (aerosol shedding probability and rate). We attempted to achieve acceptable balance

across these confounders with propensity score model adjustment, however, were unable to do so because the populations were simply too different in their distributions for these variables.

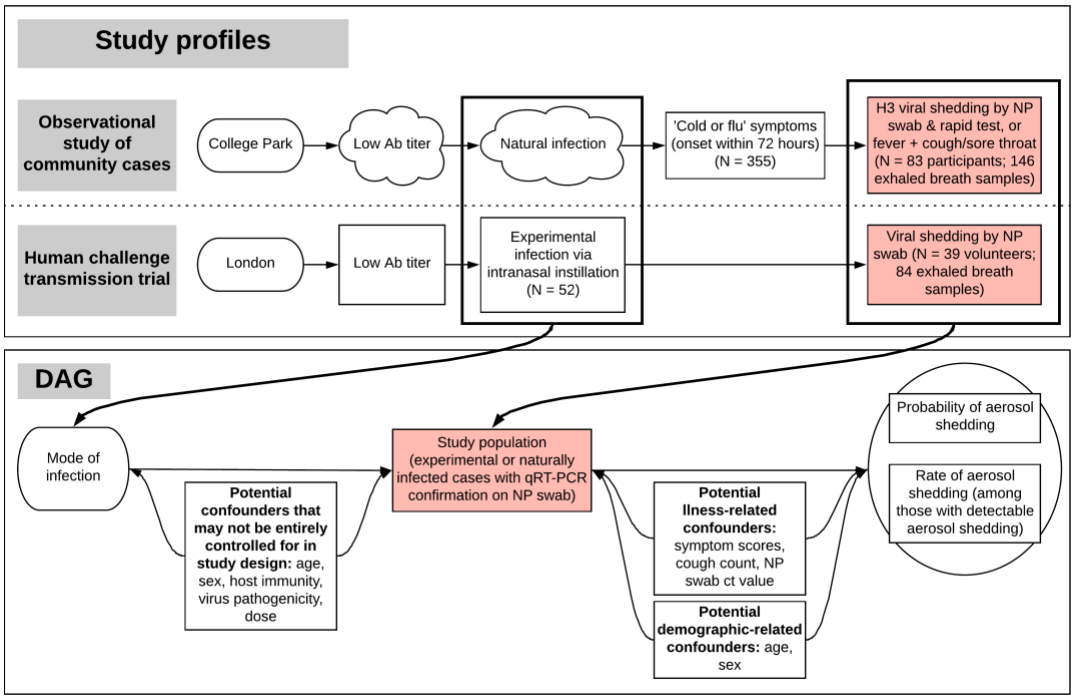

Figure S3.5. Profiles of the EMIT studies and DAG. (Top) study profiles used to make comparisons between experimental and naturally infected populations. Cloud shapes depict unobserved variables that are believed to be true. DAG (directed acyclic graph, bottom) for comparing aerosol shedding in the study populations.

CHAPTER IV SUPPLEMENTARY INFORMATION

EMIT Team Members

EMIT team members were: Walt Adamson, Blanca Beato-Arribas, Werner Bischoff, William Booth, Simon Cauchemez, Sheryl Ehrman, Joanne Enstone, Neil Ferguson, John Forni, Anthony Gilbert, Michael Grantham, Lisa Grohskopf, Andrew Hayward, Michael Hewitt, Ashley Kang, Ben Killingley, Robert Lambkin-Williams, Alex Mann, Donald Milton, Jonathan Nguyen-Van-Tam, Catherine Noakes, John Oxford, Massimo Palmarini, Jovan Pantelic, and Jennifer Wang. The Scientific Advisory Board members were: Allan Bennett, Ben Cowling, Arnold Monto, and Raymond Tellier.

SI.4 Tables

Table S1. Fine particle aerosol shedding strength from detected samples

Quarantine	Exposure Group	Day 2	Day 3	Day 4	Daily Average***
1	A	8.8E+3 (1, 2)	1.6E+5 (1, 2)	ND (0, 2)	5.6E+4 (2, 6)
	B*	ND (0, 2)	ND (0, 1)	ND (0, 2)	ND (0, 5)
	C	ND (0, 3)	1.3E+4 (1, 2)	ND (0, 1)	4.4E+3 (1, 6)
	D*	ND (0, 2)	ND (0, 2)	ND (0, 2)	ND (0, 6)
	E	ND (0, 2)	1.3E+5 (1, 3)	1.6E+4 (1, 3)	5.0E+4 (2, 8)
2	A*	ND (0, 2)	ND (0, 4)	ND (0, 0)	ND (0, 6)
	B	2.4E+3 (1, 4)	3.5E+3 (1, 2)	ND (0, 1)	2.0E+3 (2, 7)
	C**	9.8E+3 (1, 4)	1.3E+5 (1, 4)	ND (0, 3)	4.6E+4 (2, 11)
3	A	ND (0, 2)	ND (0, 2)	4.3E+3 (1, 2)	1.4E+3 (1, 6)
	B	2.0E+3 (1, 2)	ND (0, 1)	ND (0, 2)	6.7E+2 (1, 5)
	C	ND (0, 2)	2.6E+3 (1, 2)	ND (0, 2)	8.8E+2 (1, 6)
	D	3.9E+3 (1, 2)	ND (0, 2)	ND (0, 2)	1.3E+3 (1, 6)
	E	ND (0, 2)	3.9E+3 (1, 3)	ND (0, 2)	1.3E+3 (1, 7)

RNA copies shed into fine particle exhaled breath aerosols per hour by day-EG, V_{jk}, by EG, V_k from samples with at least one detectable qRT-PCR replicate (number samples with at least 1 detectable qRT-PCR replicate, number samples tested). ND: not detected = 0/2 qRT-PCR replicates detected, or no sample collected.

* EGs with no Donors observed to shed any fine aerosols with at least one qRT-PCR replicate positive. ** EG with the transmission event. *** Not time weighted. Assumed that ND = 0.

Table S2. Infectious quanta generation rate and sigma

Change in CO2	$q_{(all\ Donors)}$	$q_{(aerosol\ shedders)}$	sigma
-50%	0.089 (0.083, 0.094)	0.32 (0.26, 0.36)	2.4E+5 (1.7E+5, 3.0E+5)
-40%	0.063 (0.059, 0.066)	0.23 (0.19, 0.26)	2.2E+5 (1.5E+5, 2.8E+5)
-30%	0.048 (0.046, 0.051)	0.18 (0.15, 0.2)	2.0E+5 (1.4E+5, 2.5E+5)
-20%	0.04 (0.037, 0.042)	0.14 (0.12, 0.16)	1.8E+5 (1.3E+5, 2.3E+5)
-10%	0.033 (0.031, 0.035)	0.12 (0.1, 0.14)	1.6E+5 (1.1E+5, 2.0E+5)
Observed	**0.029 (0.027, 0.03)**	**0.11 (0.088, 0.12)**	**1.4E+5 (1.0E+5, 1.8E+5)**
+10%	0.025 (0.024, 0.027)	0.093 (0.077, 0.11)	1.2E+5 (8.5E+4, 1.5E+5)
+20%	0.023 (0.021, 0.024)	0.084 (0.07, 0.094)	1.0E+5 (7.2E+4, 1.3E+5)
+30%	0.021 (0.019, 0.022)	0.076 (0.063, 0.085)	8.0E+4 (5.8E+4, 1.0E+5)
+40%	0.019 (0.018, 0.02)	0.069 (0.057, 0.078)	6.0E+4 (4.4E+4, 7.6E+4)
+50%	0.017 (0.016, 0.018)	0.063 (0.053, 0.071)	4.0E+4 (3.0E+4, 5.0E+4)

Effect of indoor CO_2 level changes on point estimates (95% CI).

SI.4 Figures

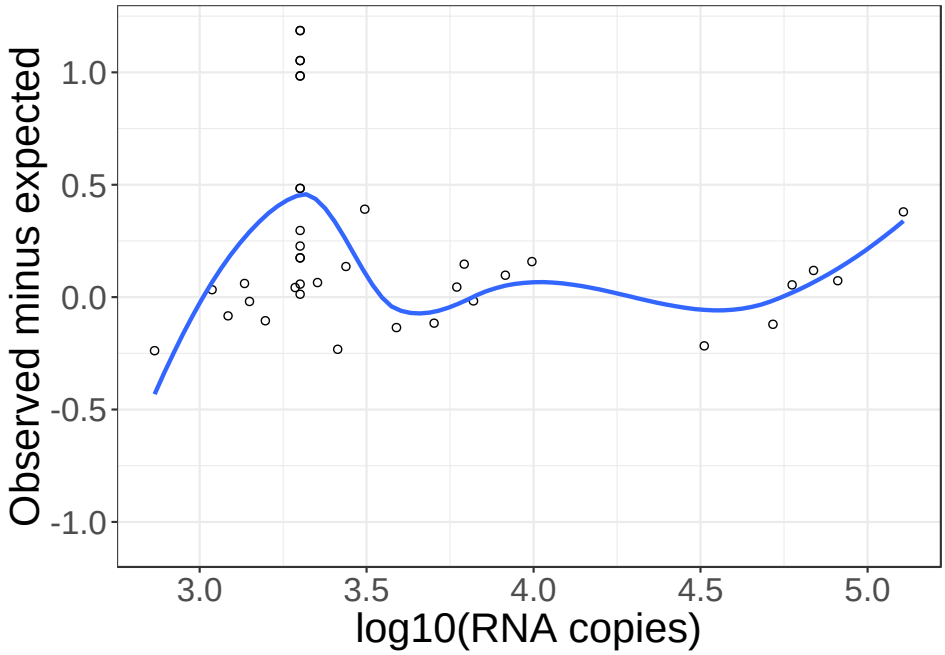

Figure S4.1. Depicts observed minus Tobit model expected values for all 33 sample values (three study days for each 11 Donors who ever shed into fine aerosol).

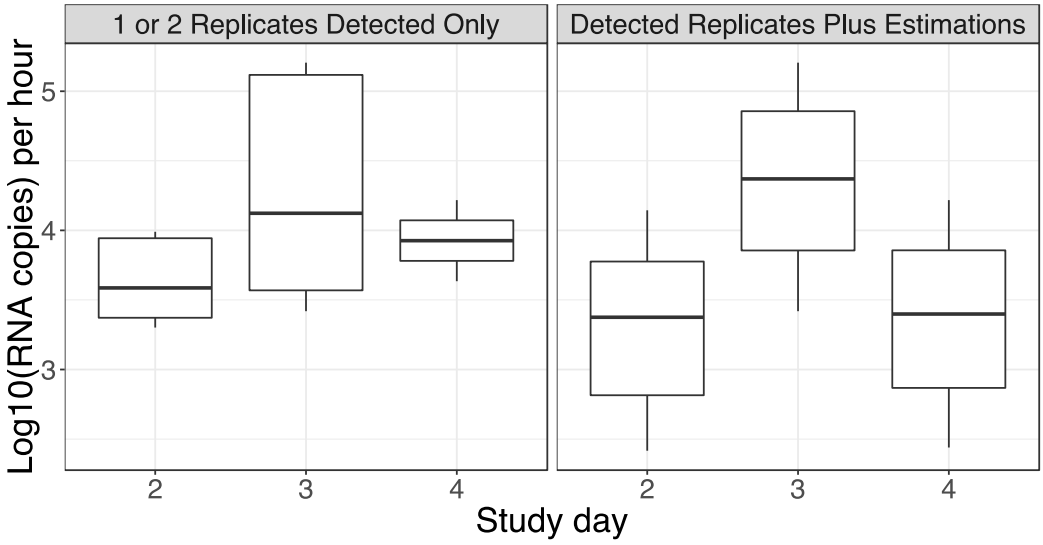

Figure S4.2. Depicts $\log_{10}$ (RNA copies) shed per hour into exhaled breath fine particle aerosol by study day, for samples with at least one detectable qRT-PCR replicate and for all samples with at least one detected qRT-PCR replicate in addition to samples below detection limit or unobserved with Tobit estimated shedding rates among ever-aerosol shedders; the boxes show the inner-quartile range (IQR) with a band to indicate the median, and whiskers extending to the highest and lowest data points within 1.5 IQR.

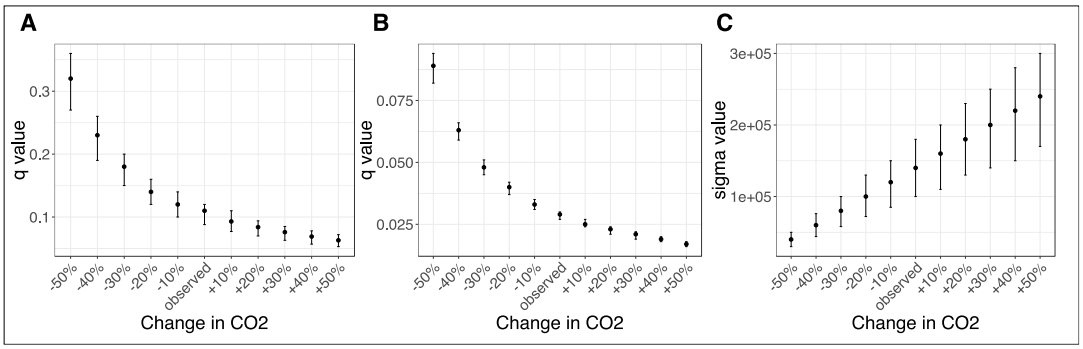

Figure S4.3. Infectious quanta generation rate and sigma. Effect of indoor CO_2 level changes on point estimates (95% CI).

SI.4 Appendices

Appendix 4.1. Note about one volunteer excluded as an infected or aerosol shedding Donor

There was an instance where a Donor (subject 109) had one replicate qRT-PCR detected for fine aerosols but no positive swabs and no indication of seroconversion, so we did not count this as a true infection and did not include their aerosols samples as positive below LOD in the final analysis.

Appendix 4.2. Tobit regression model parameters and diagnostics

I. Tobit model using 19 samples (N=10, four, and five, where two, one, and zero out of two qRT-PCR duplicates were detectable, respectively) from a total of 11 Donors who ever shed into fine particle aerosols. Model: fixed effects of cough and study day with random effect of person to predict fine aerosol shedding (RNA copies per hour).

Fit Statistics	
-2 Log Likelihood	29.9
AIC	41.9
AICC	44.6
BIC	44.3

Parameter Estimates								
Parameter	**Estimate**	**Standard Error**	**DF**	**t Value**	**Pr > |t|**	**95% Confidence Limits**		**Gradient**
Random effect of person intercept	0.3568	0.1636	10	2.18	0.0542	-0.00772	0.7214	-0.00010
Random effect of person	0.04104	0.01532	10	2.68	0.0231	0.006913	0.07517	0.001449
Intercept	2.9801	0.2074	10	14.37	<.0001	2.5180	3.4421	-0.00001
Cough score (daily average)	0.08768	0.2605	10	0.34	0.7434	-0.4928	0.6681	0.000129
Study day 3 vs study day 2	0.9946	0.1825	10	5.45	0.0003	0.5880	1.4013	0.000196
Study day 4 vs study day 2	0.02316	0.1773	10	0.13	0.8987	-0.3720	0.4183	0.000080

II. Tobit model using 14 samples (N=10 and four, where two and one out of two qRT-PCR duplicates were detectable, respectively) from a total of 11 Donors who ever shed into fine particle aerosols. Model: fixed effects of cough and

study day with random effect of person to predict fine aerosol shedding (RNA copies per hour).

Fit Statistics	
-2 Log Likelihood	27.5
AIC	39.5
AICC	43.5
BIC	41.9

Parameter Estimates								
Parameter	**Estimate**	**Standard Error**	**DF**	**t Value**	**Pr > |t|**	**95% Confidence Limits**		**Gradient**
Random effect of person intercept	0.3534	0.1626	10	2.17	0.0549	-0.00896	0.7157	2.357E-6
Random effect of person	0.04063	0.01549	10	2.62	0.0255	0.006107	0.07515	0.000011
Intercept	2.9345	0.2091	10	14.03	<.0001	2.4685	3.4005	1.893E-6
Cough score (daily average)	0.03770	0.2624	10	0.14	0.8886	-0.5469	0.6223	-0.00002
Study day 3 vs study day 2	1.0832	0.1939	10	5.59	0.0002	0.6513	1.5151	-0.00002
Study day 4 vs study day 2	0.2448	0.2353	10	1.04	0.3225	-0.2794	0.7690	0.000010

Appendix 4.3. BSRIA Report on indoor air conditions in the quarantine facility

Can be provided upon request.

Appendix 4.4. Relationship between q, fine aerosol shedding, and SIR models

Variables related to infectious dose that are absorbed by the q value include: a) host immune status (influenced by genetics, prior/recent or concurrent infectious disease exposures, vaccination history, psychosocial stress, coinfection, chemical or physical exposures, etc.), b) viral virulence, c) deposition probability in various vulnerable loci in the lung, d) number of viruses per infectious particle, e) biological and physical decay rate of infectious particles, and f) stochasticity of inhaled air viral exposure. These variables represent effect modifiers with potential to dramatically influence the relationship between inhalation exposure to air containing a quantifiable level of infectious influenza virus, and infectious risk. Understanding the strength of these effect modifiers, individually and together, improves airborne risk assessment under more specific exposure scenarios. Thus, the quantum is not solely related to the strength of airborne viral contamination, but also a function of these other variables that modify the effect of the viral exposure. A quantum could be dramatically different between individuals.

Issarow et al., 2015 builds upon the rebreathed-air equation to give the transmission risk for susceptibles as:

$$P\left(T \leq t \middle| I, n, \overline{f}, \theta, \mu, \beta\right) = 1 - e^{-\left(\left(\frac{I(\beta-\mu)\theta\overline{f}t}{n}\right)\right)}, \quad (12)$$

with T time at infection, t time until infection, I infectious individuals shedding virus into exhaled breath aerosols, n room occupants contributing exhaled breath, θ deposition fraction of particles to vulnerable loci in the respiratory tract, μ particles

that do not reach the lung due to physical decay, and β concentration of infectious particles in the environment. This formulation describes the relationship between airborne virus present in an indoor space and the effective exposure dose that reaches vulnerable loci in the respiratory tract. An alternative formulation to takes q as the product of: a) θ, the deposition fraction, b) γ, the average probability of escaping the host defenses given deposition at a vulnerable locus, and c) β, this time taken to mean the rate of viral contamination of the air through exhaled breath. Thus, compared with the Issarow, et al. version $q = (\beta - \mu)\theta$, we take $q = \theta\gamma\beta$. The multiplicative form is generally more computationally suitable for these models. This formulation for q can be generalized for various size fractions or limited to solely the fine-particle size fraction as presented here, thus introducing host immunity, virulence, and deposition considerations into to the q term. Additional nuance on risk by deposition site can be introduced and has been explored elsewhere (Cheng et al., 2016).

The effect of biological and physical decay can be addressed by using $\theta\rho\mu$ as the lung deposition equal to θ reduced by the predicted biological decay ρ and physical decay μ, which includes diffusional deposition. Biological decay is governed by environmental temperature and humidity, and by virus robustness. Physical decay would be influenced by particle size and room air turbulence.

By using the Equation 13:

$$q = \theta\rho\mu\,[1 - (1 - \gamma)^{\nu}]\beta/\nu, \quad (13)$$

where ν is the number of infectious virions per aerosol particle, we incorporate the additional risk posed by particles that may be comprised of multiple infectious agents. Multiple virions may be packaged into a fine particle during aerosol production in the lung. Vesicles carrying multiple pathogens for enteric viruses have been observed and support motivation for the investigation of similar packaging for airborne influenza virus-carrying particles (Altan-Bonnet, 2016).

Accounting for stochasticity in airborne exposure and infection risk effectively increases the upper bound for the amount of inhaled virus, given the precautionary principle and modelling for the highest risk level required to prevent transmission. Noakes and Sleigh, 2009 implemented a stochastic zonal model to deal with imperfect air mixing and report that transmission risk is otherwise underestimated by as much as 15%. A summary of improved model considerations to improve the precision of the q term is provided in ***Table S4.3***.

Table S4.3. Variables absorbed by q

Variable	Existing models	Proposed model
Host immunity	θ (Issarow et al., 2015)	γ (Population averaged probability of escaping host defenses influenced by host immunity and virulence of virus)
Virulence of pathogen	θ (Issarow et al., 2015)	γ (Population averaged probability of escaping host defenses influenced by host immunity and virulence of virus)
Deposition fraction to vulnerable loci in respiratory tract	θ (Issarow et al., 2015)	θ (Deposition fraction of particles on vulnerable loci, based on the various size fractions)
Infectious viruses per particle	None	ν (Infectious particles per aerosol particle)
Biological decay rate	θ (Issarow et al., 2015)	ρ (May be influenced by particle size and the type of virus)
Physical decay rate	μ (Issarow et al., 2015)	μ

Stochasticity of exposure and infection risk	(Noakes and Sleigh, 2009)	Incorporate stochasticity term to account for potential increases in exposure to inhaled particles and/or stochastic increases in infection risk (increases the effect of the θ term)

Linking airborne infection risk with SIR modelling

Models of airborne infection risk have been linked with SIR models to make inferences about population infection dynamics and the potential for disease control (i.e., Noakes et al., 2006). SIR models are specified as three ordinary differential equations with respect to time, t, that relate the change in the number of susceptibles, S, with the number of infectors, I, and the population removed from the susceptible pool through immunity or death, R: $\frac{dS}{dt} = -\beta SI, \frac{dI}{dt} = \beta SI - \gamma I, \frac{dR}{dt} = \gamma I,\ S + I + R = N$, where β is the contact rate between susceptibles and infectors that leads to infection, and γ is the removal rate. We point out that compared with β as discussed in SIR models β as discussed in airborne transmission risk models refers to viral exposure that leads to infection. For the purpose of assessing the effect of indoor air conditions on airborne transmission risk, Gammaitoni and Nucci, 1997 proposed a link with SIR specified as: $\frac{dS}{dt} = -\frac{-pq}{VA}IS$, where V is the volume of the shared indoor air space and A is the ventilation rate. This specification gives an SIR specification $\beta = \frac{pq}{VA}$. When we compared the SIR formulation with the rebreathed-air equation, we found SIR $\beta = fq$. Refinement of q can be directly translated back into SIR models to model population dynamics. Information from airborne risk models can be used to inform SIR models including the effect of latency period, length of infectious period, and variation in shedding on each day post infection.

The behavior of specified models can be tested extensively by parameterizing the variables from ***Table S4.3*** and the SIR equations, and by examining the relationships between the variables. This approach has been as has been successfully used in numerous studies of infection risk and population infection dynamics (i.e., Nardell et al., 1991; Gammaitoni and Nucci, 1997; Noakes et al., 2006; Issarow et al., 2015; Cheng et al., 2016). Parameterization is informed by available knowledge or reasonable estimates and models tested under a range of simulated conditions can show the extent to which individual or groups of variables influence the system. Model validation can be done using observational data.

We have shown that 1) we can estimate the relationship between observed aerosol shedding and infectious quanta, 2) synthesis and refinement of available infection risk models responds to the major critique that current models fail to accurately reflect the biological and physical process of transmission, and 3) refined infection risk models can be integrated into SIR models for powerful generalizability and application to population infection dynamics prediction and control. Models can be tested by human challenge transmission trials under controlled conditions as done in the EMIT trial. However greater external validity could be achieved using epidemiologic study designs that surveil infectious acute respiratory infection cases and their close contacts and characterize indoor air conditions in which exposure occurs. Advances in molecular epidemiology that could confirm transmission chains enables the

shifting of transmission work from the controlled experimental environment into the real-world epidemiological realm.

BIBLIOGRAPHY

Aiello, A.E., Perez, V., Coulborn, R.M., Davis, B.M., Uddin, M., Monto, A.S., 2012. Facemasks, Hand Hygiene, and Influenza among Young Adults: A Randomized Intervention Trial. PLoS One 7. https://doi.org/10.1371/journal.pone.0029744

Alford, R.H., Kasel, J.A., Gerone, P.J., Knight, V., 1966. Human influenza resulting from aerosol inhalation. Proc. Soc. Exp. Biol. Med. 122, 800–804. https://doi.org/10.3181/00379727-122-31255

Allen, J.G., MacNaughton, P., Satish, U., Santanam, S., Vallarino, J., Spengler, J.D., 2016. Associations of Cognitive Function Scores with Carbon Dioxide, Ventilation, and Volatile Organic Compound Exposures in Office Workers: A Controlled Exposure Study of Green and Conventional Office Environments. Environ. Health Perspect. 124, 805–812. https://doi.org/10.1289/ehp.1510037

Almstrand, A.-C., Bake, B., Ljungström, E., Larsson, P., Bredberg, A., Mirgorodskaya, E., Olin, A.-C., 2010. Effect of airway opening on production of exhaled particles. J. Appl. Physiol. 108, 584–588. https://doi.org/10.1152/japplphysiol.00873.2009

Altan-Bonnet, N., 2016. Extracellular vesicles are the Trojan horses of viral infection. Curr Opin Microbiol 32, 77–81. https://doi.org/10.1016/j.mib.2016.05.004

Austin, P.C., 2009. The Relative Ability of Different Propensity Score Methods to Balance Measured Covariates Between Treated and Untreated Subjects in Observational Studies. Med Decis Making 29, 661–677. https://doi.org/10.1177/0272989X09341755

Austin, P.C., Grootendorst, P., Anderson, G.M., 2007. A comparison of the ability of different propensity score models to balance measured variables between treated and untreated subjects: a Monte Carlo study. Statistics in Medicine 26, 734–753. https://doi.org/10.1002/sim.2580

Berghöfer, B., Frommer, T., Haley, G., Fink, L., Bein, G., Hackstein, H., 2006. TLR7 Ligands Induce Higher IFN-α Production in Females. The Journal of Immunology 177, 2088–2096. https://doi.org/10.4049/jimmunol.177.4.2088

Bischoff, W.E., Swett, K., Leng, I., Peters, T.R., 2013. Exposure to Influenza Virus Aerosols During Routine Patient Care. J Infect Dis. 207, 1037–1046. https://doi.org/10.1093/infdis/jis773

Boelle, P.Y., Ansart, S., Cori, A., Valleron, A.J., 2011. Transmission parameters of the A/H1N1 (2009) influenza virus pandemic: a review. Influenza Other Respi Viruses 5, 306–316. https://doi.org/10.1111/j.1750-2659.2011.00234.x

Brankston, G., Gitterman, L., Hirji, Z., Lemieux, C., Gardam, M., 2007. Transmission of influenza A in human beings. Lancet Infect Dis 7, 257–265. https://doi.org/10.1016/S1473-3099(07)70029-4

Brookhart, M.A., Schneeweiss, S., Rothman, K.J., Glynn, R.J., Avorn, J., Stürmer, T., 2006. Variable selection for propensity score models. Am. J. Epidemiol. 163, 1149–1156. https://doi.org/10.1093/aje/kwj149

Brooks-Pollock, E., Becerra, M.C., Goldstein, E., Cohen, T., Murray, M.B., 2011. Epidemiologic Inference From the Distribution of Tuberculosis Cases in Households in Lima, Peru. J Infect Dis 203, 1582–1589. https://doi.org/10.1093/infdis/jir162

Burki, T.K., 2017. The economic cost of respiratory disease in the UK. The Lancet Respiratory Medicine 5, 381. https://doi.org/10.1016/S2213-2600(17)30108-X

Buu, T.N., van Soolingen, D., Huyen, M.N.T., Lan, N.N.T., Quy, H.T., Tiemersma, E.W., Borgdorff, M.W., Cobelens, F.G.J., 2010. Tuberculosis Acquired Outside of Households, Rural Vietnam. Emerg Infect Dis 16, 1466–1468. https://doi.org/10.3201/eid1609.100281

Campbell, F., Cori, A., Ferguson, N., Jombart, T., 2019. Bayesian inference of transmission chains using timing of symptoms, pathogen genomes and contact data. PLOS Computational Biology 15, e1006930. https://doi.org/10.1371/journal.pcbi.1006930

Carrat, F., Sahler, C., Rogez, S., Leruez-Ville, M., Freymuth, F., Gales, C.L., Bungener, M., Housset, B., Nicolas, M., Rouzioux, C., 2002. Influenza Burden of Illness: Estimates From a National Prospective Survey of Household Contacts in France. Arch Intern Med 162, 1842–1848. https://doi.org/10.1001/archinte.162.16.1842

Carrat, F., Vergu, E., Ferguson, N.M., Lemaitre, M., Cauchemez, S., Leach, S., Valleron, A.-J., 2008. Time lines of infection and disease in human influenza: a review of volunteer challenge studies. Am. J. Epidemiol. 167, 775–785. https://doi.org/10.1093/aje/kwm375

Chartered Institution of Building Services Engineers, 2015. GVA/15 CIBSE Guide A: Environmental Design 2015. CIBSE, London.

Cheng, Y.-H., Wang, C.-H., You, S.-H., Hsieh, N.-H., Chen, W.-Y., Chio, C.-P., Liao, C.-M., 2016. Assessing coughing-induced influenza droplet transmission and implications for infection risk control. Epidemiol. Infect. 144, 333–345. https://doi.org/10.1017/S0950268815001739

Cohen, S., Tyrrell, D.A., Smith, A.P., 1991. Psychological stress and susceptibility to the common cold. N. Engl. J. Med. 325, 606–12. https://doi.org/10.1056/NEJM199108293250903

Colijn, C., Gardy, J., 2014. Phylogenetic tree shapes resolve disease transmission patterns. Evol Med Public Health 2014, 96–108. https://doi.org/10.1093/emph/eou018

Couch, R.B., Chanock, R.M., Cate, T.R., Lang, D.J., Knight, V., Huebner, R.J., 1963. Immunization with types 4 and 7 adenovirus by selective infection of the intestinal tract. Am. Rev. Respir. Dis. 88, SUPPL 394-403. https://doi.org/10.1164/arrd.1963.88.3P2.394

Couch, R.B., Douglas Jr., R.G., Lindgren, K.M., Gerone, P.J., Knight, V., 1970. Airborne transmission of respiratory infection with coxsackievirus A type 21. Am J Epidemiol 91, 78–86.

Cowling, B.J., Chan, K.-H., Fang, V.J., Cheng, C.K.Y., Fung, R.O.P., Wai, W., Sin, J., Seto, W.H., Yung, R., Chu, D.W.S., Chiu, B.C.F., Lee, P.W.Y., Chiu, M.C., Lee, H.C., Uyeki, T.M., Houck, P.M., Peiris, J.S.M., Leung, G.M., 2009. Facemasks and hand hygiene to prevent influenza transmission in households: a cluster randomized trial. Ann. Intern. Med. 151, 437–446.

Cowling, B.J., Ip, D.K.M., Fang, V.J., Suntarattiwong, P., Olsen, S.J., Levy, J., Uyeki, T.M., Leung, G.M., Malik Peiris, J.S., Chotpitayasunondh, T., Nishiura, H., Mark Simmerman, J., 2013a. Aerosol transmission is an important mode of influenza A virus spread. Nature Communications 4. https://doi.org/10.1038/ncomms2922

Cowling, B.J., Ip, D.K.M., Fang, V.J., Suntarattiwong, P., Olsen, S.J., Levy, J., Uyeki, T.M., Leung, G.M., Malik Peiris, J.S., Chotpitayasunondh, T., Nishiura, H., Mark Simmerman, J., 2013b. Aerosol transmission is an important mode of influenza A virus spread. Nat Commun 4, 1935. https://doi.org/10.1038/ncomms2922

Didelot, X., Fraser, C., Gardy, J., Colijn, C., 2017. Genomic Infectious Disease Epidemiology in Partially Sampled and Ongoing Outbreaks. Mol. Biol. Evol. 34, 997–1007. https://doi.org/10.1093/molbev/msw275

Erbelding, E.J., Post, D.J., Stemmy, E.J., Roberts, P.C., Augustine, A.D., Ferguson, S., Paules, C.I., Graham, B.S., Fauci, A.S., 2018. A Universal Influenza Vaccine: The Strategic Plan for the National Institute of Allergy and Infectious Diseases. J. Infect. Dis. 218, 347–354. https://doi.org/10.1093/infdis/jiy103

Fabian, P., McDevitt, J.J., DeHaan, W.H., Fung, R.O.P., Cowling, B.J., Chan, K.H., Leung, G.M., Milton, D.K., 2008. Influenza virus in human exhaled breath: an observational study. PLoS ONE 3, e2691. https://doi.org/10.1371/journal.pone.0002691

Fennelly, K.P., Davidow, A.L., Miller, S.L., Connell, N., Ellner, J.J., 2004. Airborne infection with Bacillus anthracis--from mills to mail. Emerg Infect Dis 10, 996–1002.

Fischer, W.A., Gong, M., Bhagwanjee, S., Sevransky, J., 2014. Global burden of Influenza: Contributions from Resource Limited and Low-Income Settings. Glob Heart 9, 325–336. https://doi.org/10.1016/j.gheart.2014.08.004

Fischinger, S., Boudreau, C.M., Butler, A.L., Streeck, H., Alter, G., 2019. Sex differences in vaccine-induced humoral immunity. Semin Immunopathol 41, 239–249. https://doi.org/10.1007/s00281-018-0726-5

Fraser, C., Riley, S., Anderson, R.M., Ferguson, N.M., 2004. Factors that make an infectious disease outbreak controllable. PNAS 101, 6146–6151. https://doi.org/10.1073/pnas.0307506101

Gabriel, G., Arck, P.C., 2014. Sex, Immunity and Influenza. J Infect Dis 209, S93–S99. https://doi.org/10.1093/infdis/jiu020

Gammaitoni, L., Nucci, M.C., 1997. Using a mathematical model to evaluate the efficacy of TB control measures. Emerg Infect Dis 3, 335–342.

Gao, X., Wei, J., Lei, H., Xu, P., Cowling, B.J., Li, Y., 2016. Building Ventilation as an Effective Disease Intervention Strategy in a Dense Indoor Contact Network in an Ideal City. PLOS ONE 11, e0162481. https://doi.org/10.1371/journal.pone.0162481

Gustin, K.M., Belser, J.A., Wadford, D.A., Pearce, M.B., Katz, J.M., Tumpey, T.M., Maines, T.R., 2011. Influenza virus aerosol exposure and analytical system for ferrets. Proc. Natl. Acad. Sci. U.S.A. 108, 8432–8437. https://doi.org/10.1073/pnas.1100768108

Harper, G.J., 1961. Airborne micro-organisms: survival tests with four viruses. J Hyg (Lond) 59, 479–486.

Hayden, F.G., 2012. Experimental human influenza: observations from studies of influenza antivirals. Antivir. Ther. (Lond.) 17, 133–141. https://doi.org/10.3851/IMP2062

Hayward, A.C., Fragaszy, E.B., Bermingham, A., Wang, L., Copas, A., Edmunds, W.J., Ferguson, N., Goonetilleke, N., Harvey, G., Kovar, J., Lim, M.S.C., McMichael, A., Millett, E.R.C., Nguyen-Van-Tam, J.S., Nazareth, I., Pebody, R., Tabassum, F., Watson, J.M., Wurie, F.B., Johnson, A.M., Zambon, M., Flu Watch Group, 2014. Comparative community burden and severity of seasonal and pandemic influenza: results of the Flu Watch cohort study. Lancet Respir Med 2, 445–454. https://doi.org/10.1016/S2213-2600(14)70034-7

Henle, W., Henle, G., Stokes, J., 1943. Demonstration of the Efficacy of Vaccination Against Influenza Type A by Experimental Infection of Human Beings. J. Immunol. 46, 163–175.

Henle, W., Henle, G., Stokes, J., Maris, E.P., 1946. Experimental Exposure of Human Subjects to Viruses of Influenza. J. Immunol. 52, 145–65.

Ijaz, M.K., Brunner, A.H., Sattar, S.A., Nair, R.C., Johnson-Lussenburg, C.M., 1985. Survival characteristics of airborne human coronavirus 229E. J Gen Virol 66, 2743–2748.

Ip, D.K.M., Lau, L.L.H., Chan, K.-H., Fang, V.J., Leung, G.M., Peiris, M.J.S., Cowling, B.J., 2016. The Dynamic Relationship Between Clinical Symptomatology and Viral Shedding in Naturally Acquired Seasonal and Pandemic Influenza Virus Infections. Clin Infect Dis 62, 431–437. https://doi.org/10.1093/cid/civ909

Ip, D.K.M., Lau, L.L.H., Leung, N.H.L., Fang, V.J., Chan, K.-H., Chu, D.K.W., Leung, G.M., Peiris, J.S.M., Uyeki, T.M., Cowling, B.J., 2017. Viral Shedding and Transmission Potential of Asymptomatic and Paucisymptomatic Influenza Virus Infections in the Community. Clin. Infect. Dis. 64, 736–742. https://doi.org/10.1093/cid/ciw841

Issarow, C.M., Mulder, N., Wood, R., 2015. Modelling the risk of airborne infectious disease using exhaled air. Journal of Theoretical Biology 372, 100–106. https://doi.org/10.1016/j.jtbi.2015.02.010

Jenkins, S.T., 2018. VENTILATION IMPACT ON AIRBORNE TRANSMISSION OF RESPIRATORY ILLNESS IN STUDENT DORMITORIES (Thesis). https://doi.org/10.13016/sadj-dny0

Johnson, G.R., Morawska, L., 2009. The mechanism of breath aerosol formation. J Aerosol Med Pulm Drug Deliv 22, 229–237. https://doi.org/10.1089/jamp.2008.0720

Keitel, W.A., Couch, R.B., Cate, T.R., Six, H.R., Baxter, B.D., 1990. Cold Recombinant Influenza B/Texas/1/84 Vaccine Virus (CRB 87): Attenuation, Immunogenicity, and Efficacy against Homotypic Challenge. The Journal of Infectious Diseases 161, 22–26.

Killingley, B., Enstone, J., Booy, R., Hayward, A., Oxford, J., Ferguson, N., Nguyen Van-Tam, J., influenza transmission strategy development group, 2011. Potential role of human challenge studies for investigation of influenza transmission. Lancet Infect Dis 11, 879–886. https://doi.org/10.1016/S1473-3099(11)70142-6

Killingley, B., Enstone, J.E., Greatorex, J., Gilbert, A.S., Lambkin-Williams, R., Cauchemez, S., Katz, J.M., Booy, R., Hayward, A., Oxford, J., Bridges, C.B.,

Ferguson, N.M., Nguyen Van-Tam, J.S., 2012. Use of a human influenza challenge model to assess person-to-person transmission: proof-of-concept study. J. Infect. Dis. 205, 35–43. https://doi.org/10.1093/infdis/jir701

Killingley, B., Nguyen-Van-Tam, J., 2013. Routes of influenza transmission. Influenza and Other Respiratory Viruses 7, 42–51. https://doi.org/10.1111/irv.12080

Knight, V., Kasel, J.A., Alford, R.H., Loda, F., Morris, J.A., Davenport, F.M., Robinson, R.Q., Buescher, E.L., 1965. New Research on Influenza: Studies with Normal Volunteers: Combined Clinical Staff Conference at the National Institutes of Health. Ann. Intern. Med. 62, 1307–1325. https://doi.org/10.7326/0003-4819-62-6-1307

Kormuth, K.A., Lin, K., Prussin, A.J., Vejerano, E.P., Tiwari, A.J., Cox, S.S., Myerburg, M.M., Lakdawala, S.S., Marr, L.C., 2018. Influenza Virus Infectivity Is Retained in Aerosols and Droplets Independent of Relative Humidity. J. Infect. Dis. 218, 739–747. https://doi.org/10.1093/infdis/jiy221

Larson, E.L., Ferng, Y., Wong-McLoughlin, J., Wang, S., Haber, M., Morse, S.S., 2010. Impact of non-pharmaceutical interventions on URIs and influenza in crowded, urban households. Public health reports 178–191.

Lau, L.L.H., Cowling, B.J., Fang, V.J., Chan, K.-H., Lau, E.H.Y., Lipsitch, M., Cheng, C.K.Y., Houck, P.M., Uyeki, T.M., Peiris, J.S.M., Leung, G.M., 2010. Viral Shedding and Clinical Illness in Naturally Acquired Influenza Virus Infections. J Infect Dis 201, 1509–1516. https://doi.org/10.1086/652241

Lau, L.L.H., Ip, D.K.M., Nishiura, H., Fang, V.J., Chan, K.-H., Peiris, J.S.M., Leung, G.M., Cowling, B.J., 2013. Heterogeneity in viral shedding among individuals with medically attended influenza A virus infection. The Journal of infectious diseases 207, 1281–5. https://doi.org/10.1093/infdis/jit034

Lessler, J., Reich, N.G., Brookmeyer, R., Perl, T.M., Nelson, K.E., Cummings, D.A.T., 2009. Incubation periods of acute respiratory viral infections: a systematic review. Lancet Infect Dis 9, 291–300. https://doi.org/10.1016/S1473-3099(09)70069-6

Leung, N.H.L., Xu, C., Ip, D.K.M., Cowling, B.J., 2015. Review Article: The Fraction of Influenza Virus Infections That Are Asymptomatic. Epidemiology 26, 862–872. https://doi.org/10.1097/EDE.0000000000000340

Lindsley, W.G., Blachere, F.M., Thewlis, R.E., Vishnu, A., Davis, K.A., Cao, G., Palmer, J.E., Clark, K.E., Fisher, M.A., Khakoo, R., Beezhold, D.H., 2010. Measurements of airborne influenza virus in aerosol particles from human coughs. PLoS One 5, e15100–e15100. https://doi.org/10.1371/journal.pone.0015100

Lindsley, W.G., Noti, J.D., Blachere, F.M., Thewlis, R.E., Martin, S.B., Othumpangat, S., Noorbakhsh, B., Goldsmith, W.T., Vishnu, A., Palmer, J.E., Clark, K.E., Beezhold, D.H., 2015. Viable influenza A virus in airborne particles from human coughs. J Occup Environ Hyg 12, 107–113. https://doi.org/10.1080/15459624.2014.973113

Little, J.W., Douglas, R.G., Hall, W.J., Roth, F.K., 1979. Attenuated influenza produced by experimental intranasal inoculation. J. Med. Virol. 3, 177–188. https://doi.org/10.1002/jmv.1890030303

Lowen, A.C., Mubareka, S., Steel, J., Palese, P., 2007. Influenza virus transmission is dependent on relative humidity and temperature. PLoS Pathog. 3, 1470–1476. https://doi.org/10.1371/journal.ppat.0030151

Lowen, A.C., Steel, J., 2014. Roles of Humidity and Temperature in Shaping Influenza Seasonality. J. Virol. 88, 7692–7695. https://doi.org/10.1128/JVI.03544-13

Makison Booth, C., Clayton, M., Crook, B., Gawn, J.M., 2013. Effectiveness of surgical masks against influenza bioaerosols. Journal of Hospital Infection 84, 22–26. https://doi.org/10.1016/j.jhin.2013.02.007

McCrone, J.T., Woods, R.J., Martin, E.T., Malosh, R.E., Monto, A.S., Lauring, A.S., 2018. Stochastic processes constrain the within and between host evolution of influenza virus. Elife 7. https://doi.org/10.7554/eLife.35962

McDevitt, J.J., Koutrakis, P., Ferguson, S.T., Wolfson, J.M., Fabian, M.P., Martins, M., Pantelic, J., Milton, D.K., 2013. Development and Performance Evaluation of an Exhaled-Breath Bioaerosol Collector for Influenza Virus. Aerosol Sci Technol 47, 444–451. https://doi.org/10.1080/02786826.2012.762973

McDevitt, J.J., Rudnick, S.N., Radonovich, L.J., 2012. Aerosol Susceptibility of Influenza Virus to UV-C Light. Applied and Environmental Microbiology 78, 1666–1669. https://doi.org/10.1128/aem.06960-11

Milton, D.K., 2012. What was the primary mode of smallpox transmission? Implications for biodefense. Front Cell Infect Microbiol 2, 150. https://doi.org/10.3389/fcimb.2012.00150

Milton, D.K., Fabian, M.P., Cowling, B.J., Grantham, M.L., McDevitt, J.J., 2013. Influenza virus aerosols in human exhaled breath: particle size, culturability, and effect of surgical masks. PLoS Pathog. 9, e1003205. https://doi.org/10.1371/journal.ppat.1003205

Milton, D.K., Glencross, P.M., Walters, M.D., 2000. Risk of sick leave associated with outdoor air supply rate, humidification, and occupant complaints. Indoor Air 10, 212–221. https://doi.org/10.1034/j.1600-0668.2000.010004212.x

Molinari, N.-A.M., Ortega-Sanchez, I.R., Messonnier, M.L., Thompson, W.W., Wortley, P.M., Weintraub, E., Bridges, C.B., 2007. The annual impact of seasonal influenza in the US: Measuring disease burden and costs. Vaccine 25, 5086–5096. https://doi.org/10.1016/j.vaccine.2007.03.046

Moser, M.R., Bender, T.R., Margolis, H.S., Noble, G.R., Kendal, A.P., Ritter, D.G., 1979a. An outbreak of influenza aboard a commercial airliner. Am. J. Epidemiol. 110, 1–6.

Moser, M.R., Bender, T.R., Margolis, H.S., Noble, G.R., Kendal, A.P., Ritter, D.G., 1979b. An outbreak of influenza aboard a commercial airliner. Am. J. Epidemiol. 110, 1–6.

Mubareka, S., Lowen, A.C., Steel, J., Coates, A.L., García-Sastre, A., Palese, P., 2009. Transmission of Influenza Virus via Aerosols and Fomites in the Guinea Pig Model. J Infect Dis 199, 858–865.

Myatt, T.A., Staudenmayer, J., Adams, K., Walters, M., Rudnick, S.N., Milton, D.K., 2002. A study of indoor carbon dioxide levels and sick leave among office workers. Environmental Health 1, 3. https://doi.org/10.1186/1476-069X-1-3

Nardell, E.A., Keegan, J., Cheney, S.A., Etkind, S.C., 1991. Airborne infection. Theoretical limits of protection achievable by building ventilation. Am Rev Respir Dis 144, 302–306.

Nguyen-Van-Tam, J.S., Killingley, B., Enstone, J., Hewitt, M., Pantelic, J., Grantham, M., Bueno de Mesquita, P.J., Lambkin-Williams, R., Gilbert, A., Mann, A., Forni, J., Noakes, C.J., Levine, M.Z., Cauchemez, S., Bischoff, W., Tellier, R., Milton, D.K., EMIT Consortium, 2019. Minimal transmission in an influenza A H3N2 human challenge-transmission model with exposure events in a controlled environment. In Prep.

Nikitin, N., Petrova, E., Trifonova, E., Karpova, O., 2014. Influenza Virus Aerosols in the Air and Their Infectiousness. Advances in Virology. https://doi.org/10.1155/2014/859090

Noakes, C.J., Beggs, C.B., Sleigh, P.A., Kerr, K.G., 2006. Modelling the transmission of airborne infections in enclosed spaces. Epidemiology and Infection 134, 1082. https://doi.org/10.1017/S0950268806005875

Noakes, C.J., Sleigh, P.A., 2009. Mathematical models for assessing the role of airflow on the risk of airborne infection in hospital wards. J R Soc Interface 6, S791–S800. https://doi.org/10.1098/rsif.2009.0305.focus

Noti, J.D., Lindsley, W.G., Blachere, F.M., Cao, G., Kashon, M.L., Thewlis, R.E., McMillen, C.M., King, W.P., Szalajda, J.V., Beezhold, D.H., 2012. Detection of infectious influenza virus in cough aerosols generated in a simulated patient

examination room. Clin. Infect. Dis. 54, 1569–1577. https://doi.org/10.1093/cid/cis237

Office of the Surgeon General (US), 2009. The Surgeon General's Call to Action to Promote Healthy Homes, Publications and Reports of the Surgeon General. Office of the Surgeon General (US), Rockville (MD).

Onodera, T., Hosono, A., Odagiri, T., Tashiro, M., Kaminogawa, S., Okuno, Y., Kurosaki, T., Ato, M., Kobayashi, K., Takahashi, Y., 2016. Whole-Virion Influenza Vaccine Recalls an Early Burst of High-Affinity Memory B Cell Response through TLR Signaling. The Journal of Immunology 196, 4172–4184. https://doi.org/10.4049/jimmunol.1600046

Park, J.-K., Han, A., Czajkowski, L., Reed, S., Athota, R., Bristol, T., Rosas, L.A., Cervantes-Medina, A., Taubenberger, J.K., Memoli, M.J., 2018. Evaluation of Preexisting Anti-Hemagglutinin Stalk Antibody as a Correlate of Protection in a Healthy Volunteer Challenge with Influenza A/H1N1pdm Virus. MBio 9, e02284-17. https://doi.org/10.1128/mBio.02284-17

Piralla, A., Pariani, E., Rovida, F., Campanini, G., Muzzi, A., Emmi, V., Iotti, G.A., Pesenti, A., Conaldi, P.G., Zanetti, A., Baldanti, F., Severe Influenza A Task Force, 2011. Segregation of virulent influenza A(H1N1) variants in the lower respiratory tract of critically ill patients during the 2010-2011 seasonal epidemic. PLoS ONE 6, e28332. https://doi.org/10.1371/journal.pone.0028332

Prussin, A.J., Schwake, D.O., Lin, K., Gallagher, D.L., Buttling, L., Marr, L.C., 2018. Survival of the Enveloped Virus Phi6 in Droplets as a Function of Relative Humidity, Absolute Humidity, and Temperature. Applied and Environmental Microbiology AEM.00551-18. https://doi.org/10.1128/AEM.00551-18

Ranjeva, S., Subramanian, R., Fang, V.J., Leung, G.M., Ip, D.K.M., Perera, R.A.P.M., Peiris, J.S.M., Cowling, B.J., Cobey, S., 2019. Age-specific differences in the dynamics of protective immunity to influenza. Nature Communications 10, 1660. https://doi.org/10.1038/s41467-019-09652-6

Riley, E.C., Murphy, G., Riley, R.L., 1978. Airborne spread of measles in a suburban elementary school. Am J Epidemiol 107, 421–432.

Riley, R.L., Nardell, E.A., 1989. Clearing the air. The theory and application of ultraviolet air disinfection. Am Rev Respir Dis 139, 1286–1294.

Roy, C.J., Milton, D.K., 2004. Airborne transmission of communicable infection--the elusive pathway. N. Engl. J. Med. 350, 1710–1712. https://doi.org/10.1056/NEJMp048051

Rubin, D.B., 2001. Using Propensity Scores to Help Design Observational Studies: Application to the Tobacco Litigation. Health Services & Outcomes Research Methodology 2, 169–188. https://doi.org/10.1017/CBO9780511810725

Rudnick, S.N., Milton, D.K., 2003a. Risk of indoor airborne infection transmission estimated from carbon dioxide concentration. Indoor Air 13, 237–245. https://doi.org/10.1034/j.1600-0668.2003.00189.x

Rudnick, S.N., Milton, D.K., 2003b. Risk of indoor airborne infection transmission estimated from carbon dioxide concentration. Indoor Air 13, 237–245. https://doi.org/10.1034/j.1600-0668.2003.00189.x

SeppĘnen, O., 2008. Ventilation Strategies for Good Indoor Air Quality and Energy Efficiency. International Journal of Ventilation 6, 297–306. https://doi.org/10.1080/14733315.2008.11683785

Shaman, J., Pitzer, V.E., Viboud, C., Grenfell, B.T., Lipsitch, M., 2010. Absolute Humidity and the Seasonal Onset of Influenza in the Continental United States. PLoS Biol 8, e1000316. https://doi.org/10.1371/journal.pbio.1000316

Simmerman, J.M., Suntarattiwong, P., Levy, J., Jarman, R.G., Kaewchana, S., Gibbons, R.V., Cowling, B.J., Sanasuttipun, W., Maloney, S.A., Uyeki, T.M., Kamimoto, L., Chotipitayasunondh, T., 2011. Findings from a household randomized controlled trial of hand washing and face masks to reduce influenza transmission in Bangkok, Thailand. Influenza Other Respir Viruses 5, 256–267. https://doi.org/10.1111/j.1750-2659.2011.00205.x

Snider, D., Bridges, C., Weissman, D., 2010. Meeting summary of the workshop ‘Approaches to better understand human influenza transmission’’.’ Presented at the Approaches to better understand human influenza transmission. Centers for Disease Control and Prevention (United States of America), Centers for Disease Control and Prevention, Tom Harkin Global Communications Center, Centers for Disease Control and Prevention, Atlanta, Georgia.

Sobel Leonard, A., McClain, M.T., Smith, G.J.D., Wentworth, D.E., Halpin, R.A., Lin, X., Ransier, A., Stockwell, T.B., Das, S.R., Gilbert, A.S., Lambkin-Williams, R., Ginsburg, G.S., Woods, C.W., Koelle, K., 2016. Deep Sequencing of Influenza A Virus from a Human Challenge Study Reveals a Selective Bottleneck and Only Limited Intrahost Genetic Diversification. J. Virol. 90, 11247–11258. https://doi.org/10.1128/JVI.01657-16

Sun, Y., Wang, Z., Zhang, Y., Sundell, J., 2011. In China, students in crowded dormitories with a low ventilation rate have more common colds: evidence for airborne transmission. PLoS ONE 6, e27140. https://doi.org/10.1371/journal.pone.0027140

Tang, J.W., 2012. Pre-existing immunity in human challenge studies of influenza transmission. The Lancet Infectious Diseases 12, 744. https://doi.org/10.1016/S1473-3099(12)70199-8

Tellier, R., 2009. Aerosol transmission of influenza A virus: a review of new studies. J R Soc Interface 6 Suppl 6, S783-790. https://doi.org/10.1098/rsif.2009.0302.focus

Tellier, R., 2006. Review of aerosol transmission of influenza A virus. Emerging Infect. Dis. 12, 1657–1662. https://doi.org/10.3201/eid1211.060426

Tellier, R., Li, Y., Cowling, B.J., Tang, J.W., 2019. Recognition of aerosol transmission of infectious agents: a commentary. BMC Infectious Diseases 19, 101. https://doi.org/10.1186/s12879-019-3707-y

Tsang, T.K., Cowling, B.J., Fang, V.J., Chan, K.-H., Ip, D.K.M., Leung, G.M., Peiris, J.S.M., Cauchemez, S., 2015. Influenza A Virus Shedding and Infectivity in Households. J. Infect. Dis. 212, 1420–1428. https://doi.org/10.1093/infdis/jiv225

Tsang, T.K., Fang, V.J., Chan, K.-H., Ip, D.K.M., Leung, G.M., Peiris, J.S.M., Cowling, B.J., Cauchemez, S., 2016. Individual Correlates of Infectivity of Influenza A Virus Infections in Households. PLoS ONE 11, e0154418. https://doi.org/10.1371/journal.pone.0154418

Twisk, J., Rijmen, F., 2009. Longitudinal tobit regression: A new approach to analyze outcome variables with floor or ceiling effects. Journal of Clinical Epidemiology 62, 953–958. https://doi.org/10.1016/j.jclinepi.2008.10.003

Verver, S., Warren, R.M., Munch, Z., Richardson, M., van der Spuy, G.D., Borgdorff, M.W., Behr, M.A., Beyers, N., van Helden, P.D., 2004. Proportion of tuberculosis transmission that takes place in households in a high-incidence area. Lancet 363, 212–214. https://doi.org/10.1016/S0140-6736(03)15332-9

Viboud, C., Boëlle, P.-Y., Cauchemez, S., Lavenu, A., Valleron, A.-J., Flahault, A., Carrat, F., 2004. Risk factors of influenza transmission in households. Br J Gen Pract 54, 684–689.

Volz, E.M., Frost, S.D.W., 2013. Inferring the Source of Transmission with Phylogenetic Data. PLoS Comput Biol 9, e1003397. https://doi.org/10.1371/journal.pcbi.1003397

Volz, E.M., Pond, S.L.K., Ward, M.J., Brown, A.J.L., Frost, S.D.W., 2009. Phylodynamics of Infectious Disease Epidemics. Genetics 183, 1421–1430. https://doi.org/10.1534/genetics.109.106021

Wardell, R., Prem, K., Cowling, B.J., Cook, A.R., 2017. The role of symptomatic presentation in influenza A transmission risk. Epidemiol. Infect. 145, 723–727. https://doi.org/10.1017/S0950268816002740

Wells, W.F., 1955. Airborne Contagion and Air Hygiene: An Ecological Study of Droplet Infection. Harvard University Press, Cambridge, MA.

Wong, V.W.Y., Cowling, B.J., Aiello, A.E., 2014. Hand hygiene and risk of influenza virus infections in the community: a systematic review and meta-analysis. Epidemiol. Infect. 142, 922–932. https://doi.org/10.1017/S095026881400003X

Wood, R., Johnstone-Robertson, S., Uys, P., Hargrove, J., Middelkoop, K., Lawn, S.D., Bekker, L.-G., 2010. Tuberculosis Transmission to Young Children in a South African Community: Modeling Household and Community Infection Risks. Clin Infect Dis 51, 401–408. https://doi.org/10.1086/655129

Worby, C.J., Lipsitch, M., Hanage, W.P., 2017. Shared Genomic Variants: Identification of Transmission Routes Using Pathogen Deep-Sequence Data. Am. J. Epidemiol. 186, 1209–1216. https://doi.org/10.1093/aje/kwx182

World Health Organization (Ed.), 2011. Manual for the laboratory diagnosis and virological surveillance of influenza. World Health Organization, Geneva.

Yan, J., Grantham, M., Pantelic, J., Bueno de Mesquita, P.J., Albert, B., Liu, F., Ehrman, S., Milton, D.K., EMIT Consortium, 2018. Infectious virus in exhaled breath of symptomatic seasonal influenza cases from a college community. Proc. Natl. Acad. Sci. U.S.A. 115, 1081–1086. https://doi.org/10.1073/pnas.1716561115

Yang, W., Elankumaran, S., Marr, L.C., 2012. Relationship between Humidity and Influenza A Viability in Droplets and Implications for Influenza's Seasonality. PLOS ONE 7, e46789. https://doi.org/10.1371/journal.pone.0046789

Yu, I.T., Li, Y., Wong, T.W., Tam, W., Chan, A.T., Lee, J.H., Leung, D.Y., Ho, T., 2004. Evidence of airborne transmission of the severe acute respiratory syndrome virus. New England Journal of Medicine 350, 1731–1739.

Zaas, A.K., Burke, T., Chen, M., McClain, M., Nicholson, B., Veldman, T., Tsalik, E.L., Fowler, V., Rivers, E.P., Otero, R., Kingsmore, S.F., Voora, D., Lucas, J., Hero, A.O., Carin, L., Woods, C.W., Ginsburg, G.S., 2013. A host-based RT-PCR gene expression signature to identify acute respiratory viral infection. Sci Transl Med 5, 203ra126. https://doi.org/10.1126/scitranslmed.3006280

Zaas, A.K., Chen, M., Varkey, J., Veldman, T., Hero, A.O., Lucas, J., Huang, Y., Turner, R., Gilbert, A., Lambkin-Williams, R., Øien, N.C., Nicholson, B., Kingsmore, S., Carin, L., Woods, C.W., Ginsburg, G.S., 2009. Gene

expression signatures diagnose influenza and other symptomatic respiratory viral infections in humans. Cell Host Microbe 6, 207–217. https://doi.org/10.1016/j.chom.2009.07.006